Andreas Bjørshol
Gunn Helen Nylund

Single Tank Oil Based Heat Storage for Cooking

Master's thesis in Mechanical Engineering
Supervisor: Ole Jørgen Nydal

June 2021

Master's thesis

NTNU
Norwegian University of
Science and Technology

Andreas Bjørshol
Gunn Helen Nylund

Single Tank Oil Based Heat Storage for Cooking

NTNU
Norwegian University of
Science and Technology

Acknowledgments

Abstract

This thesis concerns the design and testing of a thermal energy storage to be used for cooking by families and institutions in Sub-Saharan African countries. The system consists of an oil barrel containing a funnel and a heating element, with a pot at the top. The funnel separates the hot and cold oil flows and makes it possible to heat a small volume of oil quickly, to be stored or used for cooking. A system to test the concept was designed and built during a previous project thesis. Experiments showed that the system can be used to cook food both from the storage and while charging. The results from these experiments were used to optimize the design and, based on this, an improved system was built, with the possibility of adjusting the funnel height to control the temperature in the funnel. A pot-in-pot solution for cooking was tested, since the pot must be extracted for cleaning. With a small amount of oil in between the pots, the pot-in-pot solution provides a much more acceptable heat transfer to the cooker than without. The tank was filled with rocks to reduce the amount of oil needed. Experiments showed that the rock bed reduces the mixing of oil, which leads to better thermal behavior during charging and makes it possible to extract more energy from the oil during discharging. The funnel concept has proven inefficient while charging under reduced power, due to heat losses from the funnel to the storage. Simulations have been run to investigate the effect of insulating the funnel tube, showing the importance of the upper part of the funnel. Rice and bean cooking experiments were conducted, with the system charged by photovoltaic panels. The available energy in the fully charged system is about 5.3 kWh, which can be suitable for small institutions. With the ability to recharge the system, the daily available energy can be increased. The concept has been deemed ready for testing under more realistic conditions.

Sammendrag

I denne masteroppgaven blir design og testing av et termisk energilager som kan brukes as familier og institusjoner i land sør for Sahara i Afrika undersøkt. Systemet består av en oljetønne med en trakt og et varmeelement inni, med en kjele til matlaging øverst. Trakten skiller varm og kald oljestrøm og gjør det mulig å varme opp et lite volum olje raskt, som kan brukes til å lage mat eller lagres. Et system for å teste konseptet ble designet og bygget under en tidligere prosjekt-toppgave. Eksperimenter viste at systemet kan brukes til å lage mat både fra termisk lager og under oppladning. Resultatene fra disse eksperimentene ble brukt til å utvikle et bedre design og et nytt system ble bygd med mulighet til å endre høyden på trakten for å kontrollere temperatur. Et kjele-i-kjele-oppsett for å tilberede mat ble testet, da man må kunne ta ut den ene kjelen for rengjøring. En liten mengde olje mellom kjelene gir tilfredsstillende varmeoverføring. Tanken ble fylt med steiner for å redusere oljemengden i systemet. Eksperimenter viste at steinene senker hastigheten på oljestrømmen, noe som fører til mindre miksing av kald og varm olje og bedre temperaturoppførsel under oppladning. Dette gir en bedre energiutnyttelse av oljen ved koking. Trakt-i-tank-konseptet har vist seg å være ineffektivt om det lades opp med for lav effekt på grunn av varmetap fra trakten til det termiske lageret. Simuleringer med et isolert traktrør er gjort for å se om dette kan forbedre systemet. Eksperimenter med ris- og bønnekoking tilkoblet solcellepaneler ble gjennomført. Den tilgjengelige mengden termisk energi når systemet er fulladet er 5.3 kWt. Dette kan være passende for en liten institusjon. Med mulighet for å lade opp tanken samme dag kan den daglige tilgjengelige energien være høyere. Konseptet er klart for å testes i det virkelig liv.

Contents

Figures

Tables

Nomenclature

C	Thermal capacity $[J/(cm^3K)]$
C_p	Specific heat capacity $[J/(kgK)]$
E_X	Exergy $[J]$
$F_{buoyancy}$	Buoyancy-induced force
g	Gravitational acceleration $[m/s^2]$
Gr_x	Local Grashof number [-]
h	Convective heat transfer coefficient $[W/(m^2K)]$
H	Height of tank $[m]$
k	Thermal conductivity $[W/(mK)]$
L	Characteristic length $[m]$
Nu_L	Nusselt number [-]
q''	Local heat flux $[W/m^2]$
Q	Thermal energy $[J]$
Pr	Prandtl number [-]
Ra_x	Local Rayleigh number [-]
Str	Stratification number [-]
T	Temperature [°C]
V	Volume $[m^3]$
x	Horizontal Cartesian coordinate $[m]$
y	Vertical Cartesian coordinate $[m]$
α	Thermal diffusivity $[m^2/s]$
β	Coefficient of thermal expansion $[K^{-1}]$
μ	Dynamic viscosity $[kg/(ms)]$
ν	Kinematic viscosity $[m^2/s]$
ρ	Density $[kg/m^3]$
ϕ	Mass fraction [-]

Abbreviations

AC	Alternating current
DC	Direct current
GHI	Global Horizontal Irradiation
HTF	Heat Transfer Fluid
MPPT	Maximum Power Point Tracking
NORHED	Norwegian Programme for Capacity Development in Higher Education and Research for Development
NORPART	Program for mobility in higher education
PV	Photovoltaic
STC	Standard Test Conditions
TES	Thermal Energy Storage

Chapter 1

Introduction

1.1 Objective

This thesis is a continuation of a project thesis [1] with the objective to develop an oil-based system for storing energy from sustainable energy sources. It is to be used for cooking by a small institution, like a small school or a community of families, for developing countries in Sub-Saharan Africa. The project is made under the framework of the NORHED project: "Energy Technology Network". The system will consist of one oil barrel and can use power from photovoltaic panels and/or wind and hydro generators. The heat storage is then charged by heating elements in the oil. The internal arrangements in the oil container are such that oil circulates via natural convection between a cooking chamber and a storage chamber. The arrangement with a heating funnel and a storage part can be improved with a flow control device (overflow barrier and valve), such that the temperature in the storage part is controllable (about 220 °C).

The system has been built during the project thesis and further laboratory experiments will include:

- Temperature measurements of the moving thermocline during charging and discharging (cooking).
- Charging experiments with different power levels to determine if insulation is needed on the internal funnel.
- Testing of a method for regulating the flow across the funnel barrier for temperature control in the storage.
- Cooking experiments at different charging levels of the storage.
- Charging with PV panels and a MPPT controller.
- Testing of the system with rock bed.

1.2 Background

More people have access to electricity than ever before, but there were still 840 million people without access to electricity in 2017 and most of these were living
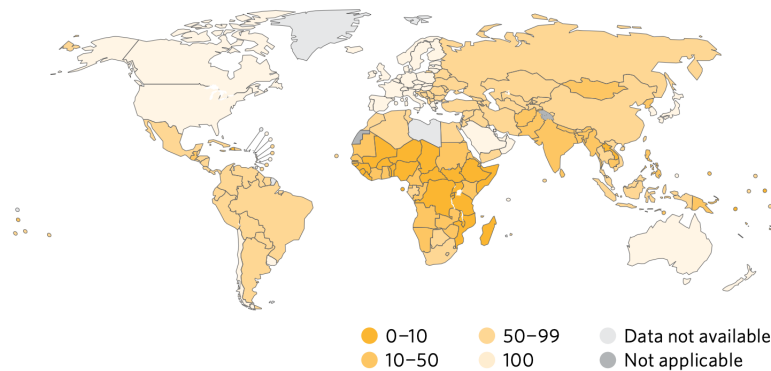
Figure 1.1: Proportion of population with access to clean cooking fuels and technologies, 2017 (percentage) [2].

in sub-Saharan Africa. A staggering 56% of the population in this area lacked access to electricity in 2017, which is approximately 573 million people [2]. Lack of electricity and lack of access to clean cooking usually go hand in hand as seen in Figure 1.1.

Unclean and highly polluting cooking systems result in nearly 4 million premature deaths every year. The use of these systems is one of the main contributors to poor health and environmental degradation in low income countries. The population growth in sub-Saharan Africa is larger than the increase in use of clean-fuel technology. Addressing these problems will require action from policymakers, as well as financing, availability, affordability, reliability, and consumer awareness [2].

Biomass accounts for the largest fuel source in sub-Saharan Africa. Wood in the form of firewood and charcoal is the most common type of biomass used [3]. To cook 1 kg of dry beans, about 2.6 kg of firewood is required. On average, a school of 500 students, in Uganda, consumes about 302 kg of firewood daily [4]. A study by Mwampamba [3] shows that medium consumption levels and low replenishment of harvested forests could deplete forests on public land in Tanzania by 2028. Not only does the use of biomass as an energy source lead to pollution and deforestation, it might also put the women and female children in danger. Women and female children are usually in charge of the cooking and collection of firewood, which subsequently requires long travel distances to collect the fuel. Karekezi *et al.* [5] states that an average wood collecting trip in southern Africa is 6 km while it is a staggering 10 km in Eritrea. These long trips not only limit time that could be used in other pursuits, but also exposes them to threats like wild animals, rape, attack, and abduction [6].

Solar cookers have long been presented as a solution for the problem of using biomass to cook. This has led to advances in solar cooking technology, but very few have researched the social context. Most projects have now realised that designing the perfect solar cooker will not result in massive product popularity [6]. A

joint study done by the South African Department of Minerals and Energy and the Deutsche Gesellschaft für Technische Zusammenarbeit [7] shows that families will use a solar cooker if they have one, but typically as an addition to their existing system, not as a replacement. Rural households traditionally use a variety of cooking options (on average two to three) and this will not change by introducing new technology. One of the biggest issues regarding solar cookers is that very few people buy them due to low awareness of the technology and the relatively high price compared to other, more established appliances. The purchase of a solar cooker represents a decent, financial risk, especially to low and middle-income households [6]. This will likely be a problem for all new, clean cooking technology.

The energy required to cook food in Uganda was investigated by Kajumba *et al.* [4]. Dry beans, rice, cassava, plantains, maize flour, fresh beans, and sweet potatoes were tested because they are the most consumed foods in Ugandan households. It was discovered that the energy required to cook high moisture food is similar to the energy required to boil water. Dry beans have the highest energy demand, with 1.65 kWh/kg to cook. This can be reduced to 1.10 kWh if the dry beans have been soaked in water first.

An institutional survey has been conducted by Kajumba *et al.* in which ten schools in Uganda took part. It was discovered that the most commonly cooked foods comprised of beans and maize flour. Three meals were prepared every day: breakfast, lunch, and dinner. On average, 140 g of dry beans and 267 g of maize flour were cooked per student, per day. For the average student in Uganda, the daily energy requirement is 0.36 kWh, so, for a school with 500 students, the daily energy requirement would be 180 kWh. Similarly, the daily energy requirement for an average household in Uganda was also investigated and was discovered to be 1.81 kWh for a household of five people.

Most of the cooking is done with stone fire technologies, which result in low thermal efficiencies, hence the need for modern cooking methods.

NTNU and partner universities in Ethiopia, Tanzania, Uganda, Mozambique, Malawi, and South Sudan have worked together on renewable energy research and education. Within the NORHED project, multiple solutions for clean cooking using thermal energy storage have been made.

One of the earlier models is the three tank system. This is a system consisting of three tanks: one with cold oil, one for heat storage of heated oil, and one for the used oil. The system is operated with valves to control the oil flow and the effect in the cooker. It has both a frying pan and a cooker. The three tank system solves the problem of cooking without a direct energy source by employing energy storage. However, it contains many parts and is designed for large-scale use. A simpler and scaled down system is, therefore, desirable.

The interest in a simpler system led to the development of the one tank system in the spring of 2020. Here, the stored oil and cooker is in the same tank. However, this requires all of the oil to be heated before cooking can begin, which is a time

intensive process. It is also desirable that one can cook even while the system is charging. This led to the idea of the two tank system. This design separates the oil tank and cooker. The cooker is a funnel shaped device that consists of a heating element and a cooker over the heating element. It has the ability to cook while charging, as well as having a thermally stratified heat storage. The system is not completely self driven and is more complicated than the one tank system.

The final iteration is the funnel-in-tank design, which is a combination of the one tank and two tank systems with a funnel inserted into the tank. The goal is a simple system that can cook both during charging and discharging. The system was designed and built during the project thesis. This thesis is a continuation of that project.

1.2.1 Structure of Report

This thesis follows a chronological structure. First, relevant theory is explained in Chapter 2. Then, the concept and the first design are explained in Chapter 3. Chapter 4 presents the method and the results obtained from the experiments conducted with the system designed during the project thesis. Chapter 5 shows a new design of the system, which is based on the results from Chapter 4. The results from experimenting with the new design are presented in Chapter 6. Simulations for testing design features regarding insulation have been run and are explained and presented in Chapter 7. Experiments with rock bed have been conducted and are presented in Chapter 8. Experiments using PV panels as a power source are presented in Chapter 9. Lastly, the conclusion and further work can be found in Chapter 10 and Chapter 11.

Chapter 2

Theory

The relevant theory for the work done in this thesis is presented in this chapter.

2.1 Heat Transfer

Heat transfer is the movement of thermal energy due to temperature differences in a medium (or between media) via conduction, convection, or radiation.

2.1.1 Conduction

Conduction is the transport of energy in a medium due to temperature gradients. The heat transfer rate equation is known as Fourier's law and can be written as

$$q''_{cond} = -k\nabla T. \tag{2.1}$$

Where q'' is the heat flux. The thermal conductivity k measures the rate of heat transfer through a medium, while ∇T represents the temperature gradient.

2.1.2 Convection

Convection is heat transfer by diffusion and bulk motion of a fluid. It occurs when there is a fluid motion over a surface with differing temperatures between the fluid flow and surface.

The convection heat flux is dependent on the temperature difference and the heat transfer coefficient, and can be expressed as

$$q''_{conv} = h\left(T_w - T_\infty\right) \tag{2.2}$$

from a wall to a freestream. Where T_w is the temperature at the wall and T_∞ is the temperature in the freestream. The convective heat transfer coefficient h is influenced by fluid motion, surface geometry, and the thermal properties of the fluid. Convection can be classified either as forced or free. Forced convection is a fluid flow caused by an external motion.

Free convection is a flow caused by buoyancy forces. Temperature differences in the fluid results in density differences, which, in turn, induces fluid motion. The buoyancy force acts on the gravitational field [8] and is defined as

$$F_{buoyancy} = \rho_{fluid} g V_{displaced} \, .$$

(2.3)

Where $V_{displaced}$ is the displaced volume. The density of oil is strongly temperature dependent. Therefore, a temperature gradient will lead to a significant change in density that induces buoyancy forces in that region. This change in density results in a change in volume, as seen in Equation (2.4).

$$V_{new} = \frac{\rho_{initial}}{\rho_{new}} V_{\text{initial}} \, .$$

(2.4)

(a) Momentum boundary layer   **(b)** Thermal boundary layer
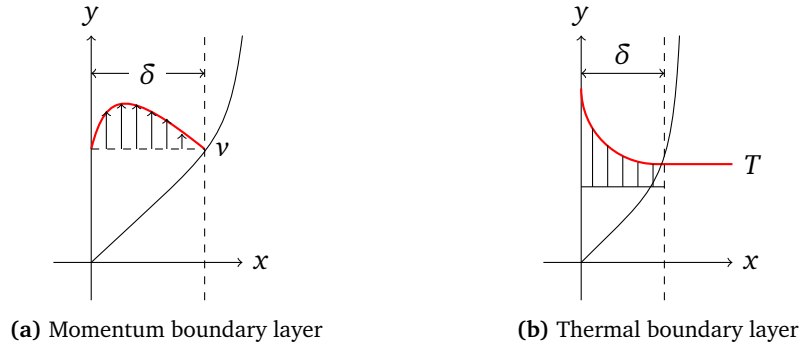
Figure 2.1: The boundary layers from free convection.

The momentum and thermal boundary layer for free convection along a warm vertical wall can be seen in Figure 2.1. The warm wall heats up the fluid close to it. This leads to a change in density and a buoyancy force is induced. This leads to free convection, the warm fluid flows upwards along the wall.

2.1.3 Correlations

The Nusselt number represents the ratio between convective and conductive heat transfer. Large Nusselt numbers signify that convection is more effective. The Nusselt number is defined as

$$Nu_L = \frac{hL}{k} \, ,$$

(2.5)

where L is the characteristic length.

The Prandtl number is a dimensionless number explaining the ratio between the thermal boundary layer and the velocity boundary layer. For Prandtl numbers below one, the thermal boundary layer will be thickest. The thickness of the boundary layers is related to the fluid properties. For air at room temperature and atmospheric pressure, the Prandtl number is 0.72. The Prandtl number varies with

temperature, such that, for soybean oil, it ranges from 50 to 500. This means that the velocity boundary layer is thicker than the thermal boundary layer.

$$Pr = \frac{\nu}{\alpha} = \frac{\mu/\rho}{k/\rho C_p} \tag{2.6}$$

"The Grashof number is a measure of the ratio of the buoyancy forces to the viscous forces acting on the fluid" stated by Bergman, Incropera, DeWitt and Lavine (2011, p.599)[8]. It is defined as

$$Gr_x \equiv \frac{g\beta(T_w - T_\infty)x^3}{\nu^2} \tag{2.7}$$

for a flow on a vertical plate where density variations are due only to temperature gradients [8]. β is the coefficient of thermal expansion.

As Bergman, Incropera, DeWitt and Lavine stated (2011, p.599)[8], "The Rayleigh number provides a measure of the ratio of the inertial to viscous forces acting on a fluid element" and is defined as the product of the Grashof and the Prandtl numbers. When the Rayleigh number exceeds a certain threshold, a convective flow will begin to develop. This flow will be laminar until the transition region is reached. This number is defined as

$$Ra_x = Gr_x Pr = \frac{g\beta(T_w - T_\infty)x^3}{\nu\alpha} \, . \tag{2.8}$$

Combining Equation (2.8) and Equation (2.1), results in

$$Ra_x = \frac{g\beta q'' x^4}{\nu\alpha k}, \tag{2.9}$$

where α is the thermal diffusivity.

The transition criterion from laminar to turbulent flow for a vertical plate is $Ra_L \approx 10^9$, according to the correlation mentioned in [8]. Not everyone agrees with this correlation, as stated by Bejan and Lage (1990, pp. 788) [9], "Although the transition Rayleigh for both air and water is of order 10^9, the Ra value increases as Pr increases". A study by Fujii [10] with ethylene glycol with a Pr of 28-33 showed that the transition was located at $Ra \approx 8.5 \times 10^9$. Another study with ethylene glycol [11] with $Pr = 40$ chose $Ra \approx 4 \times 10^{10}$ as the transition criteria. A study of natural convection in oil with $Pr \approx 200$ reported laminar flow with Rayleigh number in the range $10^8 - 2.2 \times 10^{10}$ [12]. Bejan and Lage came to the conclusion of another correlation for the transition criteria altogether, $Gr_L \approx 10^9$ which means that $Ra_L = 10^9 \times Pr$. Both correlations mentioned in [8] and [9] were studied in [13] and were compared to experimental data for vertical plates. They concluded that $Gr_L \approx 10^9$ forecasts the laminar-turbulent transition better than the well known criterion $Ra_L \approx 10^9$ for all Prandtl numbers.

2.2   Thermal Energy Storage

Energy demand varies by day, week and season. A way to match these demands is by using Thermal Energy Storage (TES) methods. The end-user's energy demand is reached through energy redistribution. Energy, both in the form of heat or cold, are placed in a storage medium for a duration of time and can be retrieved for later use. TES can be described as a thermal battery [14].

TES can be charged with a base load of energy. This means that only a minimal energy supply is needed to supply energy to the system. During discharge, the stored energy can be utilized at higher loads, normally in a short time to the end-users. The energy source that supplies the system has to be dimensioned to meet a desired base load for the TES [15].

Energy redistribution from TES can be utilized in many different ways. For a building, the energy demand that has to be met during daytime can be stored in a TES. This can be loaded overnight and supplied to the building during daytime to meet the required energy demand. For a solar-driven system, the energy from solar radiation can be stored during the day and then used at night.

There are, in general, three different ways of storing this energy: sensible heat storage, latent heat storage, and thermochemical energy storage. Sensible heat storage are storage methods that cause the storage medium to decrease or increase in temperature. Latent heat storage stores or extracts energy by changing the phase of the storage medium [14]. Latent storage mediums are called "phase change materials". Thermochemical energy storage uses a chemical interaction to store and release energy.

2.2.1   Sensible Heat Storage

In a sensible TES, the temperature of the medium of storage is increased by energy transferred to the medium. The internal energy is influenced by the added energy, which increases the temperature of the storage medium.

Sensible heat storage mediums can either be solid materials, such as rocks, bricks, etc. or liquids, like water and oil. They can also be a mix of these, for example an oil/pebble-bed TES system. The selection of the right medium has to be done based on a set of criteria for the designated system. Design and technical requirements for the system, such as thermophysical properties, are relevant. The lifespan of the medium and behaviour over time are also important factors when choosing the correct medium. A heat transfer fluid (HTF) can be used. The HTF needs good thermodynamic properties and should work in the temperature range of the system.

Packed-bed Storage   Packed bed storage uses the heat capacity of a loosely packed material to store energy. A HTF, like air or oil, flows through the material to add or extract energy [16]. These systems are suitable for solar power plants

due to their ability to store heat at high temperatures. Amongst the typical materials are ceramic bricks, alumina pebbles, or rock. Rock is easily attainable and cheap, but its use is made more complicated by the fact that they are typically comprised of various minerals that likely have different thermal expansion coefficients, heat capacities, and thermal conductivities. Thermal expansion may lead to local stresses at higher temperatures, causing the rocks to break. The composition and orientation of the grains in the rock will influence the magnitude of these stresses.

Sedimentary rocks will probably not be suitable for storage at high temperatures (around 500 °C), as they are formed by high pressure, not temperature. They may undergo thermally induced reactions at high temperatures, causing the layers to separate from one another. Sedimentary rocks may, however, still be useful as thermal storage at lower temperatures. To prevent the rocks from fracturing, one should choose those with adequate properties and avoid heating them at a rate greater than 1-2 °C/min [17].

Specific heat capacity C_p is the energy that is required to increase the temperature by one unit for a given unit of mass of a fluid. Thermal capacity is the specific heat capacity multiplied by the density, as seen in Equation (2.10). This is a useful measure when applied to rocks, as it shows energy capacity per volume unit. For most minerals, the thermal capacity is equal to 2.3 J/cm^3/K ±20% [18]. This means that, if density is known, the heat capacity can be estimated with good confidence.

$$C = C_p \rho \tag{2.10}$$

The specific heat capacity of rocks increases quite rapidly when increased from 0 °C to 400 °C. After 400 °C, the rate of increase occurs more slowly. The specific heat capacity of a rock bed can be calculated with:

$$C_{p(mixture)} = (1 - \phi)C_{p(solid)} + (\phi)C_{p(oil)}, \tag{2.11}$$

where ϕ is the mass fraction $mass_{oil}/mass_{total}$.

2.2.2 Stratification

Thermal energy storage systems with two tanks are very common in concentrating solar power plants. Using thermal stratification makes it possible to use a single tank system, which is cheaper. Thermal stratification means that the fluid in the tank is arranged in different temperature layers. This is due to gravity and the buoyancy effect: low density of the warmer fluid causes them to rise to the top of the tank, while the heavier, colder fluid settles to the bottom. Thermal stratification is a phenomenon that is often taken advantage of in thermal energy storage tanks. Comparisons between fully mixed water tanks and fully stratified tanks for solar utilization systems show that stratification increases the efficiency of the system [19, 20].

The temperature stratification zone (the area between the hot and the cold fluid) is called the thermocline. The thermocline zone moves downward when charging the tank and is pushed upward while discharging [21]. A highly stratified tank will have a thin thermocline zone, while a moderately stratified tank has a thicker zone, as can be seen in Figure 2.2. The primary factors contributing to loss of stratification and the subsequent degradation of stored energy are: heat losses to the environment, conduction from the fluid in the hot part of the storage to the cold part, and mixing during charging and discharging [22].

Mawire and Taole have evaluated different parameters describing thermal stratification. They discovered that the temperature distribution along the height at different time intervals, along with the stratification number, adequately describe thermal stratification. The stratification number, 2.12, is defined as the ratio between the mean and maximum temperature gradients for the charging or discharging process [23].

$$Str(t) = \frac{(\partial T / \partial y)_t}{(\partial T / \partial y)_{max}}, \tag{2.12}$$

where the temperature gradient is defined as

$$\frac{\partial T}{\partial y} = \frac{1}{j-1} \left[\sum_{j=1}^{j-1} \left(\frac{T_{j+1} - T_j}{\Delta y} \right) \right], \tag{2.13}$$

where j is the number of nodes and Δy is the distance between these nodes.

(a) Highly stratified   **(b)** Moderately stratified   **(c)** Fully mixed
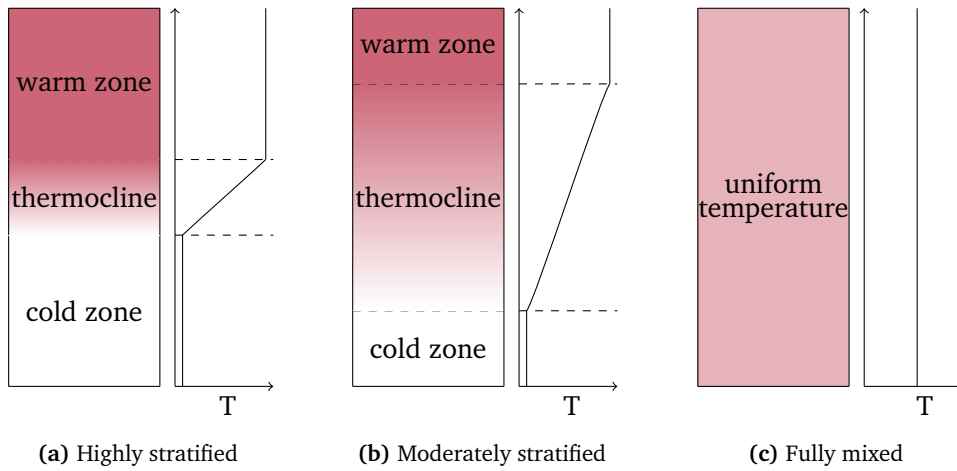
Figure 2.2: Different levels of stratification within a storage tank with equivalent amounts of stored energy.

2.2.3 Available Energy

Energy analyses are often based on the first law of thermodynamics and neglect the variation in quality of the energy. Losses and inefficiencies are, therefore,

generally not realistically evaluated [24]. Although energy cannot be created or destroyed, it can degrade in quality and eventually reach a state of equilibrium with the surroundings. This will cause it to become inadequate to perform tasks, as acknowledged by exergy analysis. Taking this into account when designing a TES system is, therefore, crucial. The objective is to recover as much of the stored thermal energy as possible, with little loss of temperature. Exergy, often called the "available energy", takes into account the quality of the energy [22].

The thermal energy of the system is expressed as

$$Q = mC_p(T_m - T_0), \tag{2.14}$$

where T_m is the average temperature along the height h_y of the tank, T_0 is the reference-environment temperature, and m is the mass of the storage fluid. The C_p of the storage fluid and T_0 are assumed constant. As T_m is the average temperature, it is equal to the temperature at any height for the fully mixed case, as this case has a constant temperature across the entire height h. Due to conservation of energy, T_m is then the same for both a mixed and thermally stratified tank.

The exergy can be expressed as

$$E_X = Q - mC_p T_0 ln(\frac{T_e}{T_0}), \tag{2.15}$$

Where

$$T_e \equiv exp[\frac{1}{H}\int_0^H lnT(h_y)dh_y] \tag{2.16}$$

for a tank with height H, where the temperature varies with height h. Note that $T_e = T_m$ only when the tank is fully mixed. The thermal energy Q is, by the principle of conservation of energy, the same for a fully mixed tank as for a stratified tank, while the exergy E_X is different between two such tanks of the same Q. A stratified tank will have higher exergy (available energy) than a mixed tank [22].

2.3 Solar Radiation and Power

Solar radiation is a term that covers all forms of radiant energy originating from the sun which is incident on the earth's surface. Solar irradiation is the sum of this energy during a given time period and is measured in kWh/m^2. Solar irradience is the instantaneous energy received by a surface, measured in W/m^2. These measurements are often hourly averages. Radiation on the earth's surface varies with location, season, time of day, local weather, and landscape. When the solar rays pass through the atmosphere, some are absorbed or reflected by obstacles such as clouds, air molecules, or dust, producing so-called "diffuse solar radiation". The radiation that reaches the earth's surface without being diffused is called direct

solar radiation. The sum of the diffuse and direct solar radiation is called global solar radiation [25].

(a) Global horizontal irradiation   **(b)** Photovoltaic power potential
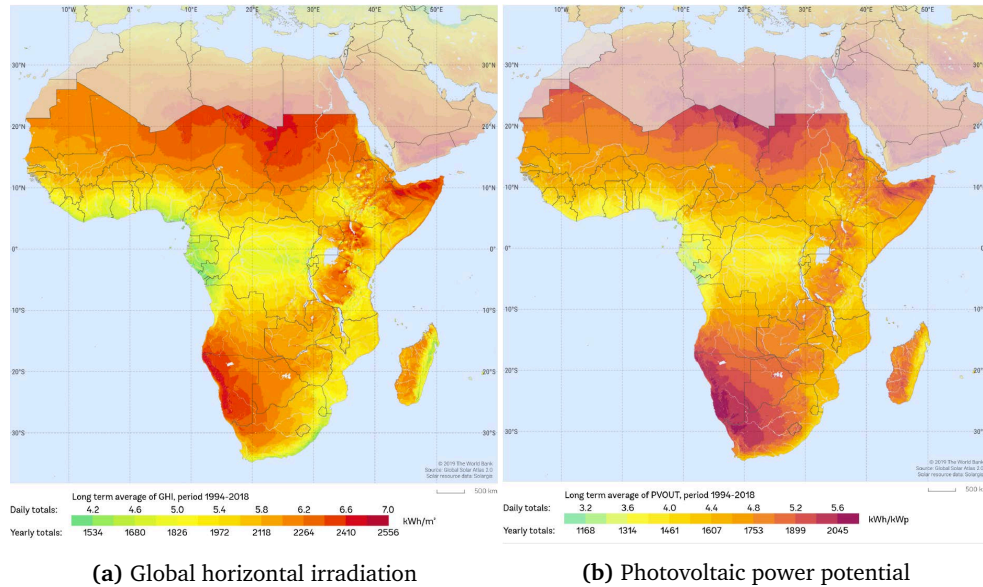
Figure 2.3: Average GHI and PV power potential in Sub-Saharan Africa. [26]

There are two types of solar power systems: photovoltaics (PV) and concentrating solar power (CSP). PV turns the radiation into electricity, while CSP turns the radiation into heat, which can also be converted into electricity. PV's are used in solar panels [27]. The International Renewable Energy Agency has reported that the price for solar PV modules has decreased by 80% during the last decade. The installed capacity has also grown massively within the same period. PV technology provides an opportunity for countries and communities to develop or transform their energy infrastructure in a more environmentally friendly way [28].

The PV power potential in Sub-Saharan Africa has been calculated by using the global horizontal irradiation (GHI) in a study funded by The World Bank [28]. The GHI is the sum of the diffuse and direct irradiation received by a horizontal surface. The GHI is used as a theoretical potential and has been modulated by local temperature, atmospheric pollution, and other geographical factors. It is to be noted, however, that it is still a simplified approximation. For example, the equatorial belt has less potential due to the frequent cloud cover. As well as taking into account the GHI, the PV power potential study has also accounted for the effects of temperature on the system performance, system configuration, shading, topographic, and land-use constraints. The results were presented in kilowatthours per installed kilowatt-peak of the system capacity [26]. The GHI and PV power potential can be seen in Figure 2.3. By studying the figure, one can see that most of Sub-Saharan Africa has a PV power potential of 4-5.6 kWh/kWp per day, meaning

that, in one day, a PV system with a capacity of 1 kW produces, on average, 4-5.6 kWh of electricity. As a reference, southern Norway (up to a latitude of 60°) has an average PV power potential of 2.76 kWh/kWp per day, which naturally varies with the season [28]. Fact sheets from this study for Norway and Tanzania can be found in Appendix D.

A study concerning the optimum tilt angle for solar panels in different latitudes [29] concludes that, for small values of latitude, the optimum annual tilt angle is close to the latitude value itself. For higher values of latitude, however, the optimum annual tilt angle is smaller than the latitude. Climate conditions may also have a considerable influence and should be included when selecting the optimum tilt angle.

2.4   Solar Cookers

Direct solar radiation is thought to be one of the most prosperous energy sources in many parts of the world. Solar cookers enable the use of solar radiation for cooking. There exist many different types of solar cookers, which can be divided into two main categories: those with and without storage capabilities [30].

2.4.1   Solar Cookers without Storage

Solar cookers without storage have two categories: direct and indirect. The direct solar cookers immediately apply solar radiation to the cooking process, such as the box-type and concentrating-type cookers. The box-type cooker is an insulated container with a glass cover to utilize the greenhouse effect. The concentrating-type cooker, on the other hand, uses multiple mirrors to concentrate the solar ray on a specific point. Both of these these types of direct methods are commercially successful, although the popularity of the hot box has been declining gradually from 1982 to 2000 (in India) [31]. An indirect solar cooker has a pot displaced from the solar collector and a heat transferring medium to redirect the energy to the pot. The main disadvantage of solar cookers without storage (whether direct or indirect) is that they can only be used during the day when sunlight is readily available [30].

2.4.2   Solar Cookers with Storage

To solve the problem of cooking outdoors and the impossibility of cooking when there are clouds or during off-sunshine hours, a thermal energy storage can be used. Many of the concepts without storage can also be used with a storage, like the hot box. The energy storage can be latent or sensible heat storage system. Typical storage mediums for sensible heat storage-type solar cookers are sand, engine oil, or vegetable oil [30].

Figure 2.4: Flat-plate solar cooker with heat storage installed in an elementary school in Chile [32].

An example of a solar cooker with storage is the flat-plate solar cooker developed by Schwarzer and Silva [32], which consist of one or more flat-plate collectors with a coated absorber, a storage tank, cooking pots, oil as a heat storage medium, and manually controlled valves to guide the oil to the storage tank or cooking pots. An example of the system can be seen in Figure 2.4. The oil used is usually vegetable oil. About 250 of these systems were built, made in different sizes for use by families, as well as in schools and hospitals. The system showed very promising results, but the price to build the solar cooker is too high. This can only be reduced by manufacturing on a mass scale. Large-scale use of these solar cookers in developing countries will, therefore, not be possible without financial aid.

2.5 Vegetable Oils as Heat Transfer Fluid

Vegetable oils are renewable and biodegradable resources that can be used as heat transfer fluids (HTF), while also having low greenhouse gas emissions. They have good thermal properties and can be used for more applications than just food. They are highly available and can challenge conventional oils as an effective heat transfer medium and thermal oil [33].

For use in a TES, the vegetable oil should meet the criteria from Gomna *et al.*:

- Tolerate high temperatures.
- High density and heat capacity for thermal energy storage.
- High thermal conductivity for heat transfer within the fluid.
- Low viscosity to make the oil flow easily in the system.

- Low cost and high availability.
- Good environmental properties.

The thermal fluid should be stable within the operating temperatures of the system and be thermally stable, meaning that the oil can withstand permanent changes due to the effect of the heat. Many vegetable oils exhibit significant differences in composition after being exposed to heat over a period of time [33]. The main weakness of vegetable oils is the tendency to oxidize at high temperatures. The oil's level of resistance to oxidation has to be known before using it as a HTF. The level of oxidation often correlates to the smoke point, which is the point where the oil starts to destroy fatty acids and visible smoke is produced. Oxidation can change the quality of the oil and may change the thermophysical properties. For vegetable oils the smoke point is often between 230℃ and 250℃. A HTF should also have high heat capacity and thermal conductivity, allowing it to easily transfer heat to the receiving medium and, therefore, be effective as a thermal storage mechanism.

2.5.1 Thermophysical Properties of Oil

Soybean, rapeseed, and sunflower oils are the most applicable vegetable oils for a TES [33–35]. The thermophysical properties for these three vegetables oils are presented here, as well as the properties of the thermal fluid used in the experiments at the NTNU: Duratherm 630.

The specific heat capacity, the density, and the thermal conductivity are the most important properties that need to be considered when choosing a HTF. They are presented within the temperature range of 25 °C to 225 °C [36]. For Duratherm 630, the technical data sheet is used [37].

Table 2.1: Specific heat capacity $[C_p \ (\mathrm{kJ/kg} * \mathrm{K})]$

Temperature	Rapeseed	Soybean	Sunflower	Duratherm 630
25 °C	2.029	1.985	2.002	1.948
50 °C	2.074	2.042	2.078	2.030
75 °C	2.173	2.114	2.158	2.113
100 °C	2.283	2.185	2.230	2.195
125 °C	2.374	2.247	2.288	2.278
150 °C	2.435	2.299	2.331	2.360
175 °C	2.465	2.348	2.369	2.443
200 °C	2.482	2.408	2.417	2.525
225 °C	2.518	2.502	2.498	2.608

Table 2.2: Density [ρ (kg/m^3)].

Temperature	Rapeseed	Soybean	Sunflower	Duratherm 630
25 °C	911.5	915.0	910.8	862.2
50 °C	894.7	900.2	895.6	845.2
75 °C	878.0	885.4	880.4	828.2
100 °C	861.3	870.6	865.2	811.2
125 °C	844.6	855.8	850.0	794.2
150 °C	827.8	841.0	834.8	777.2
175 °C	811.1	826.2	819.6	760.2
200 °C	794.4	811.4	804.4	743.3
225 °C	777.6	796.6	789.2	726.2
$\frac{\rho_{25\,°C}}{\rho_{225\,°C}}$	1.172	1.148	1.154	1.187

Table 2.3: Thermal conductivity [k (W/m $*$ K)]

Temperature	Rapeseed	Soybean	Sunflower	Duratherm 630
25 °C	0.166	0.166	0.165	0.144
50 °C	0.162	0.163	0.160	0.143
75 °C	0.158	0.159	0.156	0.141
100 °C	0.155	0.155	0.152	0.140
125 °C	0.151	0.152	0.148	0.138
150 °C	0.149	0.149	0.145	0.137
175 °C	0.146	0.146	0.142	0.135
200 °C	0.144	0.143	0.140	0.134
225 °C	0.141	0.140	0.138	0.133

Chapter 3

Concept

In this chapter, the idea behind the concept of this master's thesis is presented. It is a simple system based on the theoretical concepts described in Chapter 2. As mentioned in Chapter 1, similar systems have been developed in earlier student projects. These systems have been large, containing several barrels. The goal for this project is to investigate the possibility of using a single oil barrel as a complete cooking solution with the ability to store thermal energy.

3.1 Description of the Concept

The purpose of this section is to describe the ideal behaviour of the system during operation.

The system is a cooking apparatus that can store thermal energy using power from a sustainable energy source for later usage. It consist of an oil barrel with a heating element inside and a cooker on top. The oil barrel is filled with oil and has an internal tube to guide the flow of the oil during use. The system utilizes the concepts of TES and thermal stratification to redistribute the energy captured. It is valuable to have a thermally stratified storage to get a TES with higher exergy.

The oil barrel should be of a manageable size, like 100 liter or 200 liter. In Figure 3.1, an overview of the system with its main components is displayed. Part 1 labels the heat storage compartment, which takes up most of the volume in the tank. The heat storage is both where the hot oil is kept after heating and where the colder oil accumulates after the cooker is used. Part 2 shows the position of the cooker with the desired initial oil level, which is at the bottom of the cooker. Part 3 is the funnel that directs the oil during operation. Part 4 shows the placement for the heating element inside the funnel tube.

During operation (charging and discharging), internal guidance of the oil is done by the funnel with natural convection as the driving force. The funnel consists of two parts: a tube and a chamber at the top. Throughout this thesis, the tube will be referred to as the funnel tube, the chamber at the top will be referred to as the top funnel, the top part of the chamber will be referred to as the funnel

wall, and the whole funnel will simply be referred to as the funnel. Inside the funnel tube there is a heating element. At the top there is a cooker.

Table 3.1: Main components of the system.

Part	Component
1	Heat storage
2	Cooker
3	Funnel
4	Heating element
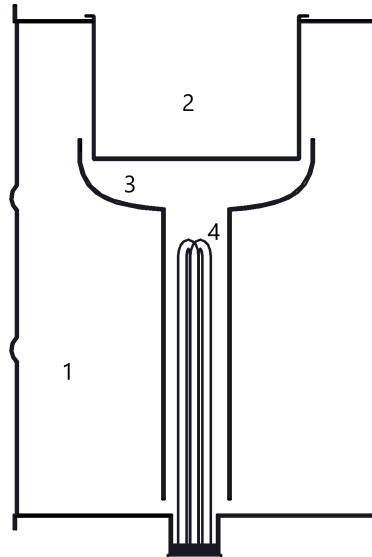
Figure 3.1: Overview of the different parts of the system.

In Figure 3.2, an illustration of the system during charging is shown. The initial oil level should be below the funnel wall. When the heating element is turned on, the oil inside the funnel will begin to heat and expand, as seen in Figure 3.2a. There should be no circulation in the tank as long as the oil level in the funnel is below the funnel wall. The oil will continue to heat and expand until it reaches the top of the funnel wall, as displayed in Figure 3.2b. At this point, the oil will begin to overflow from the funnel into the storage. Now there should be circulation of oil inside the tank and the storage is charged with warm oil. Ideally, this circulation should be very slow and lead to thermal stratification of the oil, with a thin thermocline in the storage compartment, as seen in Figure 3.2c.

A careful choice of overflow temperature is necessary. It should be between 200 °C and 220 °C to be below the smoke point for most vegetable oils. The overflow temperature can be controlled via the height of the funnel wall. The temperature of the oil inside the funnel should rise quickly because only a relatively small amount of oil is being heated. This hot oil can also be used for cooking during charging. The warm overflow temperature will result in hot oil accumulating at the top of the storage, thermal energy that can be used after being stored. This will work as a TES and the system should be designed to maximize the full potential of stratification from the warm overflow.

The temperature in the top funnel should stay constant after overflow until the storage is fully charged and the warm oil has reached the bottom of the storage. When warm oil reaches the bottom, the temperature in the funnel should increase and the system will be charged as if there were no funnel.

(a) Before overflow **(b)** Overflow **(c)** Overflow after some time
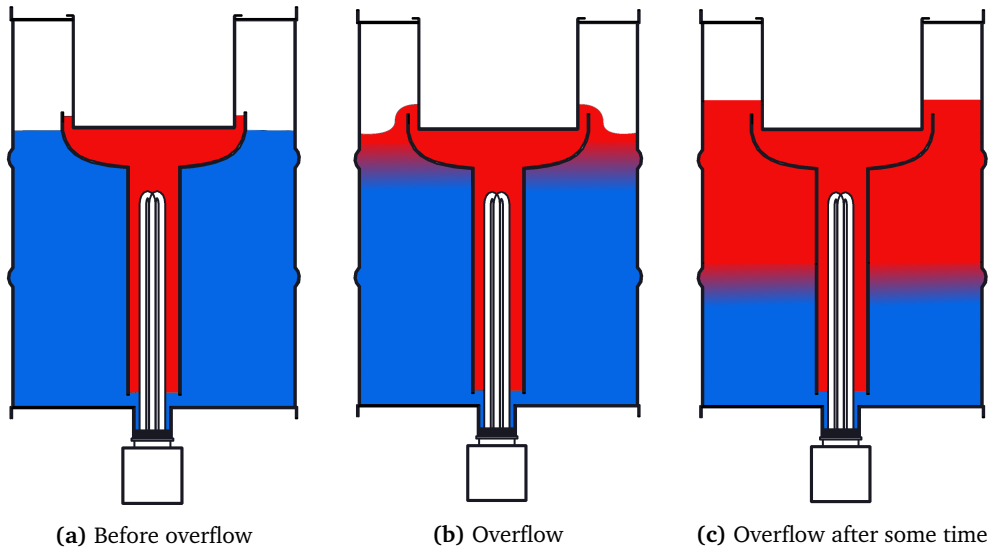
Figure 3.2: Illustration of how the system ideally should behave during charging.

(a) **(b)**
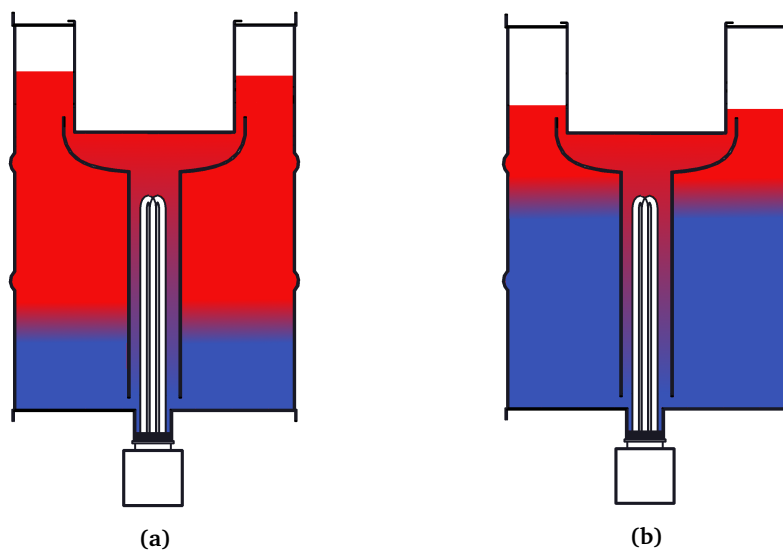
Figure 3.3: Illustration of how the system should ideally behave during dischar-ging.

The stored energy can be used to cook food. When the heating element is off and the system is being used to cook, the oil should flow the opposite way. The warm oil from the top of the storage should flow into the funnel, providing heat to the cooker. The used oil should then flow down the funnel into the storage from the bottom. There should be circulation of oil from the top storage to the cooker and then to the bottom storage. This will be referred to as discharging. In Figure 3.3 the discharging process is illustrated and Figure 3.3b shows how the system should look after being discharged for a while.

This system utilizes all the features of a modern TES, where there is a mismatch between energy supply and demand and where energy is stored (redistributed) for later use. The stored energy can be used when the energy source is not able to provide any sufficient energy to the end user. The effect of stratification is important for the system, and in Figure 3.4, an illustration of two systems with the same amount of energy is shown. In Figure 3.4b, there is no funnel and a relatively uniform heating of the oil. In Figure 3.4a, the funnel makes it possible to store energy through the use of stratification and a sharp thermocline. This means that the quality of the energy stored is higher compared to Figure 3.4b, where there is no funnel. The oil works as the storage medium. The heat capacity of oil is typically lower than water. The temperature difference between the warm oil and the cooker should, therefore, be as high as safely possible to ensure a high enough heat transfer, as indicated in Equation (2.2).

(a) **(b)**
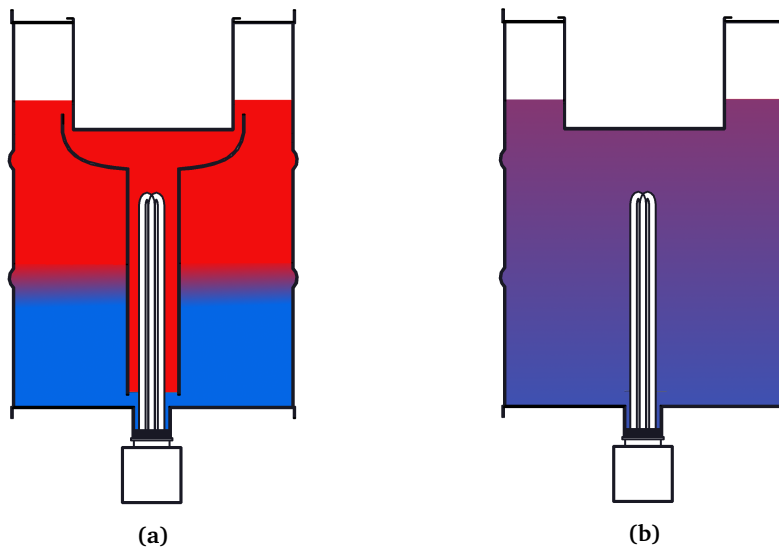
Figure 3.4: Illustration of the two systems charged with the same amount of energy, with and without a funnel.

3.2   System Designed in the Project Thesis

The initial work by S. Fjeldsæter and S. Stordal [34], a master thesis from the spring of 2020 can be seen in Figure 3.5a and is the basis for the system designed in the project thesis.

(a) Side view with dimensions in millimetres.   **(b)** Wireframe view of the design.
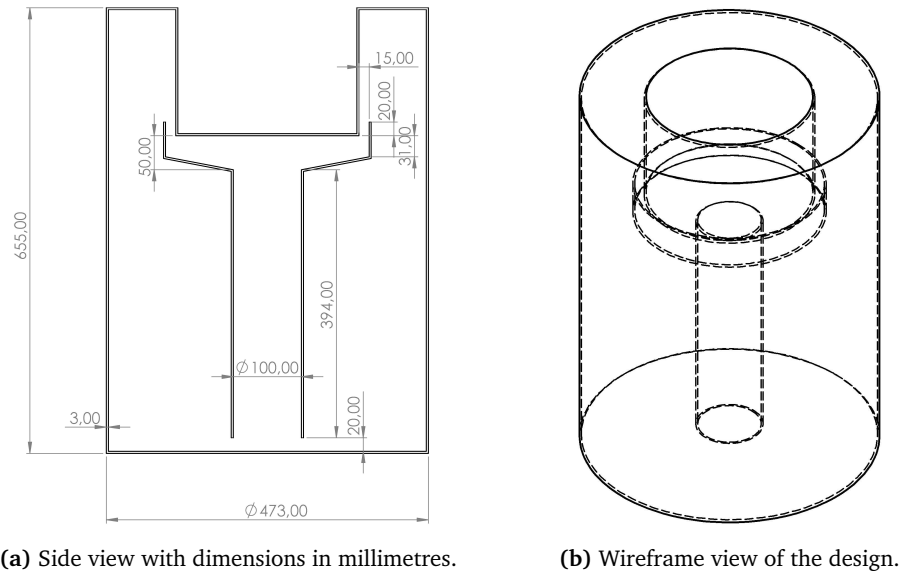
Figure 3.5: Sketch of the initial design.

The goal with this design was to have a simple and flexible design to test the concept. The system is built on a 100 liter oil barrel with a 10 liter cooker pot at the top with a diameter of 26 cm. The tank is designed to be filled with approximately 78 liters of oil, then it is room for the oil to expand with 12 liter, or about 15 %. Simulations done in the project thesis [1] showed that insulation around the funnel tube was not of great importance when charging with full power. The distance between the funnel wall and the cooker was also investigated and it was discovered that the boundary layer flowing down the cooker is thin, so a gap of 15 mm gives plenty of room for the oil to flow.

In Figure 3.6, CAD renders of the system made in the project thesis can be seen. The funnel is attached to the top of the tank with four support brackets. There are four sockets on the funnel to place the cooking pot. There is no insulation around the funnel tube. The tube itself has a diameter of 100 mm. After the system was built, it was insulated with Aerogel, with a thickness of 10 mm, and FyreWrap©, with a thickness of 50 mm at the side wall. Fyrewrap was used to insulate the bottom, covering the junction box to the heating element. The bottom had to be insulated a second time (explained in Section 4.6) so that the junction box was not covered. The area underneath the tank was then insulated with Aerogel with a thickness of 15 mm. The insulation was kept in place with aluminum foil and insulation tape. The insulated tank can be seen in Figure 3.7a.
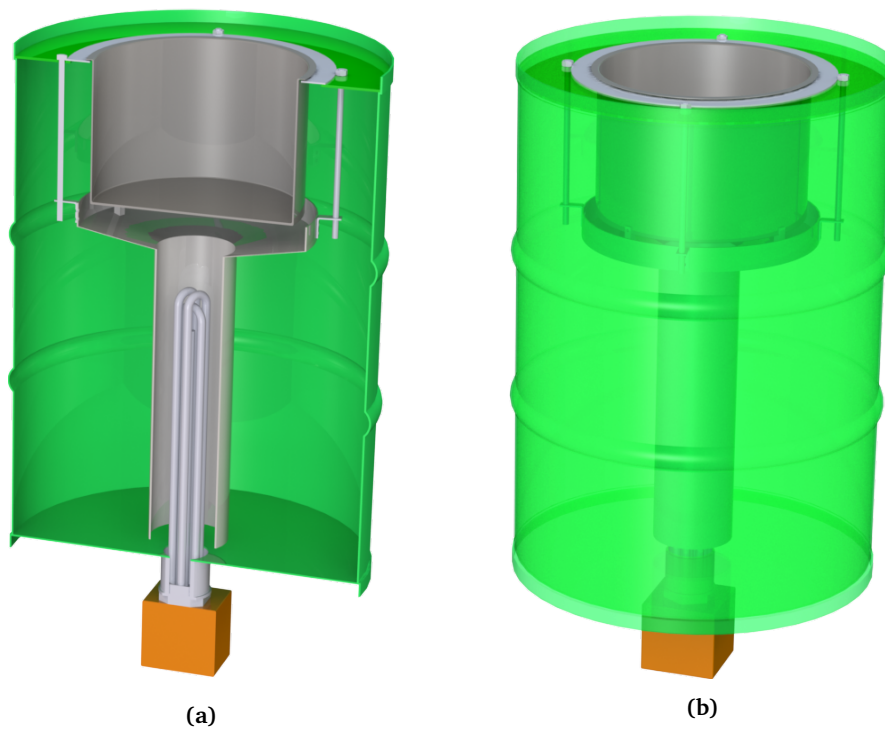
Figure 3.6: SolidWorks render of the system made in the project thesis. In Figure 3.6a there is a half-view of the system and in Figure 3.6b the barrel is a transparent view.

Heating Element   The heating element is 30 cm long and has a diameter of 45 mm. Maximum power for the heating element is 1800 W. The power of the heating element can be regulated by using a transformer, where the output voltage is changed.

Explanation of Terms   For the rest of the thesis the following terms will be used: When referring to the system, the tank with the funnel and the heat storage medium (oil/rocks), the insulation around the tank and the heating element is referred to as a unit. When referring the tank, the tank with the heat storage medium (oil/rocks) is referred to as a unit.
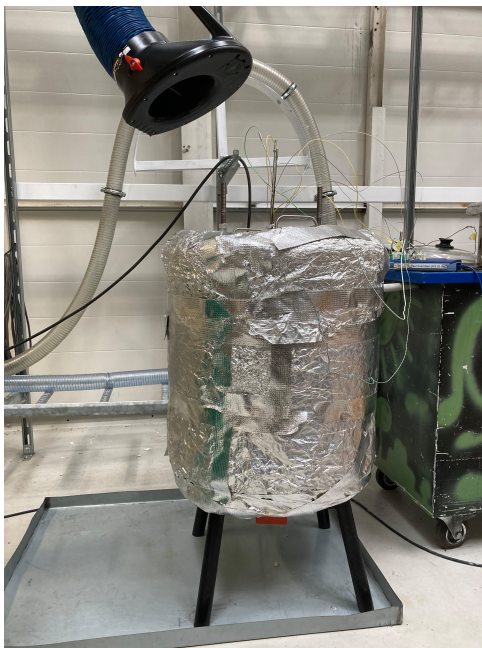
(a) The system with insulation and the extractor fan above.

(b) The transformer used to change the voltage.

Figure 3.7

Figure 3.8: The heating element.

Chapter 4

Experiments with Initial System

Using the system previously built, experiments have been conducted to determine its efficacy. The motivation for conducting the experiments, methodology, and results are presented in this chapter. A short discussion is presented, followed by suggestions for the improved design.

The experiments in this chapter include the following bullet points from the outline discussed in Section 1.1:

- Temperature measurements of the moving thermocline during charging and discharging (cooking).
- Charging experiments with different power levels to determine if insulation is needed on the internal funnel.
- Cooking experiments at different charging levels of the storage.

4.1   Motivation for the Experiments

The goal with the experiments is to validate the concept and understand the fluid flow and heat transfer in the system. Based on this, the system can be further developed.

To validate the concept, the effect of the funnel must be investigated. The funnel should provide significant improvements when it comes to heat storage and cooking compared to a system without a funnel. It is of interest to investigate if the funnel leads to thermal stratification of the oil in the storage. A stratified storage would be beneficial, as more energy can be extracted from a thermally stratified system.

A requirement for this design is the ability to cook while charging the system. To analyze the effectiveness of the funnel, water will be heated while simultaneously charging the system.

The effect of reduced power to the heating element is also of interest due to the fluctuating access to energy that might occur when using renewable energy sources. It is, therefore, of interest to study the system's behaviour when being charged with reduced power. Rapid heating of the oil in the funnel is desired

even under reduced power. The need for insulation around the funnel in such circumstances will, therefore, be investigated.

The heat loss of the system to the surroundings during the still phase (without charging and discharging) will also be investigated. It is important to have an accurate assessment of the heat loss to reduce it as much as possible.

Due to safety concerns, the system must be closed if it is to be used outside of the laboratory, which requires the cooker pot to be fixed at the top of the tank. It should, however, also be easy to clean the cooker. Different cooker solutions should, therefore, be investigated to find a solution that is both safe and hygienic.

4.2 Experimental Setup

4.2.1 Method

Charging and discharging experiments are conducted by changing one parameter at a time (initial oil temperature, initial oil level, power to the heating element, and the cooker) to ensure a systematic and scientific procedure.

Charging The charging experiments have been conducted by using power from the electrical network. These experiments use both the maximum power of the heating element (1800 W) and the system under reduced power (500 W). For the experiments with reduced power, the power to the heating element has been regulated using the transformer from Figure 3.7b. The transformer is set to an output voltage of 121 V, resulting in 500 W output to the heating element. The Norwegian electrical network has an output voltage of 230 V.

To test the effect of the funnel, experiments have been conducted with initial oil level below and above the funnel wall. There will be circulation from the start when the initial oil level is above the funnel wall. This can be assumed as a system without a funnel. With the initial oil level below the funnel wall, the effect of the funnel as a barrier is tested. There is approximately 78 liters of oil inside the tank when the oil is leveled with the top of the funnel wall. The amount of oil is not changed when conducting the experiments, but it has been changed between some experiments to get an adequate overflow temperature. Vegetable oil has been replaced with Duratherm 630 for all the experiments conducted at NTNU, the thermophysical properties of Duratherm 630 is similar to vegetable oil as described in Section 2.5.1.

The experiments started with oil at ambient temperature will be referred to as initial cold. Experiments started at higher temperatures due to stored heat from previous use will be referred to as initial warm.

Charging experiments have been done with and without water in the cooker. The cooker is insulated in the experiments without water and referred to as insulated cooker. This means that insulation is inserted inside the cooker pot, which is inserted into the tank as seen in Figure 4.1a. For the experiments with water in

(a) Insulated cooker.

(b) Water in the cooker with a lid.
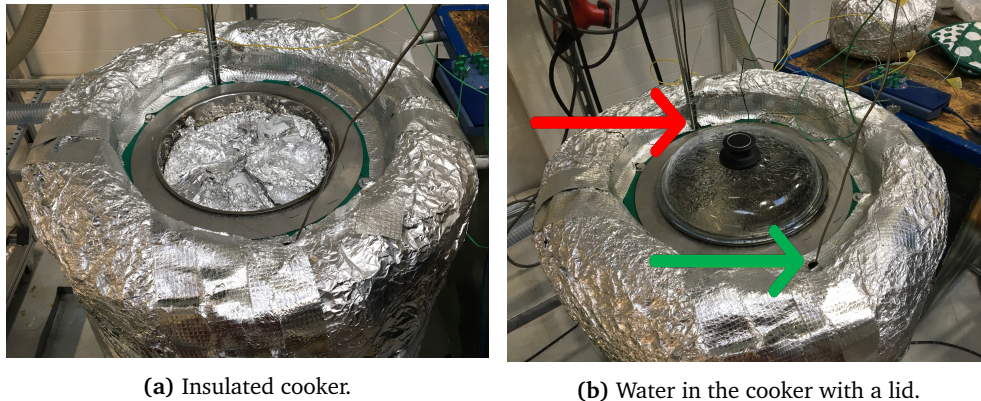
Figure 4.1: The cooker. In Figure 4.1b the red arrow shows the hole for the rod with thermocouples. The green arrow shows the hole for the thermocouple used to measure the front.

the cooker, as seen in Figure 4.1b, water at ambient temperature has been added to the cooker before the charging started. Water was chosen to be used in the experiments since it is easy to measure. The energy required to heat water represent the energy required to cook food with high content of moisture, like fresh beans and sweet potatoes [4].

To avoid overheating, a safety temperature of 220 °C has been set, meaning that the charging is stopped when one of the thermocouples reaches 220 °C. This temperature is close to the smoke point of vegetable oils, which is why it has been chosen. The limit has been exceeded on purpose for some experiments, up to 230 °C, because the overflow temperature has been at bit higher and there has been good momentum with the experiment.

Discharging Discharging experiments have been conducted by charging the system until the safety temperature is reached, then turning the heating element off and pouring water into the cooker. The time it takes for one thermocouple to reach the safety temperature is dependent of the overflow temperature and the initial oil level, the amount of stored energy in the system will, therefore, vary. For most discharging experiments, it has been attempted to have the same temperature at the top storage when the experiment begins, around 200 °C - 210 °C.

Different cooking solutions have been tested during discharging, by trying three different pot-configurations. One by directly heating water in the cooker pot submerged into the tank, which is referred to as single pot. One by boiling water in a pot inserted into the cooker pot, referred to as pot-in-pot with air in between. One by having Duratherm 630 oil in between the pots in the pot-in-pot solution, referred to as pot-in-pot with oil in between. There is enough oil in between the pots to ensure that there are no air gaps between the pots ensuring good heat transfer in the pot-in-pot with oil solution.

In all the experiments presented, water at ambient temperature ($\approx$20 °C) has been heated in the cooker and a lid has been used.

Thermocouples For these experiments, type K Thermocouples have been used, which have an accuracy of about +/- 2.2 °C or +/- .75%°C, depending on which is greater [38]. The thermocouples are plugged into a Pico Data Logger, which is a PC-based thermocouple, temperature data logger. The software used is PicoLog 6 [39].

Five thermocouples were placed at fixed positions in the system. This is to ensure that all the data from these thermocouples are consistent. Three thermocouples were placed in the storage of the system: one at the bottom, one in the middle, and one at the top (2 cm, 23 cm, and 43 cm from the bottom of the storage respectively). They were fixed to a rod that was inserted into the storage from a hole at the top of the system (see the red arrow in Figure 4.1b). Attached to the same rod, two thermocouples were placed to measure the temperature at the top of the funnel and close to the heating element. The placement of the thermocouples can be seen in Figure 4.2.

To measure the temperature profile in the storage, a hole was made opposite of the other, represented by the green arrow in Figure 4.1b. A thermocouple could easily be moved up and down in this hole without interfering with the measurements of the other thermocouples. The profile was measured every 15 minutes during the experiments. The thermocouple was moved from the bottom to the top of the storage, measuring the temperature every 9-10 centimeters. It was held still for 15 to 30 seconds at each interval to get stable readings.
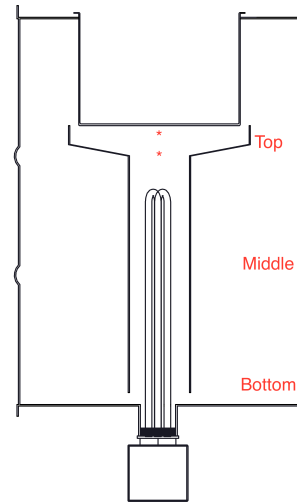
Figure 4.2: Approx placement of thermocouples.

4.3 Overview of the Experiments Conducted

Three different sets of experiments have been conducted, referred to as "test sets". Multiple experiments have been conducted in each test set. They have been categorized this way to get a better overview of the experiments.

Experiments with different initial oil temperatures and levels have been conducted within each test set. This has been done to study the impact that the change of these parameters has. Using the system for two days in a row will result in an increase of initial oil level and temperature by the second day. The column labeled "Initial oil level on funnel wall" in the tables 4.1, 4.3 and 4.4, indicates the height of the oil inside the tank relative to the funnel wall at the beginning of the experiments.

4.3.1 Test Set 1

The charging experiments were conducted with full power (1800 W) and an insulated cooker. The experiments can be seen in Table 4.1.

Discharging experiments were also done. Some of the discharging experiments in Test Set 1 were not able to boil. A lid was, therefore, bought for use in Test Set 2. The results from discharging in Test Set 1 are, therefore, not presented nor discussed.

Nº	Initial oil temperature	Initial oil level on funnel wall	Top heated to	Heating time
1	20 °C	Bottom	220 °C	250 min
2	21 °C	Bottom	220 °C	250 min
3	27 °C	Bottom	220 °C	230 min
4*	21 °C	Bottom	-	60 min
5	90 °C	Just above bottom	230 °C	245 min
6	50 °C	Middle	210 °C	215 min

Table 4.1: Overview of charging experiments done in Test Set 1. Charging 4* was done to test the height rings and is explained later.

4.3.2 Test Set 2

In Test Set 2, the cooker was tested both during charging and discharging. The three different cooking solutions were tested with one liter of water to find the effectiveness of the different solutions. The different cooking solutions are illustrated in Figure 4.3. The results are seen in Table 4.2.

Charging was done with full power and five liters of water using the pot-in-pot solution with oil in-between (Figure 4.3b) .These experiments can be seen in Table 4.3.

(a) Single pot   **(b)** Pot-in-pot with oil in-between.   **(c)** Pot-in-pot with air in-between.
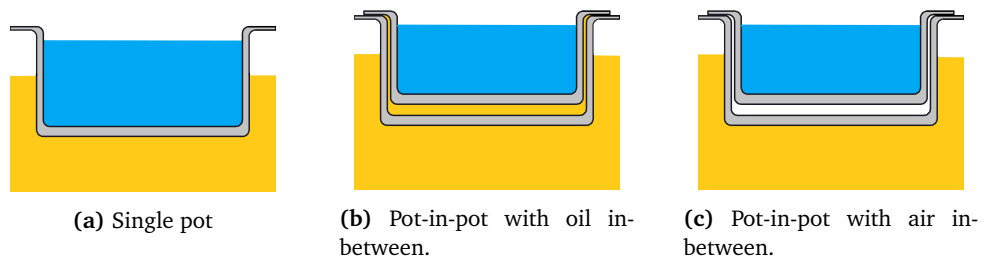
Figure 4.3: The three different cooking solutions tested.

№	How	Initial oil temperature: top	Initial oil temperature: bottom	Initial water temperature	Time for water to boil
1	Pot-in-pot	210 °C	190 °C	19 °C	25 min 20 sec
2	Pot-in-pot with oil	210 °C	168 °C	20 °C	9 min 41 sec
3	Single pot	210 °C	180 °C	20 °C	3 min 48 sec

Table 4.2: Overview of discharging experiments done in Test Set 2, heating up one liter of water from fully charged system.

№	Initial oil temperature	Initial oil level on funnel wall	Initial water temperature	Time for water to boil
1	21 °C	Bottom	19 °C	118 min
2	21 °C	Above	15 °C	160 min
3	100 °C	Middle	16 °C	105 min
4	26 °C	Bottom	20 °C	75 min

Table 4.3: Overview of charging experiments done in Test Set 2.

4.3.3 Test Set 3

Test Set 3 was done to test how the system behaves when it is being charged with reduced power (500 W). Experiments with both an insulated cooker and five liters of water with the oiled pot-in-pot were done in this test set. These can be seen in Table 4.4.

№	Initial oil temperature	Initial oil level on funnel wall	Initial water temperature	Time for water to boil
1	100 °C	Middle	-	-
2	25 °C	Bottom	-	-
3	60 °C	Right above bottom	21 °C	268 min
4	25 °C	Bottom	19 °C	> 440 min

Table 4.4: Charging experiments done in Test Set 3. Experiment 1 and 2 were done with insulated cooker.

4.4 Results and Discussion

4.4.1 The Effectiveness of Different Cooker Solutions

The three different discharging experiments in Test Set 2 were conducted in order to study the loss of heat transfer by the use of a pot-in-pot solution for cooking. One liter of water was heated from ambient temperature with the three different

cooking solutions and the time it took for it to boil was measured. Obtaining exactly the same temperature at the bottom of the storage proved difficult, but this difference will likely not affect the results of the experiments due to the short time periods involved.

Cooker	Time till boil	Average Power	Power reduction
Single pot	3 min 48 sec	1455 W	-
Pot-in-pot with oil between	9 min 41 sec	571 W	61 %
Pot-in-pot	25 min 20 sec	218 W	85 %

Table 4.5: The results from the three different cooking solutions.

The results from the experiments can be seen in Table 4.5. The single pot provides the best heat transfer from the oil to the water. There is a significant loss in efficiency from the single pot solution to the dry pot-in-pot solution. Having oil in-between the pots improves the pot-in-pot solution quite drastically, due to the thermal conductivity of oil being so much higher than that of air. As a result, all the cooking experiments presented in the remainder of this thesis are done with the pot-in-pot solution with oil in-between.

4.4.2 The Effect of the Funnel

Experiments 2 and 4 from Table 4.3 are compared in this section. Experiment 2 was done with initial oil level above the funnel wall to introduce circulation from the start of the experiment, representing a system without a funnel as a barrier. This is referred to as "without funnel". Experiment 4 was done with the initial oil level below the funnel wall, referred to as "with funnel". These experiments were conducted to investigate which contribution the funnel makes during charging. They were done with initial cold oil and with five liters of water in the pot while charging.

A problem with the charging experiments conducted in Test Set 2 is that the funnel walls are not high enough for the initial oil level to touch the cooker. This means that there is reduced heat transfer from the oil to the cooker in the start of the experiment. The problem is further explained in Section 4.4.6.

Figure 4.4a shows the temperature in the top funnel for both experiments, while Figure 4.4b shows the temperature in the top storage. There is a significant difference between the temperature development in the two experiments. In the experiment with a funnel, the temperature in the top funnel increases rapidly after the heating element is turned on, reaching 170 °C in 20 minutes. The temperature at the same thermocouple, after 20 minutes, is just 40 °C in the experiment without funnel. The water in the pot started to boil after 75 minutes with the funnel, while 160 minutes were required without the funnel. There is a small deviation in initial oil and water temperature, which is believed to make little difference for the end result. However, the difference in oil level is significant. The experiment

(a) Top funnel
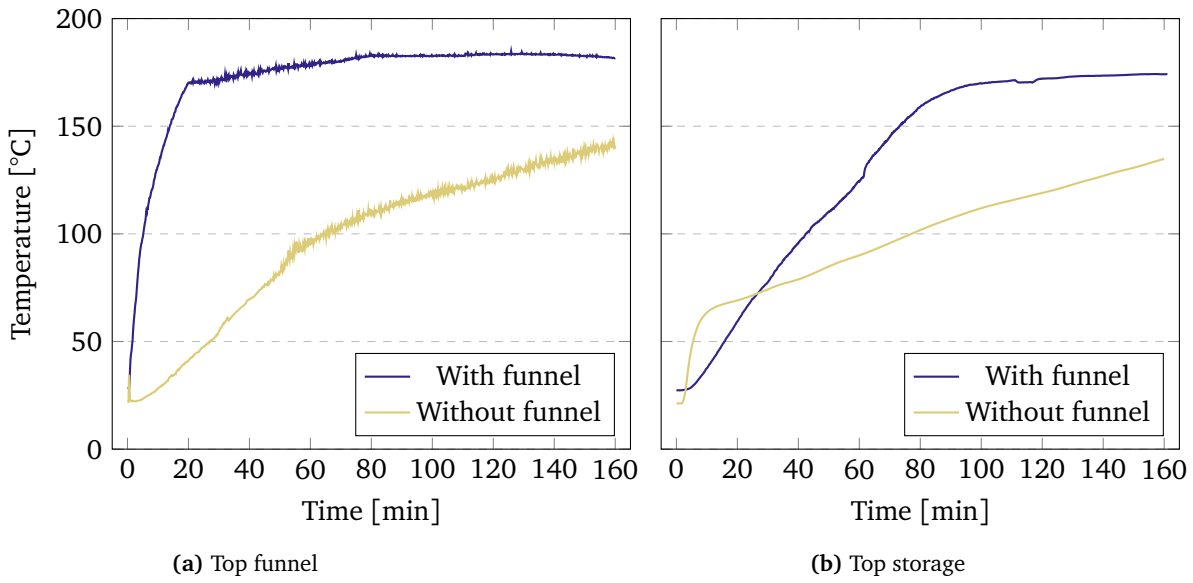
(b) Top storage

Figure 4.4: The temperature in the top funnel and in the top storage during charging with five liters of water in the cooker, experiment 2 (without funnel) and experiment 4 (with funnel) from Test Set 2.

(a) With funnel
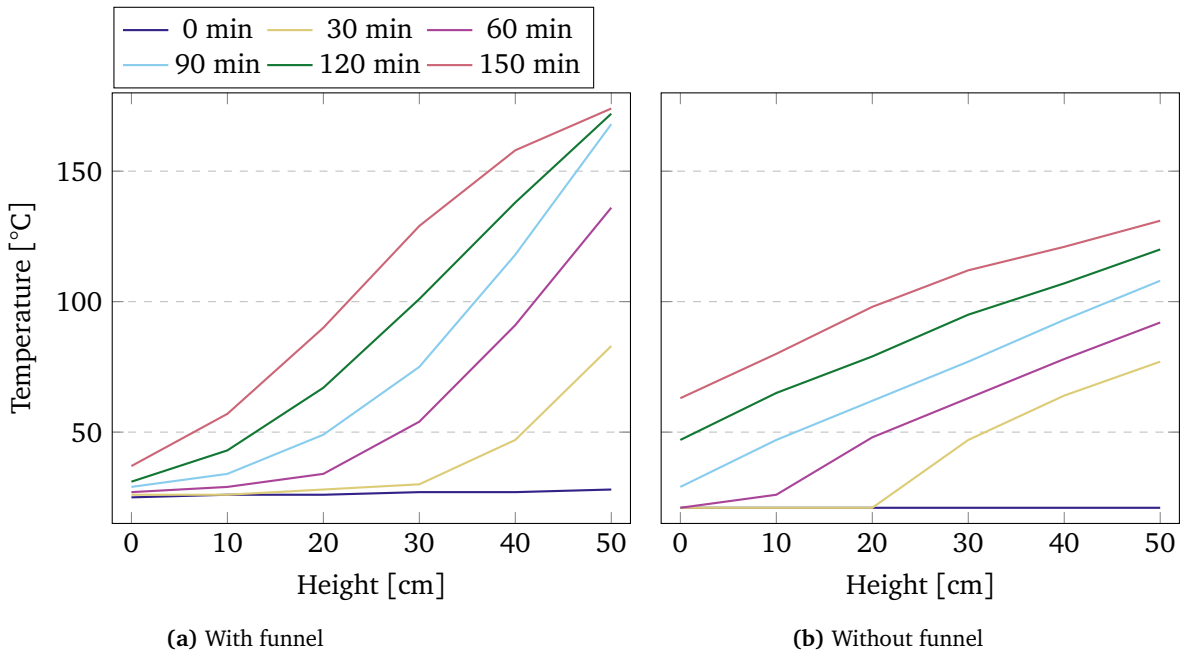
(b) Without funnel

Figure 4.5: Temperature in the storage during charging from experiment 2 (without funnel) and experiment 4 (with funnel) from Test Set 2.
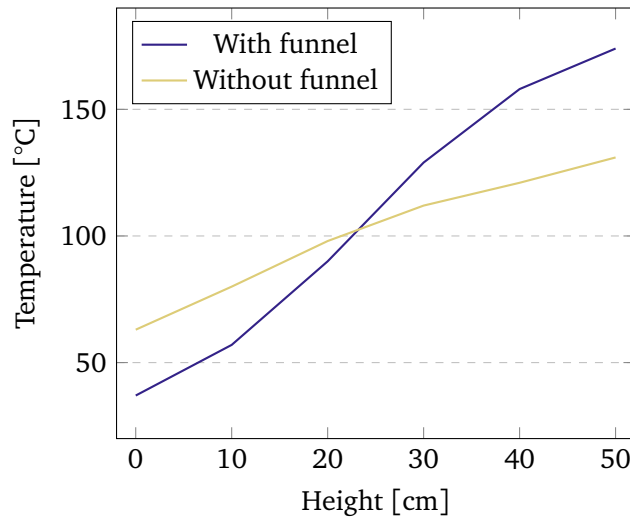
Figure 4.6: Temperature in the storage after 150 minutes from experiment 2 (without funnel) and experiment 4 (with funnel) from Test Set 2.

without the funnel has an initial oil level that touches the bottom of the pot, which is advantageous since direct heat transfer will take place right from the start. The experiment with the funnel does not have contact from the start. If both experiments started with the same configuration (either with or without contact), then the difference in time for the water to boil would likely be even bigger than the 85 minutes found in these experiments.

Figure 4.5 shows the temperature in the storage every half hour for both experiments. It can be seen that the funnel leads to an abrupt temperature increase in the top storage, while the temperature in the bottom storage hardly increases during the experiment. The oil temperature increases linearly in the experiment without a funnel, where the circulation from the start results in a gradual heating of the storage. Figure 4.6 shows the temperature profiles in the storage for both experiments after 150 minutes of charging. The experiment with a funnel had a temperature difference of 137 °C between the bottom storage and the top storage, while the experiment without had a temperature difference of 68 °C. It is clear that having a funnel results in better thermal stratification in the storage.

The results above correspond well to the concept presented in Section 3.1. Heating up a small amount of oil inside the funnel not only makes it possible to start cooking earlier than without having a funnel, but also results in a more thermally stratified TES.

4.4.3   The Effect of Stored Thermal Energy

From the first experiments done in Test Set 1, it was discovered that the initial temperature of the oil affected the system's behaviour during charging. Experiments 1 and experiment 5 from Table 4.1 were conducted with the same amount

of oil inside the tank, with the only difference being the initial oil temperature. This means that no oil was added or removed from the tank between the two experiments. Experiment 1 was done with the initial oil level at the bottom of the funnel wall with an oil temperature of 20 °C, referred to as "initial cold". Experiment 5 was done the day after, with the only difference being a higher initial oil temperature resulting in a higher initial oil level. This is due to the expansion illustrated in Figure 4.7 and is referred to as "initial warm". The average initial temperature was 86 °C for the warm oil.

(a) Cold oil   **(b)** Warm oil
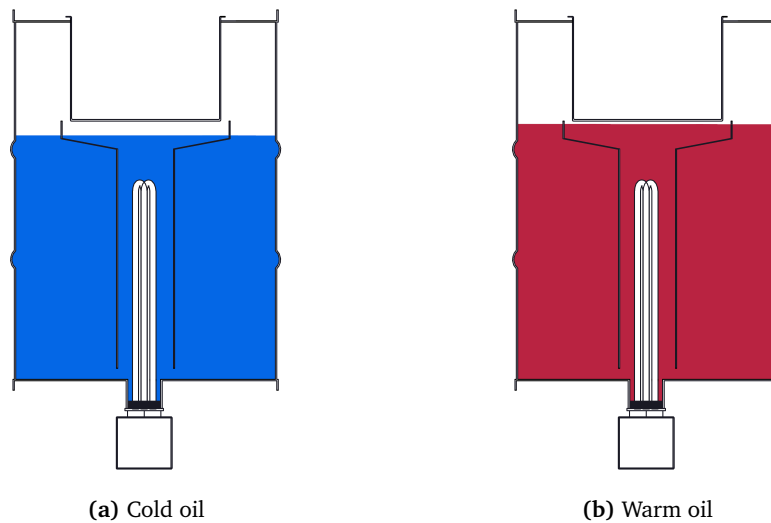
Figure 4.7: Illustration of the height difference due to expansion of the oil when the oil is warm from previous use.

The difference during charging can be seen in Figure 4.8a. It can be seen that the overflow temperature for the experiment with initially cold oil was approximately 190 °C, while it was 160 °C for the initially warm oil. The overflow temperature has been defined as the highest temperature in the funnel before the dip happens. The dip is where the temperature falls before increasing again. This dip can be seen in Figure 4.8a at 50 minutes for the initial warm oil and 145 minutes for the initial cold oil. The dip happens when the oil level in the storage reaches the oil level in the funnel. At this point the oil from the funnel will flow more rapidly and mix with the oil in the top of the storage, decreasing the temperature in the funnel.

With a higher initial temperature, causing increased expansion, the reduction in overflow temperature is approximately 30 °C. With a lower overflow temperature, the effect of stratification in the heat storage is reduced. This can be seen in Figure 4.8b, where the temperature at the top storage for the two cases are plotted. It takes almost two hours before the initial warm tank gets a higher temperature at the top storage compared to the initial cold tank, which can be explained by the fact that the effect of having a funnel disappears when the oil expands enough

to flow over the funnel wall. The circulation in the system results in a linear temperature increase in the storage.

(a) Top funnel
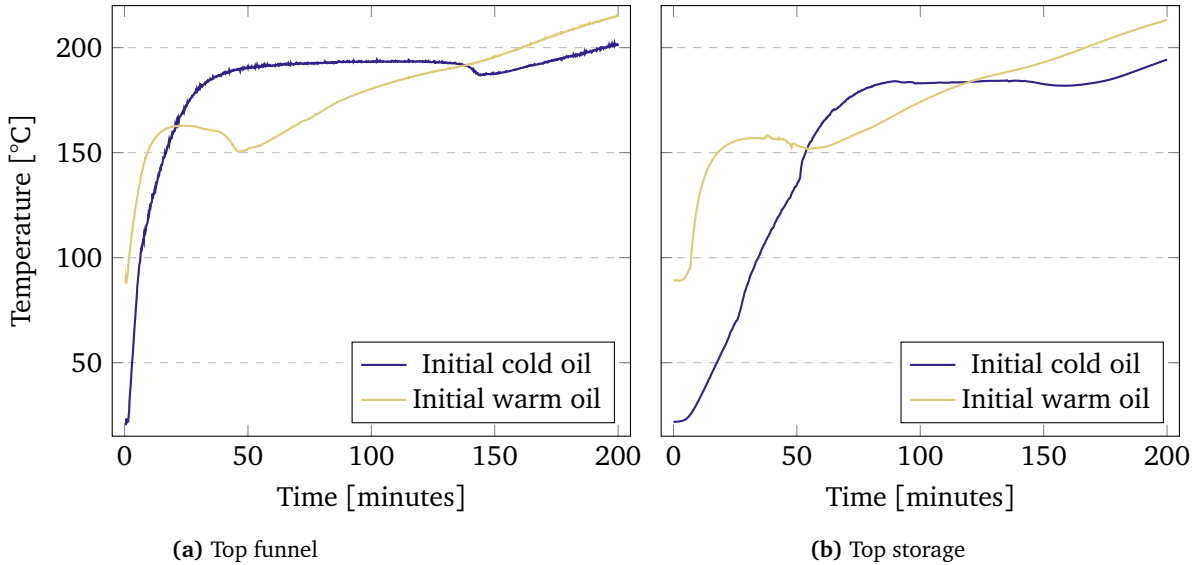
(b) Top storage

Figure 4.8: The temperature in the top funnel and in the top storage during charging, experiment 1 (cold oil) and experiment 5 (warm oil) from Test Set 1.

4.4.4 Effect of Reduced Power

The experiments with reduced power from Test Set 3 are discussed in this section. Figure 4.9 shows experiment 2 from Table 4.4. Experiment 2 had initial cold oil, initial oil level at the bottom of the funnel wall, and an insulated cooker. In Figure 4.9, it can be see that, after just 10-15 minutes, the temperature at the top storage started to increase. The temperature growth in the funnel switches to a linear growth with a small, positive slope after approximately one hour. This indicates that there is a significant heat loss from the funnel to the storage, which results in slower heating of the funnel.

The reduced power also results in slower charging of the storage. No overflow was experienced during the charging experiments. This means that the heat in the storage comes from heat emitted from the funnel to the storage, leading to an almost uniform heating. This diffusion of heat from the funnel to the storage is also present before overflow with full power. This can be seen in Figure 4.10, where the temperature increase in the storage shows a similar behaviour as when charging without a funnel, seen in Figure 4.5b.

With reduced power to the heating element, there is not enough power to get the desired temperature in the funnel and the wanted overflow temperature. Experiments with five liters of water in the cooker were conducted and showed that it took at least five hours to get the water to boil. Improvements, like insulating

the funnel tube or reducing the funnel volume, should be considered in order to make the system more efficient when charging under reduced power.
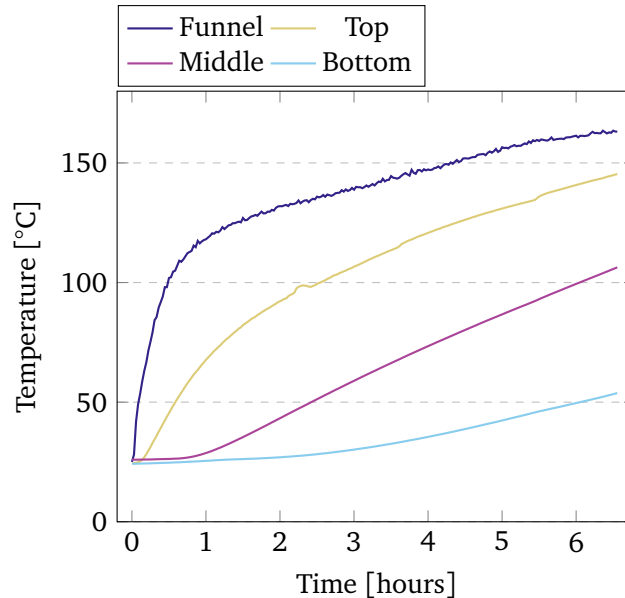
Figure 4.9: Temperature in the funnel and the storage from bottom to top during charging with reduced power and an insulated cooker (Test Set 3, experiment 2).

4.4.5 Degradation of Stratification

Figure 4.11 shows that the storage loses both heat and thermal stratification when not in use. Although the storage is still stratified after both 20 and 24 hours, the temperature difference between the bottom and top is small compared to the temperature difference right after charging. It may be difficult to minimize the degradation of stratification in the storage since the system will, by nature, work towards reaching equilibrium, which in this case is uniform temperature.

4.4.6 Design Difficulties

The Challenge with Internal Leakage From the project thesis, it was believed that a good way to test different funnel heights to control the overflow temperature would be to have rings that could be inserted on the funnel wall to change the height, as seen in Figure 4.12a. Experiment 4*, from Table 4.1, showed that it was difficult to seal these height rings properly, which resulted in overflow happening almost instantly with this feature. It was discovered that the system is very sensitive to internal leakages of oil from the funnel to the storage. The concept of height rings is not investigated any further due to the difficulty of sealing them.

Something similar took place in the project thesis when there was a problem with a screw fixing the funnel to a rod. This also resulted in overflow when the
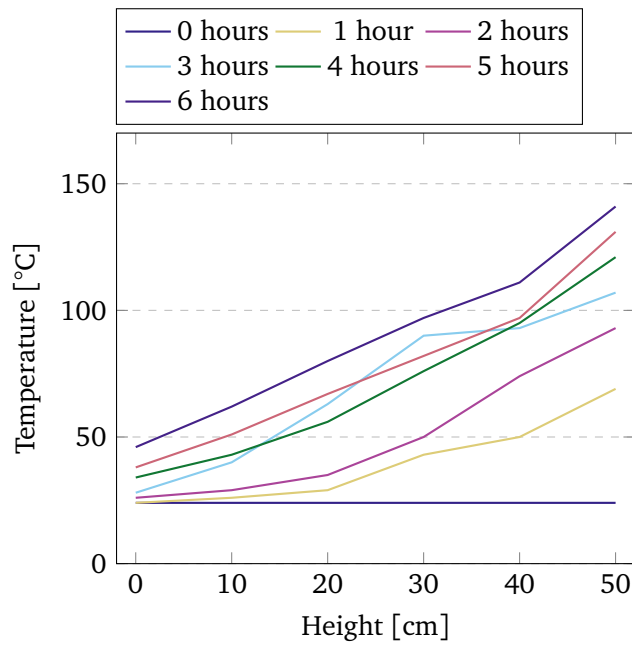
Figure 4.10: Temperature in the storage during charging with reduced power (Test Set 3, experiment 2).
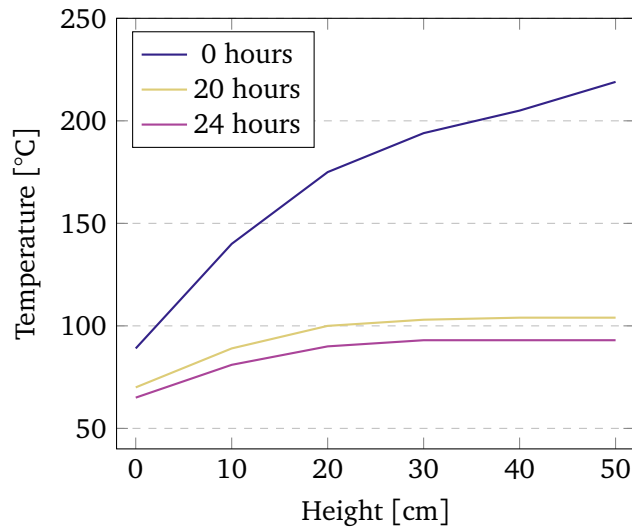
Figure 4.11: Temperature measures of the front in the storage after charging.

(a) Funnel wall with height ring.　　**(b)** Funnel wall without height ring.
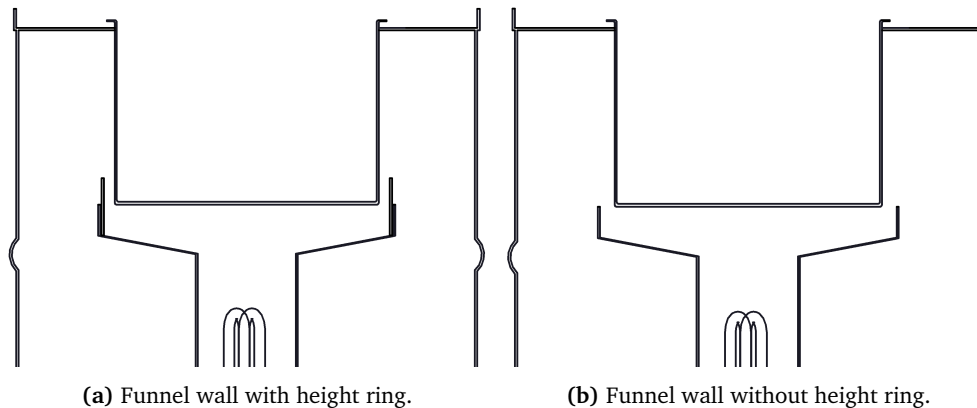
Figure 4.12

oil level reached the screw.

Some other solutions for changing the funnel height were presented in the project thesis. These consisted of some sort of rotating device that would open up holes in the funnel wall and another rotating device that would lift the funnel wall from the rest of the funnel. It is believed that the problem of sealing the funnel would also be present with these solutions.

Challenges with Wrong Initial Oil Level　Due to the problem with the height rings, the initial oil level had to be lowered to the bottom of the funnel wall to get the desired overflow temperature. Having the initial oil level at the bottom of the funnel wall (Figure 4.7a) means that the oil will not be in contact with the cooker until it has expanded enough to touch the cooker. Throughout this phase, the heat transfer from the oil to the cooker will be through air, which has a lower thermal conductivity compared to oil. This means the heat transfer will be reduced, until the oil touches the cooker and heat transfer from the oil is ensured. The funnel wall needs to be higher, so that the initial oil level is at the bottom of the cooker. The wall has to be high enough so that the oil in the funnel has space to be heated up and expand without getting overflow at an inadequate temperature.

4.5 Summary

4.5.1 Does the System Work?

From the results in Section 4.4.2, it can be concluded that the idea behind the funnel works. However, the experiments conducted show that the system still needs to be improved to utilize the full potential of the concept. The system works as a TES, where the energy is stored and can be used later to cook food. It also has the ability to cook food when it is being charged.

The temperature in the funnel rises quickly after the heating element is turned on with full power (1800 W), while the oil in the storage is slowly heated by the heat emitted from the funnel until overflow occurs. The storage becomes highly stratified, as hot oil from the overflow moves downwards in the storage compartment as a thermal front.

The oiled pot-in-pot solution works well enough for it to be used in further experiments. It gives the user the possibility to extract the pot for cleaning and it still provides enough heat transfer to boil water relatively quickly.

With reduced power, the system works poorly and the desired effect of the funnel is not achieved.

4.5.2   Improvements

Since this is a system that should be further investigated, a new system should be designed and tested. When designing a new system, the results from Section 4.4, as well as the practical experience from experimenting, should be considered.

The challenges with internal leakage, described in Section 4.4.6, showed that a design should reduce the chance of leakages between the funnel and the storage. Solutions to regulate the overflow must consider the probability of leakages.

Due to the challenges of controlling the overflow temperature, as discussed in Section 4.4.3, it should be possible to control the height of the funnel wall to get the desired overflow temperature. With regard to the challenges with internal leakages, any lifting of just the funnel wall, as suggested in the project thesis, should be avoided. Instead, the entire funnel should be lifted up and down to control the height of the funnel wall.

In Section 4.4.6, it is explained that when the oil level is too low, the heat transfer to the cooker is reduced, due to the oil not touching the pot from the start. The funnel wall should be made higher. It must be high enough for the initial oil level to be at the bottom of the cooker and still achieve an adequate overflow temperature.

In Section 4.4.4, it was seen that reduced power to the heating element resulted in difficulty reaching the desired temperatures and getting overflow. Reduction of the funnel volume should be tested, because there would then be less oil in the funnel to be heated. Finding a way of insulating the funnel should also be investigated to get higher temperatures in the funnel.

4.5.3   Sources of Error

For all the experiments, there are errors present from the thermocouples, as mentioned in Section 4.2.1. The standard deviation and the offset of the temperatures provided from the thermocouple submerged in water during boiling is measured. During boiling, the standard deviation of the temperature is measured to be +/- 0.044 °C. The average temperature is measured to be 101.29 °C, so 1.29 °C above

the boiling point. From this, a 1.29 °C offset, with a standard deviation of +/- 0.044 °C during the experiments, is observed.

It was also observed that, if the thermocouples were unintentionally touched, the temperature measured from the thermocouple would jump. The results where this strange behaviour was present are not presented here. All the results presented can be assumed to be fairly accurate, since the same temperatures and behaviours have been reproduced several times during experiments.

Measuring the front by hand proved to be a source of error, since it was impossible to lift the thermocouple exactly the same height every time. This way of measuring was, therefore, replaced through the addition of multiple thermocouples in the storage after the experiments with the initial system.

It was discovered during the first experiments in this chapter that the cooker had to be pressed down after the water was poured into it when the initial temperature of the oil was cold to ensure heat transfer from the oil as quickly as possible. This small change produced very different results and is why experiments 1 and 4 from Table 4.3 have similar initial parameters, but different outcomes in boiling time. This error is avoided with the improved design by always having the initial oil level touching the cooker.

4.6   Safety concerns

During the first round of experiments in the lab, some safety concerns arose.

The mix of hot oil and water can be dangerous and having an open system increases the risk of injury. Finding a safe way of conducting the experiments with water in the cooker was time consuming, but important. Extracting the pot from the cooker when the system is fully charged is difficult and presents a safety risk if the pot is full with water. It was concluded that an amount of five liters of water should be used in the discharging and charging experiments, even though the pot can take ten liters. This amount is big enough to be realistic and small enough for it to not be an unnecessary safety risk.

After some experiments, a leakage from two lids in the bottom of the tank was discovered. It happened after the whole system had been heated up to over 200 °C. Hot oil leaked out and both soaked the insulation at the bottom and melted the junction box of the heating element.

To fix the problem, the heating element was sealed with copper silicone, as well were the two lids for the openings. The bottom of the tank was then insulated with Aerogel and it proved to be a much more elegant and practical solution. The new insulation provides easier access to the junction box as well as cooling.

Chapter 5

Improved Design

In this chapter, an improved design of the system is presented based on feedback and the suggested improvements mentioned in Section 4.5.2.

The suggested improvements can be summarized in the following:

- The funnel should be continuous with no holes or anything that may lead to leakage from the funnel to the storage.
- The height of the funnel should be adjustable.
- The funnel walls must be high enough so that the oil always touches the cooker.
- The funnel volume should be reduced.
- Insulation around the funnel tube should be considered.

5.1   Adjustable Funnel

A funnel that can be moved up and down is desired. This will hopefully make it easier to cook during charging and provide a more stratified storage. The system will experience different oil levels based on the temperature of the oil. The moving funnel provides a possibility to control the overflow temperature for different oil levels.

The funnel tube will now be placed inside a guide tube, as seen in Figure 5.1. This guide tube centres the funnel, the funnel can slide up and down in this tube. Around the funnel tube, small metals pieces are fitted close to the top and bottom. The moving funnel can slide up and down inside the guide tube with a firm fit, seen in Figure 5.1b. The guide tube stands on three feet that lifts it 20 mm up from the bottom of the tank and centres the funnel around the heating element. Around the guide tube there is another tube to reduce the circulation of oil around the funnel and guide tube. This tube will then work as an insulating tube. Aluminum foil is wrapped between the tubes at the top to stop the motion of oil flowing between the tubes and hopefully provide an insulating effect. The aluminum foil can be removed. There is also a possibility of inserting insulation around the funnel and guide tube if desired.

(a) **(b)**
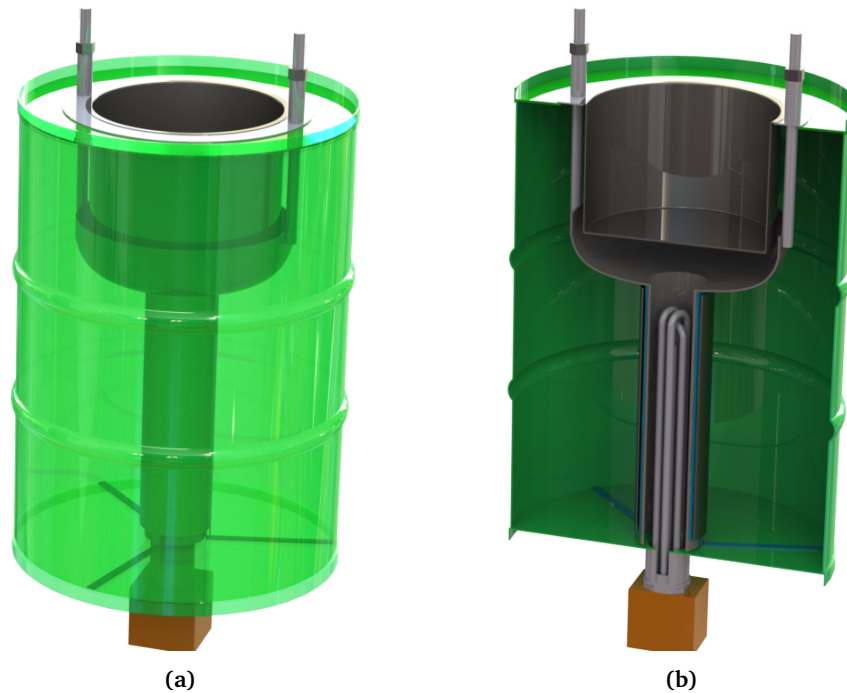
Figure 5.1: SolidWorks render of the improved design. In Figure 5.1b there is a half-view of the system and in Figure 5.1a the barrel is a transparent view.

The lifting mechanism is quite simple and consist of two rods that are welded to the top of the funnel wall. These two rods go through the top of the barrel and each has a nut mounted at the top to hold the funnel in place. There are also fitted spacers around the rods to lift the nuts up a bit, so that the nuts do not become too warm, making it easier to adjust the height by hand. By adjusting the two nuts, the funnel can be lifted up and down. The funnel can be adjusted 50 mm with this mechanism, which can been seen in Figure 5.2.

5.2   New Funnel Top

It can also be seen in Figure 5.1 that the shape of the funnel top has been changed from the previous design. The top of the funnel now consist of an end cap with a hole at the bottom. The end cap is welded to the funnel tube. This makes the funnel easier to build, since the end cap can be bought as a standard part from a specialist shop. The funnel walls are thicker compared to the old funnel, that should give a slightly better insulating effect to the storage. The end cap has an outer diameter of 306 mm and a wall thickness of 3 mm. The height of the end cap is 75 mm. At the top of the end cap a 20 mm high wall is welded to increase the height of the funnel wall. This is done so that the funnel wall is high enough to ensure there is contact between the oil and the cooker with cold oil. The funnel is now continuous, meaning there are no holes or gaps that can lead to leakage

(a) High funnel

(b) Low funnel
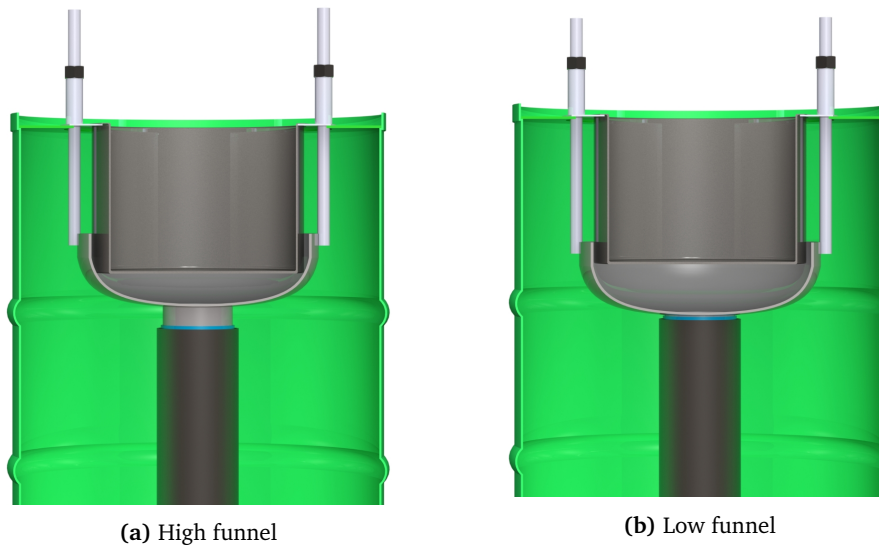
Figure 5.2: The new funnel with lifting mechanism.

from the funnel to the storage.

5.3 Technical drawing

A more detailed drawing of the new design is presented in Figure 5.4. It is a cut view of the system, with the most relevant dimensions. The inner tube has a inner diameter of 82.9 mm and a wall thickness of 3 mm. The funnel tube has a height of 376.3 mm. The solution for the guide tube was customized in the lab, an existing tube was used. The guide tube had an inner diameter of 92 mm and wall thickness of 2 mm. The outer tube had a inner diameter of 102 mm and a thickness of 2 mm. It is important to have enough space so that the funnel tube can slide up and down, and room for insulation if needed. The end cap is of standard dimensions and the wall welded at the top is 20 mm high. The lifting solution has rods with a diameter of 16 mm and spacers that are 65.2 mm high. More detailed SolidWorks drawings are provided in Appendix C. (If you are reading this with Adobe Acrobat Reader, in the Attachments on the left hand side, a 3D-model named OneTankAssem.pdf is provided. Right hand click and open the Attachment. 3D features have to be enabled).

(a)
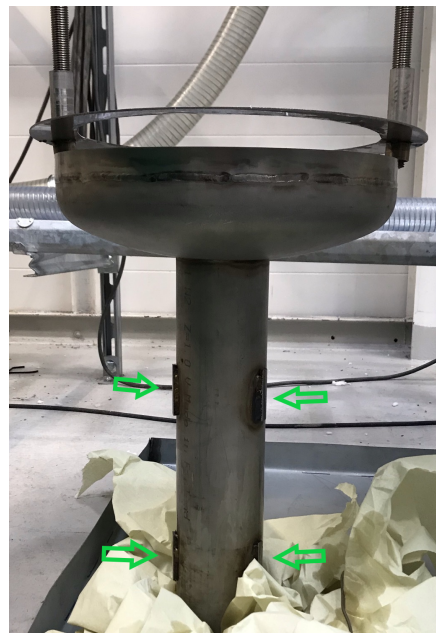
(b)

Figure 5.3: The new funnel. In Figure 5.3b, the green arrows show the spacers at the funnel tube.
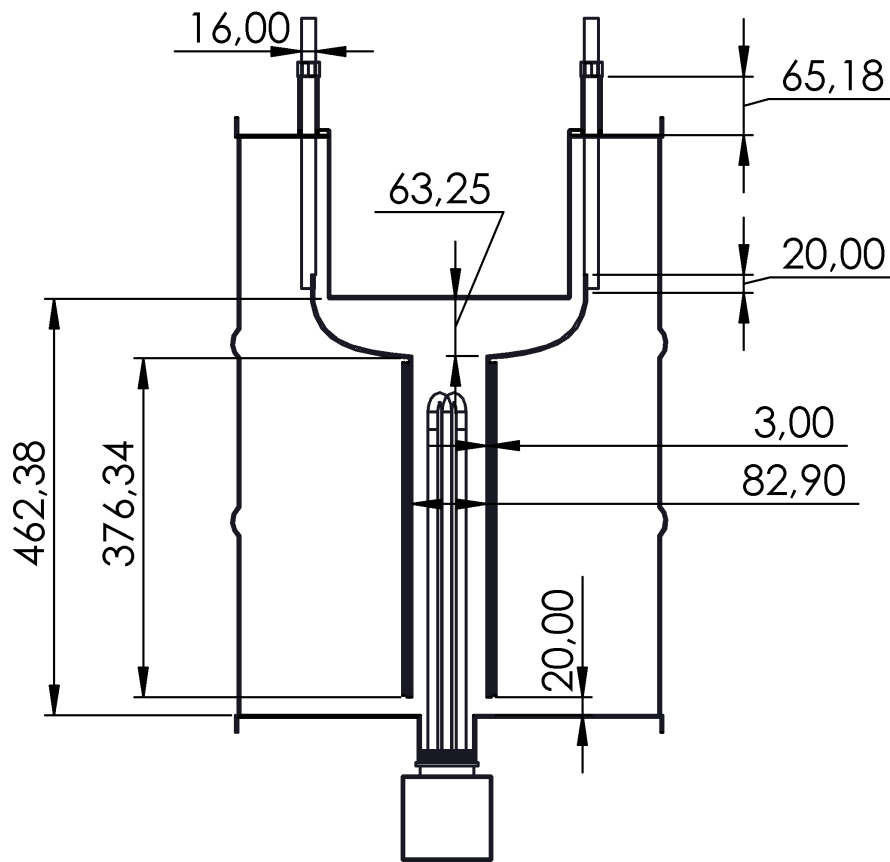
Figure 5.4: Dimensions of the new design solution in millimetre.

Chapter 6

Experiments with Improved System

Experiments with the improved system explained in Chapter 5 have been conducted. The motivation for conducting the experiments, methodology, results and discussion are presented in this chapter.

The experiments in this chapter include the following bullet points from the outline discussed in Section 1.1:

- Temperature measurements of the moving thermocline during charging and discharging (cooking).
- Charging experiments with different power levels to determine if insulation is needed on the internal funnel.
- Testing of a method for regulating the flow across the funnel barrier for temperature control in the storage.
- Cooking experiments at different charging levels of the storage.

6.1 Motivation for the Experiments

The goal of these experiments is to test the improved design: To investigate if one is able to produce a desired overflow temperature no matter what the initial oil temperature is as well as to investigate if the height adjustment provides the user with better control of the system. It is also desirable to investigate if the improved design reduces the heat transfer from the funnel to the storage and if it results in better performance when charged with reduced power.

6.2 Experimental Setup

6.2.1 Method

The setup for these experiments is quite similar to the one described in Section 4.2. The experimental method is the same as described in Section 4.2.1, but in many

experiments multiple parameters have been changed since it has been thought most important to try to keep the overflow temperature constant. Which means that when the initial oil temperature is higher than usual, the funnel height have been increased to accommodate for that. The tank is filled with approximately 80 liter of oil. The oil barely touches the bottom of the cooker when the oil is cold (ambient temperature). The oil in the tank has not been refilled nor extracted during these experiments. The amount of oil might be slightly different from the first to the last experiment conducted due to evaporation. Experiments within three different test sets have been done, the test sets are similar to the ones in Chapter 4. The first test set is with maximum power and an insulated cooker, the second is with maximum power and five liters of water in the pot, and the third one with reduced power both with and without water in the pot. Different configurations of the funnel height have been used within each test set to get the desired overflow temperature around 210 °C. The same safety temperature from Chapter 4 of 220 °C has been used. For all the cooking experiments, the pot-in-pot with oil in between and a lid have been used.

Thermocouples Two more thermocouples have been placed inside the storage (compared to Chapter 4) to obtain more accurate measurements, as well as to not having to measure the front by hand. The thermocouples in the storage have been placed 2 cm, 13 cm, 23 cm, 33 cm, and 43 cm from the bottom. All these thermocouples have been attached to the same rod as used in the first experiments.

Two thermocouples have been placed inside the funnel. These will not stay completely put due to the funnel being moved up and down. One of them is attached to the funnel wall and has a nut attached at the end to weigh it down so that it stays at the bottom of the funnel top. The other is floating in the funnel top. The placement of the seven thermocouples can be seen in Figure 6.1.
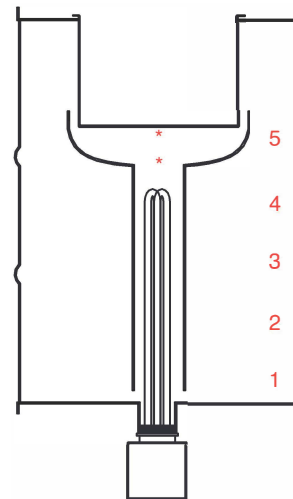
Figure 6.1: Approximate location of the thermocouples used for the experiments in chapter 6.

Adjusting the Funnel As explained in Chapter 5 the funnel can be moved 50 mm vertically. In this way, one will be able to control the overflow temperature. Experiments have been conducted with the funnel at different heights to test how this changes the performance of the system and to find a good way of controlling the height of the funnel for optimal use of the system. When the height of the funnel is 0 mm it is at the lowest possible configuration, while 50 mm is the highest configuration.

6.3 Overview of Experiments Conducted

6.3.1 Test Set 1

Charging experiments in Test Set 1 were done with full power (1800 W) and an insulated cooker. It was done with different initial oil temperatures as well as different funnel heights to understand how this changes the overflow temperature. The experiments conducted can be seen in Table 6.1. The overflow temperature has been defined as the highest temperature in the funnel before overflow.

Nº	Initial oil temperature	Funnel height	Overflow temperature
1	30 °C	21 mm	205 °C
2	90 °C	21 mm	175 °C
3	90 °C	40 mm	218 °C
4	40 °C	31 mm	218 °C
5	20 °C	25 mm	210 °C
6	23 °C	30 mm	223 °C

Table 6.1: Overview of charging experiments done in Test Set 1.

6.3.2 Test Set 2

Charging experiments in Test Set 2 were done with full power (1800 W) and with five liters of water in the pot. Discharging experiments were done with different funnel heights and by heating five liter of water in the pot. The experiments conducted can be seen in Table 6.3 and Table 6.2.

Nº	Initial oil temperature	Funnel height	Overflow temperature	Time for water to boil
1	39 °C	25 mm	184 °C	60 min
2	100 °C	40 mm	194 °C	45 min

Table 6.2: Overview of charging experiments done in Test Set 2. The experiments were started with water at ambient temperature.

Nº	Initial oil temperature, in funnel	Funnel height	Time for water to boil	Time boiling
1	194 °C	25 mm	32 min	3 h and 40 min
2	210 °C	0 mm	30 min	4 h and 45 min

Table 6.3: Overview of discharging experiments done in Test Set 2. The initial water temperature for experiment 1 was 17 °C and 13 °C for experiment 2.

6.3.3 Test Set 3

Charging experiments in Test Set 3 were done with reduced power (500 W) and different initial oil temperatures. Experiment 4 was done by heating up five liters of water in the pot from ambient temperature.

Nº	Initial oil temperature	Funnel height	Temperature in top storage after 3 hours
1	36 °C	21 mm	145 °C
2	86 °C	40 mm	174 °C
3	103 °C	25 mm	158 °C
4	22 °C	25 mm	84 °C

Table 6.4: Overview of charging experiments done in Test Set 3. Experiment 4 was done with five liters of water in the pot.

6.4 Results and Discussion

### 6.4.1 The Effect of the Funnel Height when Charging

Changing the funnel height while having the same initial oil temperature changes the overflow temperature as seen in Figure 6.2. These graphs show a comparison between experiment 2 and 3 from Table 6.1. In these experiments, the oil is warm from the previous day with an initial oil temperature at 100 °C. With a funnel height of 40 mm, the overflow temperature is 215 °C, close to the desired overflow temperature. A funnel height of 21 mm, which gives the desired overflow temperature of 210 °C when the initial oil temperature is cold, leads to an overflow temperature around 170 °C with initial warm oil, 40 °C lower than the high funnel.

The stratification number, has been calculated for the different cases using Equation (2.12), where the maximum stratification number has been set to be the most stratified point in Figure 6.3. Figure 6.4 shows the stratification numbers for charging from initial warm oil with the funnel height at 21 mm and 40 mm. It is very clear that being able to have overflow at the desired overflow temperature results in a more stratified storage, and that the stratification decreases after overflow.

6.4.2 The Effect of the Funnel Height when Discharging

Discharging experiments in Test Set 2 have been conducted to evaluate the effect of different funnel heights during discharging. The system was charged until the temperature in the storage reached an adequate temperature. Five liters of water was heated in the pot from ambient temperature.

Experiment 1 was done with a funnel height of 25 mm (normal funnel) and experiment 2 with a funnel height of 0 mm (low funnel) as seen in Table 6.3. It

(a) Top funnel

(b) Top storage
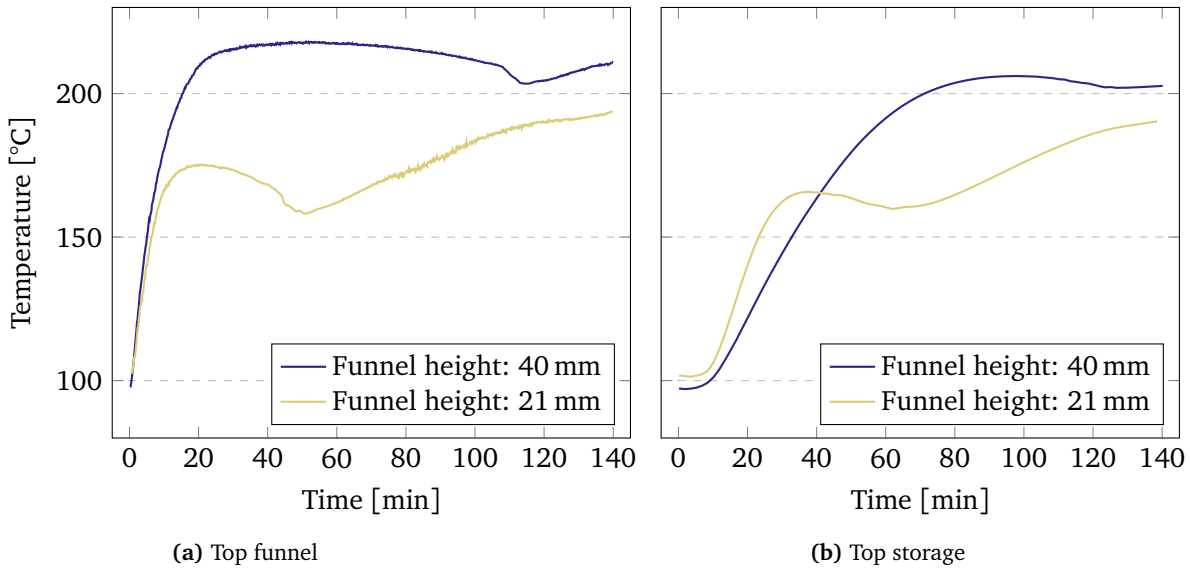
Figure 6.2: Temperature in the funnel and the storage during charging with the same initial oil temperature and different funnel heights (Test Set 1; experiment 2 - Funnel height: 21 mm and experiment 3 - Funnel height: 40 mm).
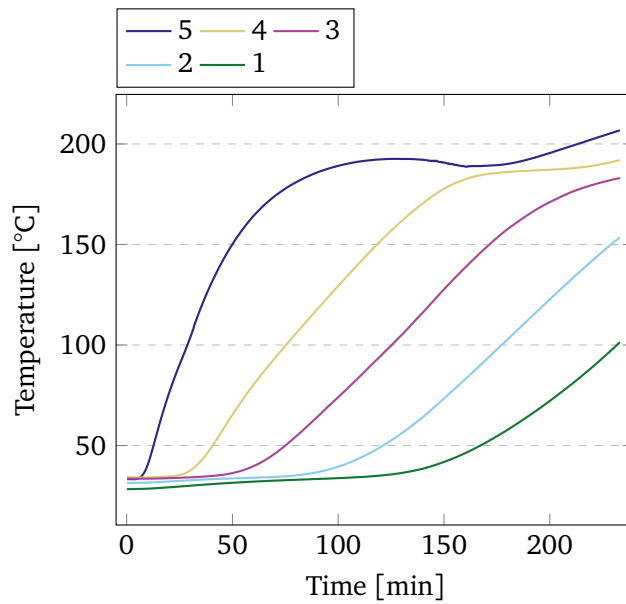
Figure 6.3: Temperature in the storage from bottom (1) to top (5) during charging from cold oil, with a funnel height of 21 mm.
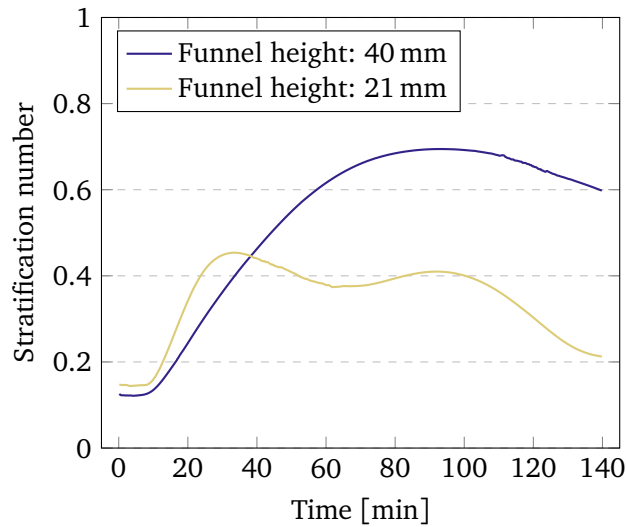
Figure 6.4: Stratification number during charging (Test Set 1; experiment 2 - Funnel height: 21 mm and experiment 3 - Funnel height: 40 mm).

takes the same amount of time for the water to start boil, but the experiment with the low funnel boils for about one hour longer than the normal funnel height. The oil level decreases during discharging and when the oil level is beneath the funnel wall there is no longer circulation of hot oil into the funnel. This can be seen in Figure 6.5 after 4-5 hours, where the temperature in the funnel decreases shortly after the water stops to boil, meaning that there is no circulation in the tank. There is, however, more energy left in the storage that can be used to boil the water for a longer time. Lowering the funnel will enable the use of the available stored energy.

Nº	Funnel height	Initial stored energy	Energy after boiling	Stratification number at t=0
1	25 mm	6.84 kWh	4.75 kWh	0.026
2	0 mm	6.11 kWh	4.13 kWh	0.62

Table 6.5: Energy and stratification number from discharge experiments in Test Set 2 with different funnel heights.

In Table 6.5 the energy before and after discharging of the system with the low and normal funnel is showed. The energy after boiling is the energy left in the tank when the boiling stops. It can be seen that there is left more energy in the tank with the normal funnel compared to a low funnel. The initial energy is a bit different between the two experiments, the experiment with a normal funnel had more stored energy and an initially uniform temperature in the storage and the experiment with low funnel had an initially stratified storage. Nevertheless, the experiment with low funnel boiled for 55 minutes longer than the one with
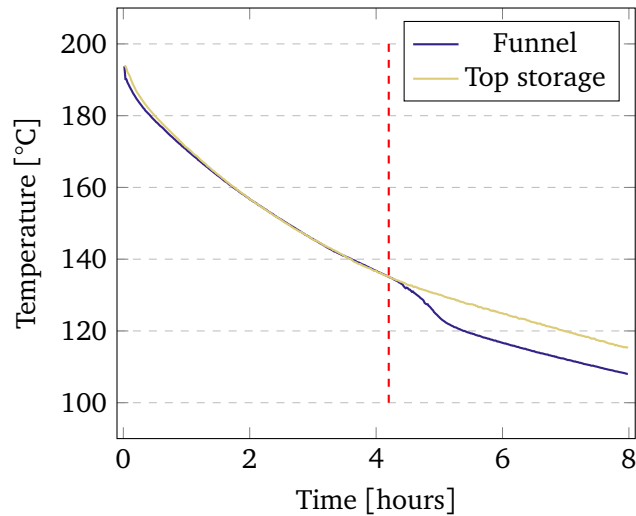
Figure 6.5: Temperature in the funnel and the top storage while discharging with a funnel height of 25 mm (normal funnel). The red line is where boiling stops. (Test Set 2; discharge experiment 1)

normal funnel due to the circulation lasting longer. This indicates that with a low funnel one is able to utilize the stored thermal energy at lower oil temperatures from the storage before boilings stops.

6.4.3   The Effect of Discharging from a Stratified Storage

Another interesting observation from Table 6.5 is that the energy used (the difference before and after cooking) is almost the same for both experiments. This means that the extra energy in the bottom of the storage from the uniform storage is not utilized and one can see for both experiments that there is still a lot of energy left in the storage. The time it takes for the water to start to boil is almost the same for the two experiments in Table 6.5. This means that the effect of stratification is important. As long as the temperature in the top of the storage is high enough, the time to reach boiling will be almost the same. This is because the heat transfer to the cooker depends on the temperature difference (Equation (2.2)) from the oil in the top funnel to the water in the pot. The problem by comparing these two experiments is of course the different funnel height for the two experiments, nevertheless 30 minutes was also the average time to reach boiling for five liters of water in the experiments with the previous design. Based on this, the only important factor in the beginning of the discharging, seems to be to have a high enough temperature in the oil in the top storage and funnel.

Figure 6.6 shows the temperature in the top and bottom of the storage while discharging. The storage was stratified when the discharging started with a temperature difference of $\approx 100\,°C$. The graph shows that when the discharging begins, hot oil from the top of the storage flows down the funnel tube to the bottom
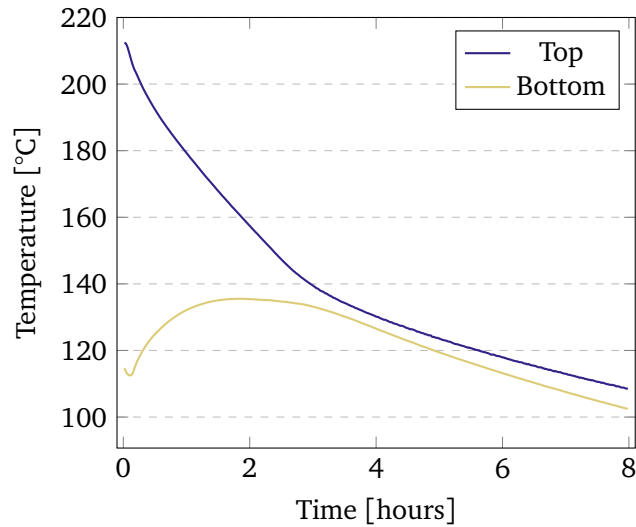
**Figure 6.6:** Temperature in the top and bottom storage while discharging from a stratified storage.

of the storage, destroying the stratification. The oil should, ideally, (to take advantage of all the energy in the storage) have transferred enough heat to the cooker, before it reaches the bottom of the storage, to not increase the temperature there. This is the reason for the large amount of energy left in the tank, observed in Table 6.5.

6.4.4 Boiling Water when Charging with Full Power

Two experiments were done with five liters of water in the pot while charging the system at full power. Table 6.2 shows the two experiments. The system was charged from two different initial temperatures. The funnel height was set to 25mm and 40mm to obtain the same overflow temperature, the overflow temperatures were 184 °C and 194 °C. The water in the experiment with initially higher oil temperature started to boil after 45 minutes while the other boiled after 60 minutes. Figure 6.7 shows the temperature in the funnel during these two experiments. One can see that although there is an initial temperature difference of 61 °C the experiments show very similar behaviour. The temperature in the funnel and the overflow temperature seem to be more important than the initial oil temperature regarding how long it takes for the water to start boil. This experiment shows that heating a small volume of oil inside the funnel results in high temperature of the oil, which can be used to cook and/or stored for later usage.

6.4.5 The Effect of Lifting the Pot while Boiling

It is desirable to have some control over the heat transfer to the pot so that it does not boil over or food get burned. A way of doing this, could be to lift the inner
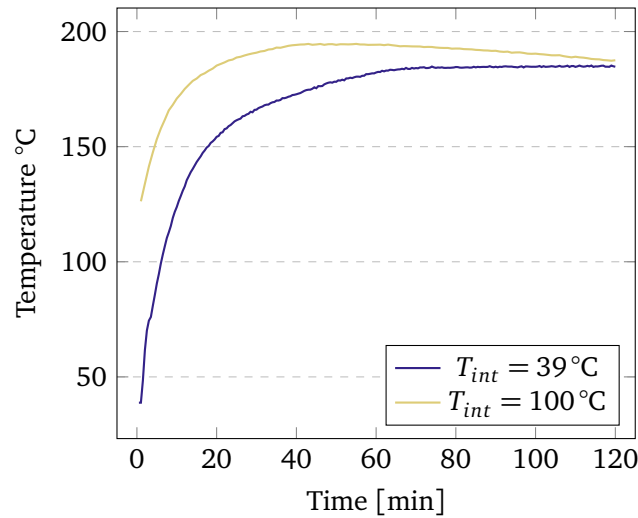
Figure 6.7: Temperature in the funnel during charging experiments with five liters of water in the cooker (Test Set 2; Experiment 1 and 2)

pot some millimeters while boiling. This would result in a gap of air between the two pots which would decrease the heat transfer due to an increase in the thermal resistance. An experiment was conducted to check if it worked as expected. Five litres of water was brought to boiling. When the water started to boil, the inner pot was lifted 18 mm, two nuts were placed in between the pots to keep the inner pot lifted. Lifting the pot did not result in reduction of temperature in the water, but one could clearly see that the water boiled less vigorously. A lifting device would be an easy controlling mechanism to implement.

6.4.6 The Effect of Having Double Funnel Tube

Chapter 4 pointed out that there is a heat loss from the funnel to the storage which turns problematic when charging the system with reduced power. The improved design has two funnel tubes with a smaller diameter, as well as a thicker wall on the funnel top. Experiments were conducted with reduced power to see if the improved design has reduced the heat transfer between the funnel and the storage. The results showed little difference compared to the results with reduced power in Chapter 4. This could indicate that the insulating effect with two more tubes is poor. Or that the biggest heat losses are from the funnel top which is not insulated and contains the highest temperatures. The surface area at the top funnel is also quite high compared to the funnel tube, meaning there will be a higher heat transfer from the top funnel compared to the funnel tube. Insulating the top funnel is believed to be too complicated and not practical for this system.

6.4.7   The Effect of Cooking with Reduced Power

Experiment 4 in Test Set 3 was done to test the effect of cooking during charging from a cold tank with reduced power. It took 5 hours and 45 minutes to boil five liters of water from ambient temperature. The temperature profiles can be seen in Figure 6.8. There was a quick temperature increase in the water the first hour, due to a high temperature difference between the oil in the funnel and the water. However, when the temperature in the top funnel reached 100 °C the temperature profile flattened out and started to increase linearly with a small slope. When this happened the heat transfer decreased.
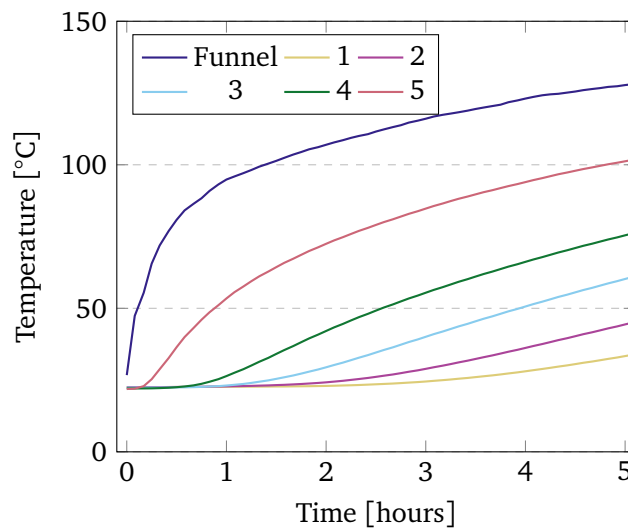
Figure 6.8: Temperature in the top funnel and the storage from bottom (1) to top (5) during charging with reduced power, with five liter of water in the cooker (Test Set 3; experiment 4).

In Figure 6.9 the temperature difference between the funnel top and the water in the pot is plotted together with heat added to the water. It can be seen that the temperature difference and heat transfer to the cooker follow each other as long as the temperature difference between the oil and the water is larger than 30 °C. After three hours the temperature difference stabilizes around 30 °C and when this happens the heat transfer decreases slowly towards zero. This indicates that to have a sufficient heat transfer from the oil to the cooker the minimum temperature difference has to be a couple degrees above 30 °C. Something similar has been seen in the discharging experiments where the boiling often stops when the oil reaches 130 °C.

6.4.8   Insulation

In Table 6.6 the heat loss of the system with different power to the heating element can be seen. The average temperature in the storage during charging and
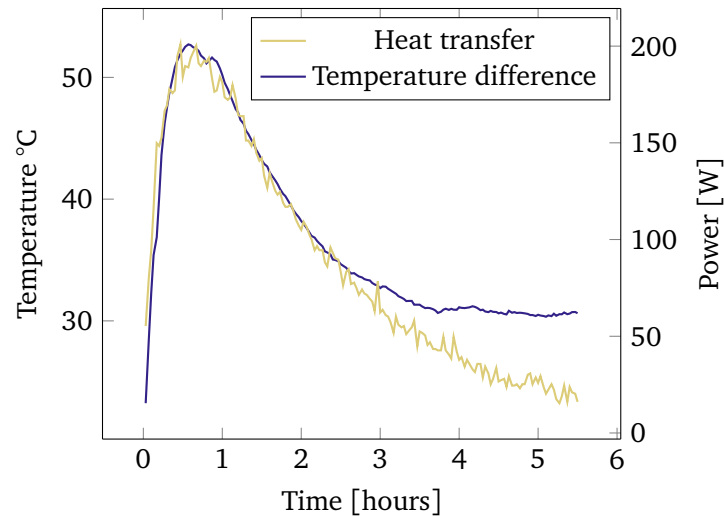
Figure 6.9: The temperature difference between the oil in the funnel and the water in the cooker and the heat to the cooker with reduced power (Test Set 3; experiment 4).

	Energy added	Energy change	Energy loss	Heat loss
No power	-	-0.15 kWh	-0.15 kWh	-0.157 kW
Full power (1.8 kW)	1.8 kWh	1.23 kWh	-0.56 kWh	-0.56 kW
Reduced power (0.5 kW)	0.5 kWh	0.45 kWh	-0.05 kWh	-0.045 kW

Table 6.6: Overview of energy losses of the system during one hour with different power to the heating element.

discharging behaves linearly in the temperature range of 100 °C to 200 °C. The heat losses have been calculated using the slope of the average temperatures in that range. Energy change in the system is the change of thermal energy calculated with Equation (2.14). Energy loss is the difference between energy added from the heating element and the change of the thermal energy in the tank. There is a significant heat loss at full power, while the heat loss for reduced power is calculated to be quite small. There is an uncertainty of the provided power during experiments with reduced power. The provided power should be 500 W, however the transformer might have an output that is higher because of the low heat loss.
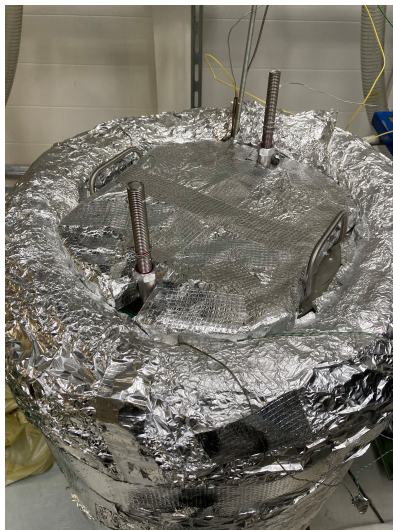
Figure 6.10: Insulation lid.

When the power is turned off, after being charged, the system has a heat loss of 157 W. This loss is fairly constant over time, this can be seen later in Figure 8.5. It is desirable that the heat losses are as small as possible and that the storage stays stratified. An insulation lid was made to avoid some of the heat losses from the top of the tank. Figure 6.10 shows the lid made of two layers of Aerogel and aluminum foil. The hot tank was left for a weekend with the lid on, the results showed that the lid made little difference.

When insulating the tank, insulation from an old system was reused. The insulation was cut of the oil tank and wrapped around the tank with aluminum foil and duck tape. This resulted in uneven insulation thickness some places and small gaps between the end parts of the insulation when wrapped around the tank. Better insulation work on the tank may result in less heat losses.

6.5   Summary

6.5.1   Does the System Work?

The experiments conducted in this chapter has proved that being able to change the height of the funnel provides the user with better control over the system. It makes it possible to change the overflow temperature which is valuable to obtain a stratified storage when the system has been used the previous day. This can be very useful if the initial temperature in the tank varies from day to day.

It is also valuable to be able to change the funnel height when discharging. Lowering the funnel will result in circulation from the storage to the funnel for a longer time, and in that way more stored energy is extracted.

Charging the system with reduced power still leads to lower temperature in the funnel, due to heat losses from the funnel to the storage. Cooking during charging with reduced power also proved difficult because the temperature difference between the oil and the water is not high enough over time. A double funnel was implemented in the new design to hopefully minimize the energy loss from the funnel to the storage, it proved to not make much of a difference.

6.5.2   Improvements

The tank should be insulated by professionals to reduce the heat losses.

Being able to control the temperature in the pot would make cooking easier. Lifting the inner pot up 18 mm did not change the temperature in the water, but it made the water boil less vigorously. More experiments lifting the inner pot should be conducted to investigate this idea, as well to find a suitable height. A lifting mechanism to lift the inner pot could be implemented in a new design.

Chapter 7

Simulations

Dynamic simulations of the system before overflow are done in *COMSOL Multiphysics*®
[40], to investigate the effect of insulation around the funnel tube when charging
with reduced power. The simulations are validated with the experiments.

The goal laid out in the following bullet point from the outline discussed in
Section 1.1 acted as the focus of these simulations:

- Charging experiments with different power levels to determine if insulation
  is needed on the internal funnel.

7.1 Motivation for the Simulations

In the project thesis [1], it was concluded that, at full power (1800 W), insulation
was not necessary around the funnel tube. The oil inside the funnel tube heated
quickly and the effect of stratification was still present. Insulation on the funnel
tube would, therefore, not have made much of a difference. Finding suitable in-
sulation also proved difficult.

Experiments from Chapter 4 and 6 have shown that the temperature in the
funnel increases slowly when charged with reduced power, and reaching overflow
temperatures was not possible. There is a significant heat loss to the storage from
the funnel. The goal with these simulations is to investigate if the conclusion of
the project thesis will be different when the system is being charged with reduced
power (500 W). It is beneficial to have a higher temperature in the funnel, but the
benefit of having insulation must also be big enough for it to be worth insulating
the funnel tube. Hence, simulations have been run to investigate how large of a
temperature difference one can expect to achieve by insulating the funnel tube.
To investigate this, simulations have been run with different insulations around
the funnel tube.

7.2   Setup

The setup for the COMSOL simulations are presented here. They are quite similar to the simulations done in the project thesis [1], with some improvements. In the project thesis, significant time was spent investigating different possibilities for simulating the system with the accessible computing power. Simulating the thermodynamic behaviour with expansion of the oil and overflow proved difficult with the computing power at hand. Different setups were made to simulate charging before overflow, charging during overflow, and discharging. It proved difficult to simulate overflow and to obtain results that could be verified. Based on this, the behaviour of the system before overflow is simulated.

Charging before overflow should provide an accurate image of the system and help to understand the heat transfer in the system with reduced power. Reduced power will also ease the computing power needed because the system experiences smaller temperature changes.

Heat Transfer Physics   In COMSOL, the Laminar Flow (spf) and the Heat Transfer in Solid and Fluid interfaces have been used, described in *CFD Module User's Guide* [41]. The Laminar Flow interface computes the velocity and pressure fields in the flow. The Heat Transfer in Fluid and Solid interfaces computes the temperature in the flow. The equations solved in the Laminar Flow interface is the Navier-Stokes equations for conservation of mass and momentum. The Heat Transfer interface solves the energy equation and the heat transfer with Fourier´s Law in the flow.

The Laminar Flow interface and the Heat Transfer in Fluid and Solid interface have been coupled using the Nonisothermal Flow interface in the Multiphysics interface. The temperature variables are coupled with the laminar flow. The equations used in COMSOL can be found in the *CFD Module User's Guide* [41] for the respective interfaces used. The Grashof number (Equation (2.9)) for the simulations are calculated to be around $5.2 \cdot 10^7$. The Grashof number indicates that the flow is experiences laminar behaviour, as discussed in Section 2.1.3. A laminar solver is, therefore, used to investigate the problem.

Geometry and Boundary Conditions   The geometry used in the simulations can be seen in Figure 7.1. The computations are done in 2D axissymmetric space. The left vertical line is the symmetry line. Five measure points in the storage have been added at the same places as in the experiments and two in the top funnel, so the temperatures from the simulations can be compared with the temperatures from the experiments. At the the outer walls, a heat loss to the surroundings is added. This is added as a convective heat flux at the outer wall, with the heat transfer coefficient set to 4.07 W/(m^{2}K) and the ambient temperature to 21 °C. The heat transfer coefficient is an estimate based on earlier work done by S. Fjeldsæter and S. Stordal [34].

The gravity option has been applied to the geometry. This adds gravity as a force to the governing equations. The pressure is calculated as a hydrostatic pressure. To make sure that the pressure behaves properly a pressure constraint is set at the top surface. This is done by setting a pressure point constraint at the top of the geometry to atmospheric pressure (1 atm). At the side wall and bottom wall no slip has been applied and at the top surface, which is a free surface, a slip boundary condition has been applied. The initial temperature for the fluid is set to be 35 °C to match the temperature from the similar experiment in the lab. The heating element has been added by inserting a cylindrical element with a diameter of 40 mm inside the funnel with a heat flux of 500 W.

At the funnel tube, different insulation boundary conditions were inserted, which can be seen in Figure 7.1. The setup without insulation at the funnel tube can be seen in Figure 7.1a. In Figure 7.1b the funnel tube is insulated with two more tubes, similar as done in the experiments in Chapter 6. In Figure 7.1c the funnel tube is insulated with a made up insulating material. This material has been placed around the funnel tube with a thickness of 20 mm. At last, the funnel tube is insulated using zero flux boundary condition leading to perfect insulation, this can be seen in Figure 7.1a. At the funnel top no insulation has been applied during the simulations.
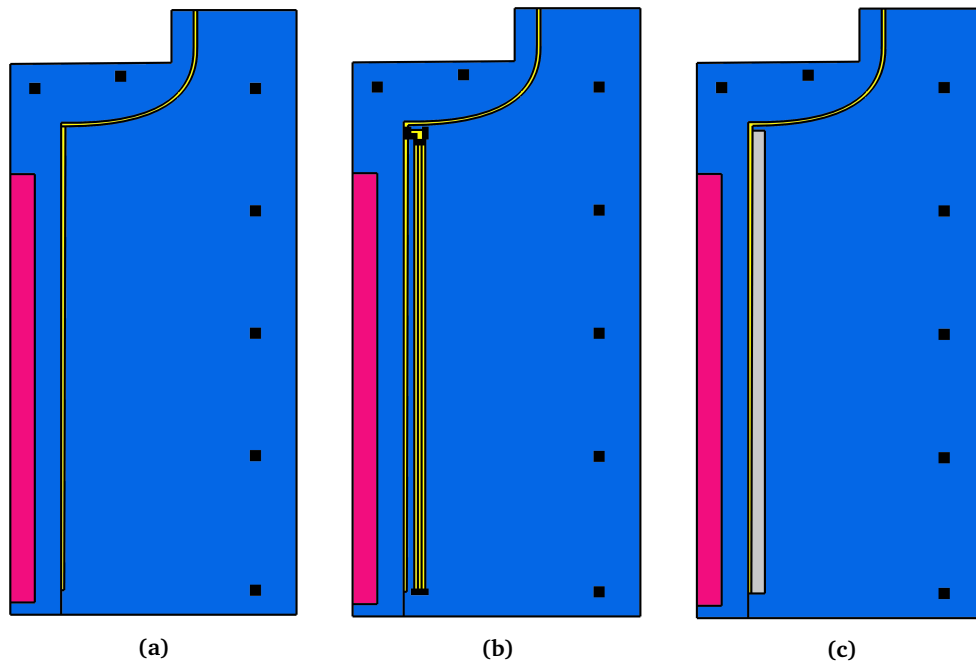
Figure 7.1: Illustration of different insulations in the geometry.

Thermophysical Properties Duratherm 630 is added as a material in COMSOL with the values from Section 2.5.1. At the funnel, AISI 4340 has been added as a

material. Nimonic Alloy is added at the heating element to represent the properties of a typical heating element. The insulation material around the funnel tube has been constructed with the following properties: Density of $128 \, \text{kg/m}^2$, thermal conductivity of $0.05 \, \text{W/(m} * \text{K)}$, and heat capacity of $2000 \, \text{J/(kg} * \text{K)}$. These parameters are chosen to reflect a good insulating material.

7.3 Results

In this section the results are presented. First, the results are validated with a mesh independence study and compared with the similar experiment done in the lab. Second, four different simulations with different insulation around the funnel tube are presented and compared with each other.

7.3.1 Validation

Mesh Independence   A mesh independence study has been done over a time interval of 200 seconds. Mesh refinement has been applied to the geometry with COMSOL's automatic mesh feature. The results can be seen in Table 7.1. From the results it can be seen that the Extra fine mesh provides an independent mesh. The Extra fine mesh has been applied to the geometry for the following simulations.

| Mesh type	Line average	Point
Normal	41.18 °C	39.37 °C
Fine	41.67 °C	39.49 °C
Finer	44.05 °C	40.24 °C
Extra fine	47.75 °C	41.76 °C
Extremely fine	48.01 °C	41.42 °C
Refine 1	47.97 °C	41.68 °C

Table 7.1: The temperatures from the mesh independence study. Line average is the average temperature at the bottom of the cooker. Point is the temperature at the measure point at the bottom of the funnel.

Compare with Experiments   To see if the simulations can be trusted, the simulation with two tubes as insulation have been compared with the similar experiment conducted in the lab (Experiment 1 from Table 6.4). In Figure 7.2, the result from the simulation with two tubes as insulation can be seen next to the experiment. It can be seen that the behaviour is quite similar and all the temperature points follow the same behaviour. The temperatures in the COMSOL simulation are a bit lower than in the experiment. The slope of the curves are also a bit steeper in the experiment.

Relevant factors to consider when comparing the results would be uncertainty form the experiments. There are some factors in the lab that can not be controlled, which gives inaccuracy. Compared to the heat loss found in Section 6.4.8, it might

(a) COMSOL

(b) Experiment 1; Table 6.4
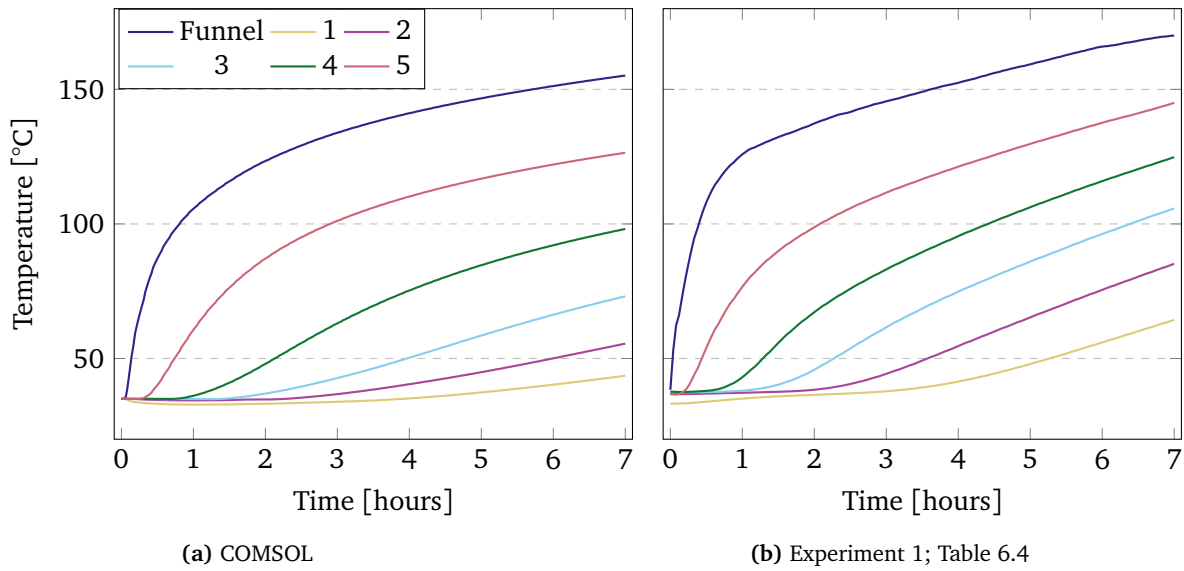
Figure 7.2: Temperature in the top funnel and the storage from bottom (1) to top (5) with two tubes used as insulation.
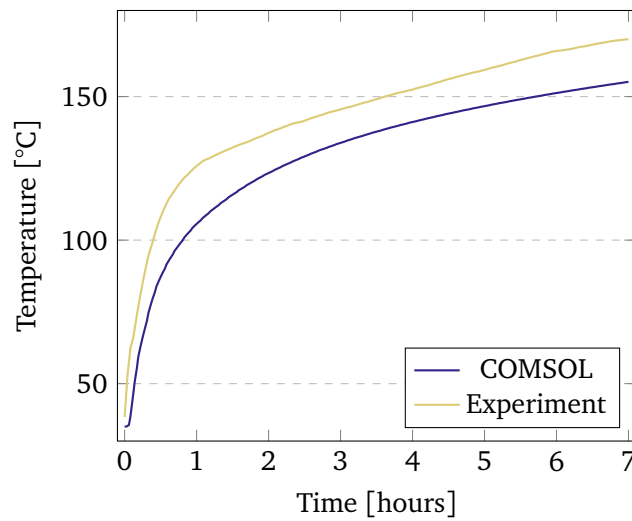
Figure 7.3: Comparison of the temperature in the top funnel between COMSOL and experiment.

indicate that the heating element in the experiments has a slightly higher power than the desired 500 W. It looks like the COMSOL simulation heat the funnel a bit slower than the experiment. The heat loss applied in COMSOL from the tank to the surroundings may not be identical with the experiment and this may also affect the results.

Figure 7.3 show a comparison between the simulation and the experiment, at the top funnel. It can be seen that the temperatures follow the same behaviour and the temperature in the simulation are around 10-15 °C offset from the experimental temperatures. The error for the experimental thermocouples, discussed in Section 4.5.3, is so small that it has not been considered in this comparison. Since the simulation and the experiment correlates well in behaviour, it is believed that COMSOL can be a good tool to investigate the potential of the funnel at reduced power before overflow. Temperature difference between simulations with different insulation may be an indication for how much the system can improve. This should be further investigated.

7.3.2 COMSOL Results

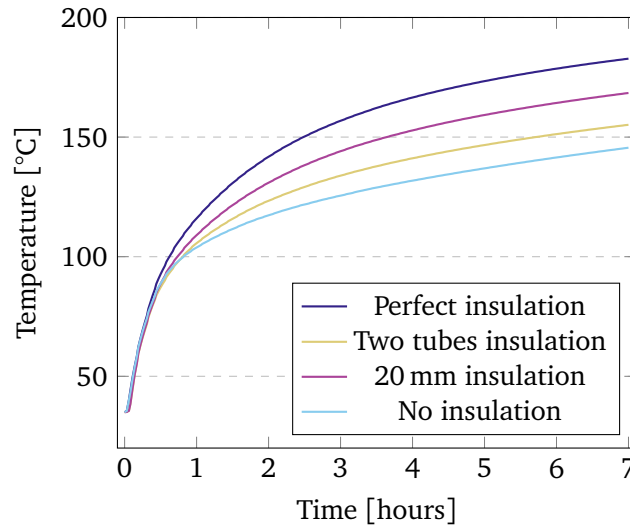| Simulation	Temperature funnel	Temperature top storage	Temperature bottom storage
No insulation	145 °C	119 °C	45 °C
Two tubes	157 °C	127 °C	43 °C
Insulating material	167 °C	132 °C	45 °C
Perfect insulation	182 °C	141 °C	39 °C

Table 7.2: Temperatures in the tank after seven hours, simulated with COMSOL with different insulation around the funnel tube.

The temperatures from the simulations are presented in Table 7.2. The behaviour of all the simulations are similar to the results with two tubes as insulation in Figure 7.2. The only differences is that with better insulation the temperature in the top funnel and top storage increases. The temperature in the bottom is quite similar for all the simulations. Additional graphs for all the simulations are provided in Appendix A.

7.3.3 Discussion

In Figure 7.4 the temperatures in the top funnel for the different cases are compared over time. It can be seen that for the first half hour there is no difference, but after that, the temperatures in the funnel starts to differ a bit. Insulating the funnel tube has a positive effect on the temperature in the funnel, and perfect insulation results in the highest temperatures in the funnel. Just having two tubes

Figure 7.4: Temperature in the top funnel compared for different insulation around the funnel tube with COMSOL.

that reduces the movement of oil around the funnel tube also provides an insulating effect. Using the made up material with 20 mm thickness wrapped around the funnel tube gives an even higher temperature.

The biggest heat loss in the funnel is from the top funnel to the storage, showing the importance of this part in the system. The effect of diffusion is quite high and dominates the heat transfer inside the system at reduced power. The heat emitted from the funnel and into the storage diffuses further down the storage. Better insulation around the funnel tube will probably cost more than it will improve the system, as long as the funnel top is difficult to insulate and the highest temperatures are present there.

It can be concluded that insulation around the funnel tube can result in higher temperature in the funnel. However, the best effect will only be reached if a suitable insulating material is found, that can be submerged in oil, and one is able insulate the top part of the funnel. Insulation materials were investigated in the project thesis [1] and it proved difficult to find a material that could be submerged in oil. Based on this, other solutions to improve the system should be investigate before insulating the funnel tube. Both due to the difficulty in finding a suitable insulation material as well as the fact that the cost may exceed the gains.

Chapter 8

Rock Bed

In this chapter experiments with a rock bed are presented. The experiments in this chapter include the following bullet points from the outline discussed in Section 1.1:

- Temperature measurements of the moving thermocline during charging and discharging (cooking).
- Charging experiments with different power levels to determine if insulation is needed on the internal funnel.
- Testing of a method for regulating the flow across the funnel barrier for temperature control in the storage.
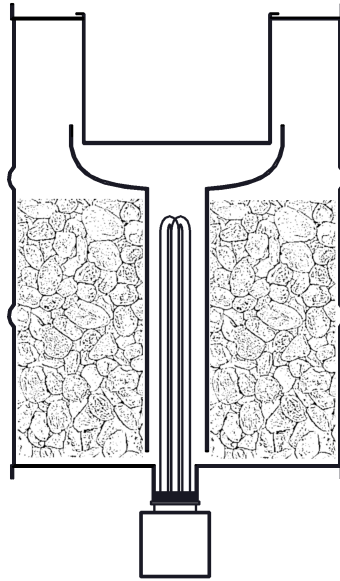- Testing the system with rock bed.

8.1   Motivation for the Experiments

As explained in Section 2.2.1, a packed bed storage uses the heat capacity of a loosely packed material to store energy. As a way of minimizing the amount of oil to make the system cheaper, the tank was filled with rocks. Experiments were conducted to evaluate if the rocks would improve the system both during charging and discharging.

8.2   Experimental Setup

Method   The experimental setup was the same as in Chapter 6, except that the tank was filled with rocks. The experiments were conducted similarly as in Chapter 4 and Chapter 6. One discharging experiment and multiple charging experiments were conducted.

Rock Bed   The amount of rocks placed in the tank replaced 36 liters of oil. The rocks filled the tank up to 34 cm, as illustrated in Figure 8.1, which is beneath the funnel top. River rocks were used, which can be seen in Figure 8.2. A total

Figure 8.1: Illustration of the system with rock bed.

amount of 43 liters of Duratherm 630 oil was added, enough for the oil to touch the bottom of the cooker at ambient temperature.

Most of the rocks were of the Chert type. Chert is a sedimentary rock composed of quartz. It is formed under low pressure and low temperatures, typically less than 1 kbar and temperatures lower than 100 °C. It was also found that most of the other rocks in the rock bed contained large amounts of quartz. Based on this, it was assumed that the thermal properties of the rock bed equaled those of rocks with a high quartz content. The rocks will be exposed to temperatures around 200 °C, which may fracture the rocks. It is, however, believed that the rocks should be able to withstand these temperatures, as discussed in Section 2.2.1.

Thermocouples   To better investigate how the temperature in the rock bed varied, four more thermocouples were placed in the storage. These new thermocouples have been placed in-between those used in Chapter 6, so that there is a measurement of temperature every 5 cm.

8.3   Relevant Properties

Using data from Waples and Waples [18], the specific heat capacity of the rock bed at 150 °C is set to 800 J/(kgK). A temperature of 150 °C has been chosen because it is often the average temperature in the storage when the system is charged and stratified. The heat capacity is an estimate and, therefore, will have a certain degree of uncertainty. The density of the rocks is 2648 kg/m^3. The mass of rocks in the tank is 95.3 kg and the total mass of rocks and oil combined is 128.7 kg.

(a) (b)

Figure 8.2: The rocks used in the rock bed.

Using Equation (2.11), the total specific heat capacity of the system is calculated to be 1204.8 J/(kgK). The total thermal capacity at 150 °C calculated with Equation (2.10) is 155.0 kJ/K. The total thermal capacity in the system without rocks, at 150 °C, is 144.9 kJ/K. With rocks, the thermal capacity of the system has increased by approximately 7%.

8.4 Expansion of Oil

With the rock bed there is now less oil in the tank. However, since a change in cross section does not affect the expansion of the oil in height, the oil in the storage with a rock bed will expand the same height as with no rock bed. This can be seen with Equation (8.1).

$$h_{oil} = \frac{m}{A \rho_{temp}} = \frac{A h_0 \rho_0}{A \rho_{temp}} = \frac{h_0 \rho_0}{\rho_{temp}} \tag{8.1}$$

$$h_{oil} = \frac{h_m \rho_m}{\rho_{temp}} \tag{8.2}$$

Here, h_{oil} is the height of the oil. m is the mass of the oil that can be expresses as $m = A h_0 \rho_0$, and h_0 and ρ_0 are constant values from the initial temperature of the oil before heating. The area A will be canceled out. In Equation (8.2) with all the terms cancelled out, it can be seen that the density is the only factor that

changes due to temperature changes in the oil. Hence the density is the only factor that affects the height of expansion. As a results of this, the expansion of oil with a rock bed will be the same as without rocks.

8.5 Results and Discussion

The main goal with the rock bed experiments is to investigate if it improves the system. Therefore, results from charging and discharging are presented and compared to the similar experiments done earlier in this thesis.

8.5.1 Charging

The charging experiments can be seen in Table 8.1.

| N$^{\underline{o}}$	Initial oil temperature	Funnel height	Charging power	Overflow temperature
1	24 °C	25 mm	1800 W	217 °C
2	35 °C	29 mm	1800 W	232 °C
3	78 °C	22 mm	500 W	No overflow

Table 8.1: Overview of charging experiments done with rock bed.

Full Power In Figure 8.3, charging of the system with rock bed is compared to experiment 5 in Table 6.1 and is referred to as the experiment "without rock bed". The heating element is set to full power (1800 W), with a funnel height that produces an overflow temperature around 215 °C.

It can be seen in the graph that the behaviour is quite familiar to the results seen in the earlier experiments without rock bed. However, there are some notable differences, especially when it comes to the overflow. Without rock bed there is a quite drastic dip in the temperature during overflow, seen after 3 hours in Figure 8.3b, followed by a steep and linear increase in temperature at the top of the funnel.

With rock bed, the temperature in the funnel during overflow is more stable and the typical dip behaviour is not as dominant. The dip with rock bed can be seen after 4 hours in Figure 8.3a. After the dip, the temperature in the top funnel does not increase as much as it does without rock bed. This indicates that the circulation is negatively affected by the rock bed and probably reduced. With the more stable temperature in the top funnel, the system is able to charge the storage for a longer time before the temperature in the funnel top reaches the critical temperature of 220 °C, marked with the red dashed line in Figure 8.3. With rock bed, one is able to charge the system for 4 hours and 51 minutes, which is 41 minutes longer than without rock bed. This leads to 1.00 kWh more energy in

the system before reaching the safety temperature. As a reference, charging the system for one hour at full power increases the energy in the system by 1.42 kWh.

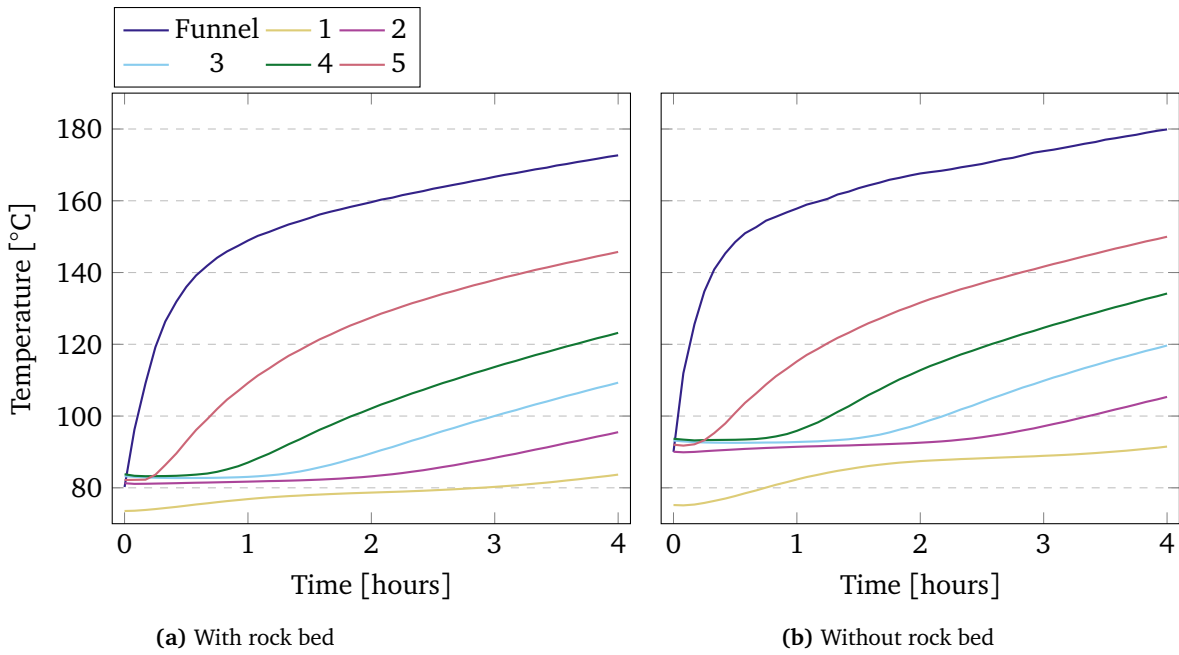**(a)** With rock bed
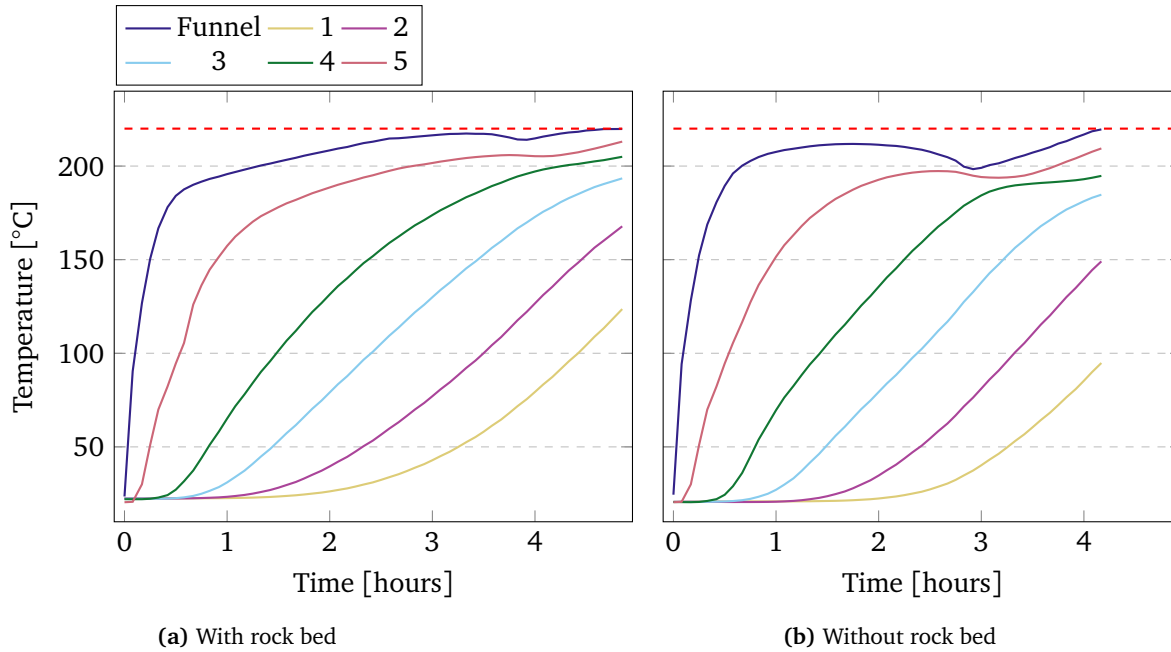
(b) Without rock bed

Figure 8.3: Temperature in the top funnel and the storage from bottom (1) to top (5) during charging with and without a rock bed. The red, dashed line is the critical temperature of 220 °C.

Reduced Power   Figure 8.4 shows the charging of the system with reduced power compared to experiment 2 from Table 6.4 referred to as "without rock bed". It can be seen that the differences between the two experiments are small. With rock bed, the temperature difference between the top storage (5) and point 4 in Figure 8.4 is a bit larger than in the experiment without rock bed. This is probably due to the increased thermal capacity that the system with rock bed has. The thermocouple at the top storage is the only one presented that is not submerged in rocks.

8.5.2   Ability to Store Energy

The loss of the average temperature from the system with rock bed is compared to the system without rock bed after being fully charged and left overnight. It can be seen in Figure 8.5 that the average temperatures in the tank are the same overnight. Since the system with rock bed has a higher thermal capacity compared to the one without, it can store more energy overnight. However, there are no differences when it comes to the heat losses.

(a) With rock bed

(b) Without rock bed

Figure 8.4: Temperature in the top funnel and the storage from bottom (1) to top (5) during charging with reduced power, with initial warm oil from the previous day.
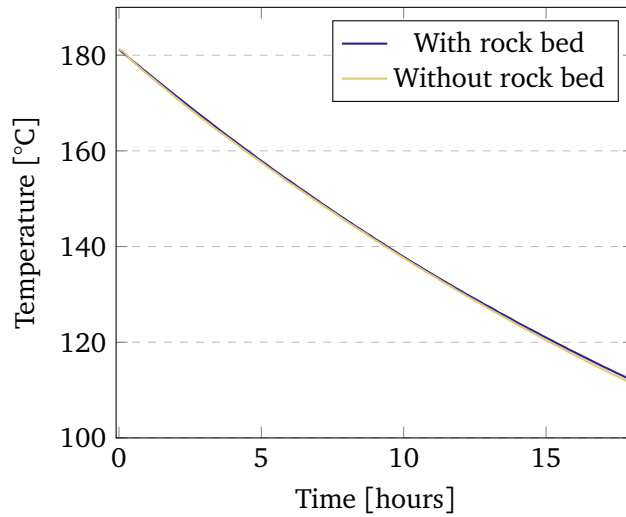
Figure 8.5: The average temperature in the tank with and without rock bed after the system is charged and left overnight.

8.5.3   Discharging

A discharging experiment was conducted with thermally stratified oil in the storage when the experiment started. The temperature at the bottom storage was 109 °C and top storage was 220 °C. It took 28 minutes for the five liters of water to boil. This is quite similar to what we have seen in previous discharging experiments.

The system kept the water boiling for 6 hours and 15 minutes. This is a significant improvement compared to the 4 hours and 45 minutes with experiment 2 in Table 6.3, which is the similar experiment without rock bed.

In Figure 8.6, the temperature in the top and bottom of the storage, as well as the funnel temperature, is plotted for both with and without rock bed. It can be seen that the temperatures in the storage are similar in the beginning of the experiments. During discharging, the temperatures in the top storage behave quite similarly for both experiments, but there are significant differences in the temperatures in the bottom of the storage.

The temperature at the bottom of the storage increases during the first hours of discharging in both experiments. This increase in temperature is smaller for the system with rock bed. The temperature difference between the top storage and funnel is also significantly higher for the system with rock bed. This indicates that the rock bed reduces the circulation of oil in the tank. The oil flows slower down the funnel, resulting in better utilization of energy from the oil in the top funnel to the cooker. The oil that flows down the funnel and into the bottom storage is, therefore, colder because more heat has been transferred. The slight improvement of thermal capacity cannot explain why one is able to boil for 1 hour and 30 minutes longer, but the reduction of circulation is the most likely cause.

Table 8.2 shows the thermal energy that is stored in the system before discharging, the thermal energy left in the system after the water stops boiling, and the thermal energy utilized by the system during boiling. It can be seen that the system with rock bed is able to utilize more energy than without rock bed, as a result of the reduced circulation.

-	Energy stored	Utilized energy	Energy after
With rock bed	6.86 kWh	2.42 kWh	4.44 kWh
Without rock bed	6.27 kWh	2.14 kWh	4.13 kWh

Table 8.2: The thermal energy in the system before and after being discharged, with and without rock bed.

There is still a lot of energy left in the system when the water in the cooker stops boiling. The average temperature in the oil is, at this point, 130 °C. If it is possible to cook food until the temperature in the pot reaches 50 °C, then the lowest usable temperature in the oil would be 80 °C, which is found by using the 30 °C limit discovered in Section 6.4.7. When the system is charged with 6.86 kWh, one can extract 2.42 kWh before the water stops to boil and 4.31 kWh before the

(a) With rock bed   **(b)** Without rock bed
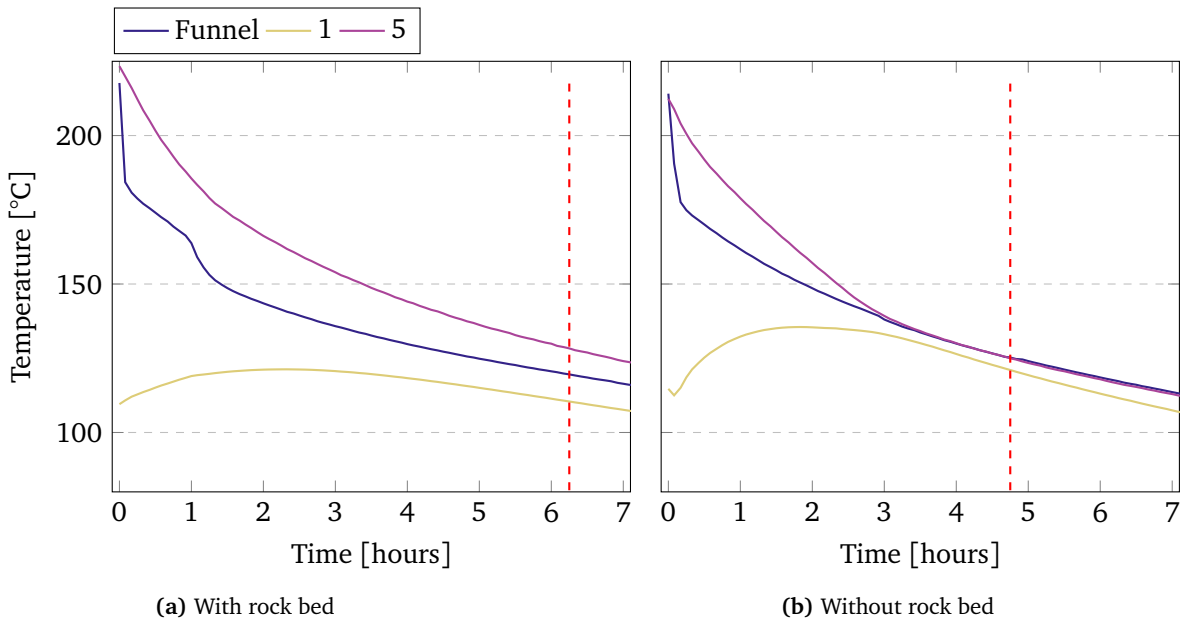
Figure 8.6: Discharging of the system with rock bed compared to discharging without rock bed. 1 and 5 is the temperature in the top and bottom storage. The red, dashed lines show where the boiling stopped.

oil is 80 °C. This gives the user 1.9 kWh more energy that perhaps can be used to cook food. It is important to remember that these experiments are done with a stratified storage.

If the system is fully charged and with uniform temperature, the system would have 8.18 kWh of thermal energy stored and 3.45 kWh of that energy is above the boiling limit at 130 °C.

By using the numbers for average energy requirements for cooking food, as mentioned in Chapter 1, one can calculate how many people the system can cook for based on the energy stored in the storage. The total daily energy requirement for cooking food for an average student in Uganda is 0.36 kWh, which means that this system is able to provide enough boiling energy for at least nine students when cooking from a fully charged storage. If one is able to cook at lower temperatures, the maximum number of students fed can be as high as 14. One can say that 5.3 kWh of available energy is stored in the system when fully charged and can be utilized to cook food, which gives enough energy for 14 students throughout a day. This calculation is based on a fully charged storage and does not take into account recharging of the system during the day, which would result in larger capacity. Real life experiments should be conducted to determine the actual capacity.

8.6   Summary

Comparisons of the system with and without rock bed have been conducted. The comparisons showed that the system with rock bed can charge for longer because the overflow temperature is more even, resulting in a more stratified storage. This is a result of the rock bed that slows down the circulation of oil, which also results in better utilization of the stored energy during discharging. The rock bed neither improves nor worsens the heat losses to the surrounding, so both systems have the same losses. Having a rock bed decreases the amount of oil needed in the tank. This is valuable, especially since the oil may eventually have to be replaced. A disadvantage of the rock bed is that it makes the system much heavier. Moving it requires not just extracting the oil, but also the rocks, which may result in transportation difficulties. However, it is still believed that the rock bed is beneficial to the system overall.

Energy calculations have been done and the system can provide enough energy to cook for at least nine students in Uganda when fully charged. If one is able to cook at lower temperatures, the number of students fed could increase by as much as five.

Chapter 9

Experiments with a Solar Photovoltaic System

In this chapter an experiment using a photovoltaic (PV) system is presented. The experiments in this chapter include the following bullet point from the outline discussed in Section 1.1:

- Charging with PV panels and a MPPT controller.

9.1 Experimental Setup

Method   The experimental setup is the same as in Chapter 8, but instead of using power from the electrical network, PV panels have been used as a power source. Charging experiments, as well as a rice cooking and bean cooking experiment, have been conducted. For the rice cooking experiment, the system was charged from the morning when initially cold and rice was cooked at lunch time. For the beans, the system had been charged the previous day to give the experiment a more realistic character. The system was charged from the morning and, around lunch time, the beans were cooked.

The PV System   It consists of six PV panels mounted in series on the roof of the Varmetekniske building at NTNU. They are faced southwards and are installed vertically, as seen in Figure 9.1. A vertical installation is not optimal, but will probably not make a significant difference due to Trondheim being situated at a latitude of 63° North.

The PV panels are polycrystalline cells from GetTek with an efficiency of 15.98% at Standard Test Conditions (STC), which is defined as a temperature of 25 °C and with a solar irradiance of 1000 W/m^2. Each panel is comprised of 60 PV cells with an area of 1.46 m^2, leading to a total area of 8.76 m^2. Each PV panel has a watt peak [Wp] of 260 at STC. Since the PV panels are connected in series the installed capacity for the PV system is 1.56 kWp. The technical datasheet for the PV panels is provided in Appendix F.

A disadvantage of connecting the PV panels in series is that shade on even one panel results in reduced overall power output. This is because the current through the connected PV panels is constant for a given irradiance. When there is shade on one of the panels, all other panels have to operate with the limited current from this panel [42]. An analogy to this is water flowing through a pipe, where an obstacle reduces the water flow for the entire pipe.

It was discovered that a shadow from one of the neighbouring roofs hit the panel at the bottom at around 13:30, which resulted in a much lower power output.

Figure 9.1: The PV panels used.

A Maximum Power Point Tracking (MPPT) charge controller is connected to the PV panels. The MPPT controller is a DC/DC converter that optimizes the voltage between the PV panels and utility grid. The voltage and current changes continuously due to fluctuating sunlight. The MPPT algorithm in the controller maximizes the power generated by the PV panel by carefully controlling the voltage. This ensures that the system operates at the maximum power point. This point is the voltage that ensures the maximum power from the PV system and is the optimal combination between voltage and current. The MPPT algorithm used by the controller is the Perturbation and Observation (P&O) version, which alters the operating voltage to ensure maximum power [43]. The user guide for the MPPT charge controller is provided in Appendix F.

## 9.2 Results and Discussion

9.2.1 The Rice Experiment
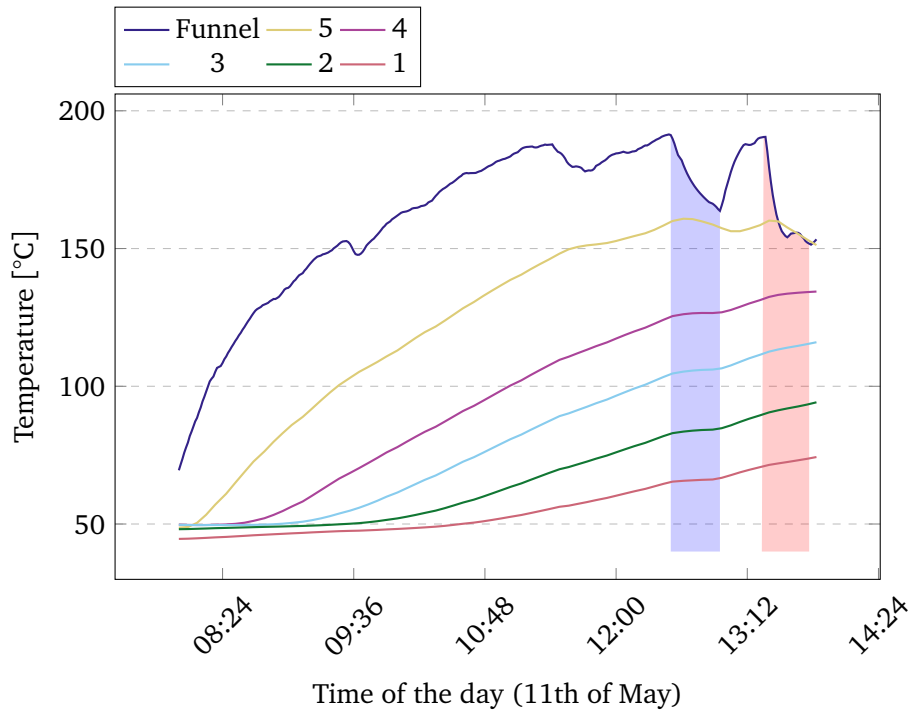
Figure 9.2: Temperature in the top funnel and the storage from bottom (1) to top (5) during charging with PV panels. The blue shaded area is when the heating element was turned off due to a fire alarm. The red shaded area is when rice was cooked.

Charging   The experiment was started at 07:50 on the 11th of May, which was a mostly sunny day. A detailed weather report is provided in Appendix E. The temperature in the funnel and the storage can be seen in Figure 9.2 and the provided power from the PV system can be seen in Figure 9.3, together with the solar irradience. The solar conditions the morning of the experiment were good, but became slightly more cloudy around 12:00. At 12:30 there was a fire alarm in the lab, which resulted in the heating element being turned off for 20 minutes. This is highlighted in blue in Figure 9.2. The temperature in the funnel decreased significantly when the system was turned off. A rice cooking experiment was completed and it was shown that it is possible to use the PV system to heat up the oil.

Before the fire alarm, the average power from the PV panels was 981.9 W, with an average solar irradience of 502 W/m^2. The temperature in the funnel was 191 °C at 12:30. The solar irradience was around 200 W/m^2 at 08:00. This increased to around 1000 W/m^2 at 11:00.

It can be seen that the behaviour of the temperature in the system during

charging is quite similar to what has been seen earlier in this thesis. The biggest difference is that the temperature in the funnel is very sensitive to the output power from the PV panels, meaning that the temperature in the funnel is a direct consequence of the power provided to the heating element. The behaviour in the storage is more stable and the fluctuating funnel temperature does not affect the temperature in the storage. The diffusion of heat from the funnel to the storage, seen earlier in this thesis, is present.
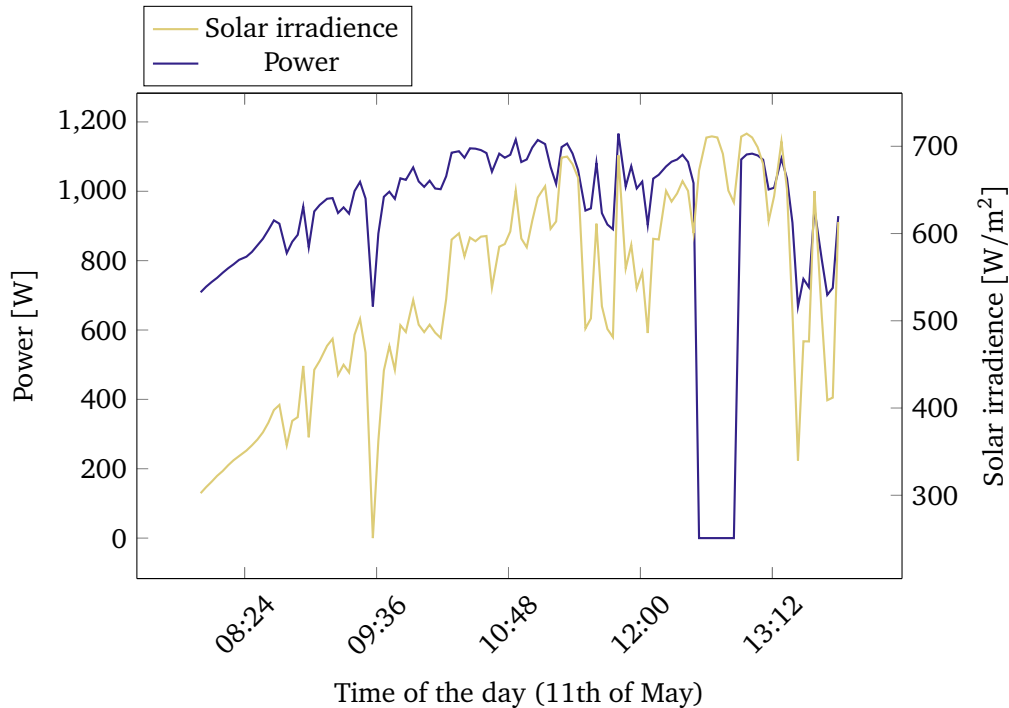
Figure 9.3: The power from the PV panels and the solar irradience during charging with the rice cooking experiment.

Rice Cooking At 13:21, after the system had been charged for six and a half hours with the PV panels, half a liter of rice, with one liter of water at ambient temperature, was set to cook. The system was still charging while the rice cooking experiment was conducted. The water started to boil after 18 minutes, and the rice was fully cooked after 28 minutes. The pot was not stirred while boiling. The rice was perfectly cooked. The cooker shows promise by being able to cook rice fast without burning.

9.2.2 Dry Beans Experiment

The experiment with dry beans was conducted on the 2nd of June, a warm and sunny day. The charging started at 08:00. The results from the experiment are

Figure 9.4: The beans during boiling.

provided in Appendix B. It was discovered that, although the solar irradiation was slightly higher, with an average of 567 W/m^2 compared to 502 W/m^2 the day of the rice cooking experiment (11th of May), the average power output was slightly smaller, with 932.5 W compared to 981.9 W. The outdoor temperature difference between the two experiments was around 8 °C throughout charging (Appendix E). The temperature coefficient for the PV panels shows that the output power decreases/increases 0.42% per °C above/below 25 °C. This means that the experiment on the 2nd of June would have had a decrease in power output of approximately 3-4% compared to the 11th of May, if the solar irradiation had been the same. A further potentially significant issue in the power output of the PV panels is the presence of pollen layers at this time of year. The quantitative impact is unknown, but it is believed that the effect is significant enough for it to be monitored in future experiments. Lastly, the angle of the sun was also 4° higher on this day, which may also have made a small difference on the power output.

Dry Beans Cooking Two kilos of dry beans were left to soak in 5.3 liters of water the night before the experiment. This amount of beans will, according to the data mentioned in Chapter 1, be enough to cover the daily bean ration for approximately 14 students. The beans were soaked to reduce the cooking time.

The pot with the beans was placed in the cooker at 12:02, with a temperature in the top funnel of 200 °C. It started to boil within an hour. The beans were fully cooked after one and a half hours.

9.2.3 Discussion

One has to be careful when cooking rice, as it can easily be burnt if the power is too intense. The cooking experiments conducted show that the system with the oiled pot-in-pot solution, is able to cook rice and beans effectively without burning the

food. The power to the cooker is evenly spread out at the bottom and side walls of the cooker, which seems to be advantageous. Given the high cooking quality of the system, it could guaranteed be sold as a bean or rice cooker and likely extended to other foods.

With PV panels connected, one seems to be able to cook multiple rounds of beans per day. The exact number needs to be investigated, but likely 3-4 batches. This will cover the daily need for beans for approximately 40-55 students in Uganda, where the daily need is 140 g of dry beans and 267 g of maize flour per student, per day. This indicates that the system has a higher potential than discussed in Chapter 8. These numbers cannot be compared directly, since the total daily energy need to cook food for a student was examined in Chapter 8, without recharging the system. However, it can clearly be seen that the potential calculated in Chapter 8 will increase when the PV panels are charging the system the whole day. With the ability to charge and cook at the same time, given good solar conditions, and later being able to cook with the stored energy at night, the system has high flexibility and good capacity.

It was also discovered that the oil between the pots emits fumes when the cooking pot is taken out of the cooker. Duratherm 630 oil was used, but vegetable oil should be tested to see how it functions as a heat transfer medium between the pots. In addition, the fuming of the vegetable oil in comparison to that of Duratherm 630 oil should be analyzed. This may be a health risk that must to be addressed before the system can be sold. When cooking beans, the chance of boiling over is quite high. This did not happen during the experiments, but if it happens, the water may come in contact with the oil between the pots and could rapidly vaporise. This may also prove to be a health risk that must, similarly, be addressed.

Previous experience with edible oils as heat transfer fluids indicate less fuming and equal well temperature tolerance to Duratherm 630 oil, which was used in the experiments.

Nevertheless, the system should be tested in real life situations. It would be of interest to see how the system works when being used daily. To do so, some improvements have to be made: the system must be closed, a valve for extracting and refilling oil must be added, and a temperature security switch must be installed to avoid overheating. The system is too small to be used by more than a small school, so it must be up-scaled if it is to be used in a large institution. Scaling up could result in either the same system with a bigger oil barrel or separating the system into two tanks (one for storage and one for the funnel and the cooker), which makes it possible to have a much bigger storage.

Charging the system with 1000 W seems to be sufficient for the system to work adequately and the PV system should, therefore, be designed with this power output as a requirement. The PV system used for the experiments in this thesis consisted of six PV panels. The amount of PV panels needed for a similar system in Sub-Saharan Africa will probably be less, due to the solar irradiation being

much higher.

A PV system is costly and it may be too expensive to acquire enough PV panels if it is to be used by a community of families, which means that the system will, in that case, be charged with lower power. Charging with low power has shown to be inefficient, but it will hopefully work well enough as long as the system is charged every day so that the initial oil temperature remains high.

Chapter 10

Conclusion

A single tank heat storage system for food preparation has been tested experimentally. The heating element is powered by photovoltaic (PV) panels and positioned inside an internal funnel below the cooking pot. As the oil expands with increasing temperatures, the vertical position of the funnel will determine at what oil temperature the overflow to the heat storage compartment on the outer side occurs. Heat extraction from the storage to the cooker happens by natural convection during discharging.

Experiments have been conducted to validate the concept and to compare the performance with the addition of rocks in the storage compartment instead of purely liquid oil.

The conclusion is that the concept of having a funnel works well, as long as the power to the heating element is sufficiently high and the funnel height is suitably adjusted. The system can cook during charging or from the stored thermal energy. The temperature in the funnel rises quickly after the heating element is turned on with full power (1800 W), while the oil in the storage is slowly heated by the heat emanating from the funnel until overflow occurs. The storage becomes highly stratified as hot oil from the overflow accumulates in the top of the storage before it moves downwards as a thermal front. The funnel height must be adjustable, as the overflow temperature will depend on the temperature in the storage side. This makes it possible to always achieve the desired overflow temperature.

For safe use, the system must remain closed and it must be possible to extract the cooking pot for cleaning. Therefore, a pot-in-pot solution is tested, where the outer pot is fixed to the tank. The experiments conducted showed that this solution decreases the heat transfer significantly, but acceptable heat transfer can be achieved by adding a small amount of oil in-between the pots. This oiled system, however, results in exhaust fumes when the inner pot is taken out of the cooker.

It has been found that charging the system under reduced power results in the funnel concept working less efficiently, as the temperature in the funnel does not increase as quickly as desired due to heat transfer through the funnel wall to the storage. This means longer waiting times before cooking temperatures are reached. Tests with a double walled funnel tube to decrease the heat losses

through the funnel tube showed little differences. Dynamic simulations, using Comsol Multiphysics, showed that the improvements of having insulation on the funnel tube are minor. The upper component of the funnel undergoes the largest heat transfer, which is also the part which will be the most impractical to insulate. The experiments indicate that a power level of about 1000 W is enough to attain the desired effect of the funnel.

The system was filled with rocks to reduce the amount of oil needed. A positive side effect was that the rocks also increase the energy storage capacity of the system, as well as providing a more stable temperature increase while charging and a slower circulation of oil during discharging. This results in better energy utilization and provides a further reason for why the system should be made with a rock bed, if possible.

The experiments conducted with the PV system show that it is possible to charge the system and cook food at the same time with PV panels. This means that the system can be used as long as there is power to the heating element or enough energy in storage. The cooking experiments with rice and beans showed that the pot-in-pot solution works well for cooking these foods and is, thereby, expected to work just as well for other food items. Having heat transfer occur both through the bottom and side walls results in good heat transfer and small risks of overcooking. The system is simple and robust, can be made with local resources, and, hence, should be suitable for local business development. The credibility of the system should be further demonstrated in real life tests.

Chapter 11

Further Work

This chapter will focus on the further work that can be considered for the next phase of this project.

The system should be tested in a real life environment in Sub-Saharan Africa. The system, made with a 100 liter oil barrel, could be tested in a small school or in a small community of families, while an up-scaled version could be tested in a school or a refugee camp. It is of interest to see how the system behaves when it is being used every day. A funnel that can change between a wide range of heights to regulate the overflow temperature is advantageous in the lab, but in real life, it may not be as important. Since the PV system will charge the cooker every day, the initial temperature in the storage may become quite uniform and similar from day to day. A simplified lifting solution for the funnel should be developed, which can be done by having only two settings, one low and one high. The funnel should be lifted when heating from a warm tank to achieve the desired overflow temperature, while it should be lowered during discharging to ensure circulation even at lower temperatures in the storage.

A safety system is needed to cut the power in case of overheating of the oil. This can be made with a thermostat safety switch. A simple way of ensuring that the initial amount of oil in the system is sufficient is needed as well.

A valve to both fill and extract oil must be included to make it possible to move the system and change the oil when needed. The system should be tested with a rock bed, provided that it remains in one location.

It is difficult to lift the inner pot out of the cooker with the pot-in-pot solution, especially when the system is hot. An inner pot with handles should be made to make the extraction easier and safer.

The pot-in-pot solution can be improved by changing the oil between the pots. Some experiences with edible oils as heat transfer fluids indicate less fuming and equal temperature tolerance to Duratherm 630 oil, which was used in the experiments. Due to the acceptable cooking rates that the pot-in-pot solution provides, regulation of the heat transfer does not seem to be an important feature to include. However, it may be possible to implement a lifting device that can lift the inner pot to reduce the heat transfer if this is deemed important after testing in a

real-life environment.

A cost analysis of the system should be done to investigate if a cost reduction is necessary before producing at a larger scale. The most expensive component, excluding the PV panels, is currently the heating element. Scaling and connecting the PV panels, such that the voltage approaches the standard grid voltage, allows for the use of mass produced heating elements.

To improve the up-scaling properties of the system, the funnel and the storage could be separated into two separate tanks: one small tank with the funnel and the cooker at the top, and a larger tank where warm oil would be stored. The tanks would be connected with pipes at the top and bottom ends. This will make the storage larger and may reduce the heat losses from the storage to the surroundings, as well as from the funnel to the storage, due to the separate insulation. The cooker can also be positioned inside a building with the storage outside. An up-scaled system would be needed for the case of cooking food for schools with hundreds of students.

Bibliography

[1]   G. H. Nylund and A. Bjørshol, 'Sensible heat storage for cooking,' M.S. thesis, NTNU, Dec. 2020.

[2]   United Nations, *The sustainable development goals report 2019*, Accessed October,2020, New York, 2019. [Online]. Available: `https://unstats.un.org/sdgs/report/2019/`.

[3]   T. H. Mwampamba, 'Has the woodfuel crisis returned? urban charcoal consumption in tanzania and its implications to present and future forest availability,' *Energy policy*, vol. 35, no. 8, pp. 4221–4234, 2007.

[4]   P. K. Kajumba, K. Nyeinga, D. Okello and O. J. Nydal, 'Assessment of the energy needs for cooking local food in uganda,' Unpublished paper, 2021.

[5]   S. Karekezi, J. Wangeci and E. Manyara, 'Sustainable energy consumption in africa,' *UN-DESA Final Report. African Energy Policy Research Network, Nairobi*, 2004.

[6]   M. Wentzel and A. Pouris, 'The development impact of solar cookers: A review of solar cooking impact research in south africa,' *Energy policy*, vol. 35, no. 3, pp. 1909–1919, 2007.

[7]   E. Biermann, M. y. Grupp and R. Palmer, 'Solar cooker acceptance in south africa: Results of a comparative field-test,' *Solar energy*, vol. 66, no. 6, pp. 401–407, 1999.

[8]   F. P. Incropera, A. S. Lavine, T. L. Bergman and D. P. DeWitt, *Fundamentals of heat and mass transfer*. Wiley, 2007.

[9]   A. Bejan, J. Lage *et al.*, 'The prandtl number effect on the transition in natural convection along a vertical surface,' *Journal of Heat Transfer*, vol. 112, no. 3, pp. 787–790, 1990.

[10] T. FUJII, 'Experimental studies of free convection heat transfer,' *Bulletin of JSME*, vol. 2, no. 8, pp. 555–558, 1959.

[11] Y. S. Touloukian, G. A. Hawkins and M. Jakob, *Heat transfer by free convection from heated vertical surfaces to liquids*. 1947.

[12] W. P. Farmer and W. McKie, 'Natural convection from a vertical isothermal surface in oil,' in *MECHANICAL ENGINEERING*, ASME-AMER SOC MECHANICAL ENG 345 E 47TH ST, NEW YORK, NY 10017, vol. 87, 1965, p. 80.

[13]   P. Arabi and K. Jafarpur, 'Criteria for predicting transitions in free convection heat transfer from isothermal convex bodies in fluids with any prandtl number: A new analytical model,' *Heat Transfer Engineering*, vol. 38, no. 6, pp. 578–593, 2017.

[14]   I. Dincer and M. A. Rosen. John Wiley & Sons, Ltd Chichester, UK, 2010, ISBN: 978-0-470-74706-3.

[15]   S. Kalaiselvam and R. Parameshwaran. Elsevier Inc., 2014, pp. 1–430, ISBN: 978-0-12-417291-3.

[16]   I. Sarbu and C. Sebarchievici, 'Chapter 4 - thermal energy storage,' in *Solar Heating and Cooling Systems*, I. Sarbu and C. Sebarchievici, Eds., Academic Press, 2017, pp. 99–138, ISBN: 978-0-12-811662-3. DOI: `https://doi.org/10.1016/B978-0-12-811662-3.00004-9`. [Online]. Available: `https://www.sciencedirect.com/science/article/pii/B9780128116623000049`.

[17]   K. G. Allen, 'Rock bed thermal storage for concentrating solar power plants,' Ph.D. dissertation, Stellenbosch: Stellenbosch University, 2014.

[18]   D. W. Waples and J. S. Waples, 'A review and evaluation of specific heat capacities of rocks, minerals, and subsurface fluids. part 1: Minerals and nonporous rocks,' *Natural resources research*, vol. 13, no. 2, pp. 97–122, 2004.

[19]   Y. Han, R. Wang and Y. Dai, 'Thermal stratification within the water tank,' *Renewable and Sustainable Energy Reviews*, vol. 13, no. 5, pp. 1014–1026, 2009.

[20]   A. Mawire and S. H. Taole, 'A comparison of experimental thermal stratification parameters for an oil/pebble-bed thermal energy storage (tes) system during charging,' *Applied Energy*, vol. 88, no. 12, pp. 4766–4778, 2011.

[21]   W. Lou, Y. Fan and L. Luo, 'Single-tank thermal energy storage systems for concentrated solar power: Flow distribution optimization for thermocline evolution management,' *Journal of Energy Storage*, vol. 32, p. 101 749, 2020.

[22]   M. A. Rosen, 'The exergy of stratified thermal energy storages,' *Solar energy*, vol. 71, no. 3, pp. 173–185, 2001.

[23]   J. Fernandez-Seara, F. J. Uhı, J. Sieres *et al.*, 'Experimental analysis of a domestic electric hot water storage tank. part ii: Dynamic mode of operation,' *Applied thermal engineering*, vol. 27, no. 1, pp. 137–144, 2007.

[24]   J. E. Ahern, 'Exergy method of energy systems analysis,' 1980.

[25]   Office of Energy Efficiency & Renewable Energy, *Solar radiation basics*, Accessed May 19th, 2021, Washington. [Online]. Available: `https://www.energy.gov/eere/solar/solar-radiation-basics`.

[26]   GLOBAL SOLAR ATLAS, *Global photovoltaic power potential by country*, Accessed May 19th, 2021. From the "Global Solar Atlas 2.0, a free, web-based application is developed and operated by the company Solargis s.r.o. on behalf of the World Bank Group, utilizing Solargis data, with funding provided by the Energy Sector Management Assistance Program (ESMAP). For additional information: https://globalsolaratlas.info, 2019. [Online]. Available: `https://globalsolaratlas.info/download/sub-saharan-africa`.

[27]   Office of Energy Efficiency & Renewable Energy, *How does solar work?* Accessed May 19th, 2021, Washington. [Online]. Available: `https://www.energy.gov/eere/solar/how-does-solar-work`.

[28]   E. S. M. A. Program, *Global photovoltaic power potential by country*, 2020.

[29]   A. G. Siraki and P. Pillay, 'Study of optimum tilt angles for solar panels in different latitudes for urban applications,' *Solar energy*, vol. 86, no. 6, pp. 1920–1928, 2012.

[30]   R. Muthusivagami, R. Velraj and R. Sethumadhavan, 'Solar cookers with and without thermal storage—a review,' *Renewable and sustainable energy reviews*, vol. 14, no. 2, pp. 691–701, 2010.

[31]   N. Nahar, 'Performance and testing of a hot box storage solar cooker,' *Energy conversion and management*, vol. 44, no. 8, pp. 1323–1331, 2003.

[32]   K. Schwarzer and M. E. V. Da Silva, 'Solar cooking system with or without heat storage for families and institutions,' *Solar Energy*, vol. 75, no. 1, pp. 35–41, 2003.

[33]   A. Gomna, K. E. N'Tsoukpoe, N. Le Pierres and Y. Coulibaly, 'Review of vegetable oils behaviour at high temperature for solar plants: Stability, properties and current applications,' *Solar Energy Materials and Solar Cells*, vol. 200, 2019. DOI: `10.1016/j.solmat.2019.109956`.

[34]   O. K. S. Fjeldsæter and V. S. Stordal, 'Photovoltaic solar cooker with heat storage,' M.S. thesis, NTNU, Jun. 2020.

[35]   A. Mawire, 'Performance of sunflower oil as a sensible heat storage medium for domestic applications,' *Journal of Energy Storage*, vol. 5, pp. 1–9, 2016. DOI: `https://doi.org/10.1016/j.est.2015.11.002`.

[36]   J.-F. Hoffmann, G. Vaitilingom, J.-F. Henry, M. Chirtoc, R. Olives, V. Goetz and X. Py, 'Temperature dependence of thermophysical and rheological properties of seven vegetable oils in view of their use as heat transfer fluids in concentrated solar plants,' *Solar Energy Materials and Solar Cells*, vol. 178, pp. 129–138, 2018. DOI: `10.1016/j.solmat.2017.12.037`.

[37]   *Technical data duratherm 630*, Duratherm fluids. [Online]. Available: `https://durathermfluids.com/pdf/productdata/heattransfer/duratherm-630.pdf`.

[38] REOTEMP Instruments, *Type k thermocouples*, Accessed April, 2021, San Diego, 2011. [Online]. Available: `https://www.thermocoupleinfo.com/type-k-thermocouple.htm`.

[39] pico Technology, *Picolog 6 data logging software*, Accessed May 4th, 2021, 2011. [Online]. Available: `https://www.picotech.com/library/data-loggers/picolog-6-data-logger-software`.

[40] *Comsol multiphysics*®, version 5.5, Stockholm, Sweden: COMSOL AB. [Online]. Available: `www.comsol.com`.

[41] *Cfd module user's guide*, version 5.5, COMSOL Multiphysics®, COMSOL AB, Stockholm, Sweden, 2019. [Online]. Available: `https://doc.comsol.com/5.5/doc/com.comsol.help.cfd/CFDModuleUsersGuide.pdf`.

[42] G. M. Masters, *Renewable and efficient electric power systems*. John Wiley & Sons, 2013.

[43] MathWorks, *Mppt algorithm*, Accessed May. 2021. [Online]. Available: `https://se.mathworks.com/solutions/power-electronics-control/mppt-algorithm.html`.

Appendix A

Additional Results from COMSOL Simulations
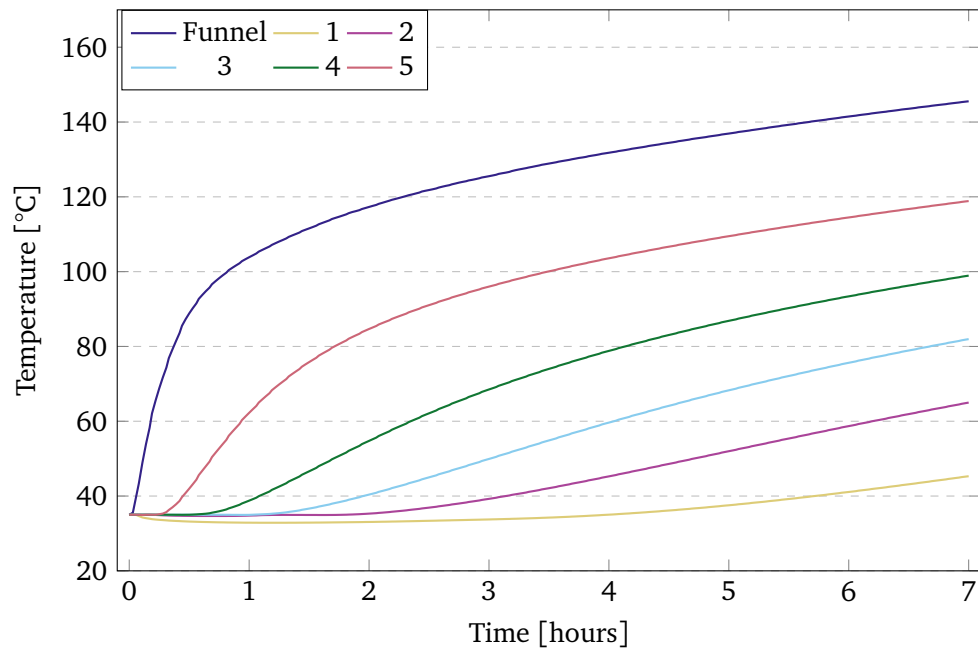
COMSOL simulation without insulation at the funnel tube. Temperature in the top funnel and the storage from bottom (1) to top (5).
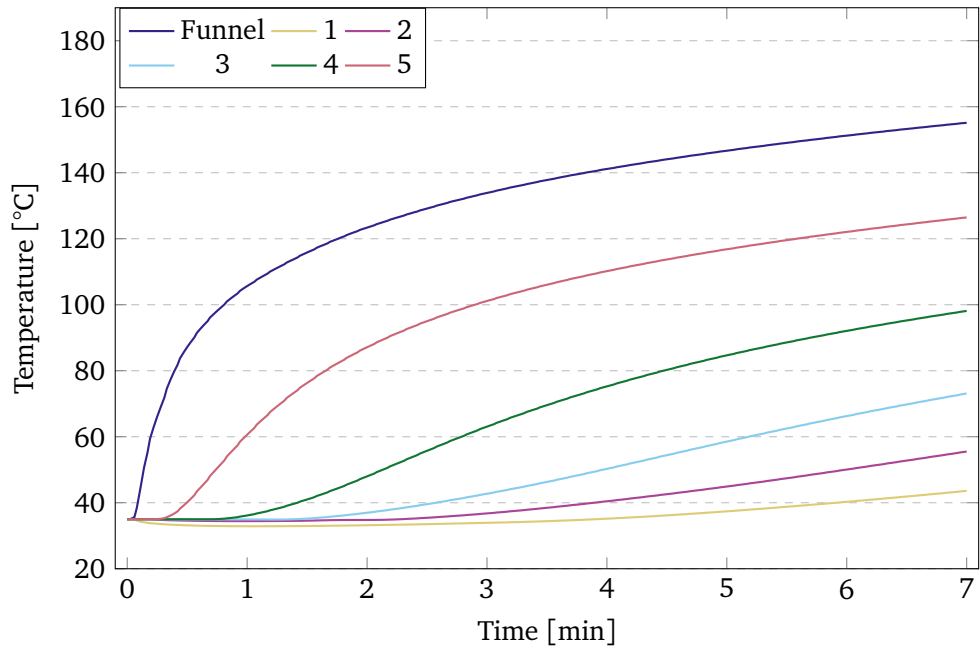
COMSOL simulation with two tubes as insulation around the funnel tube. Temperature in the top funnel and the storage from bottom (1) to top (5).
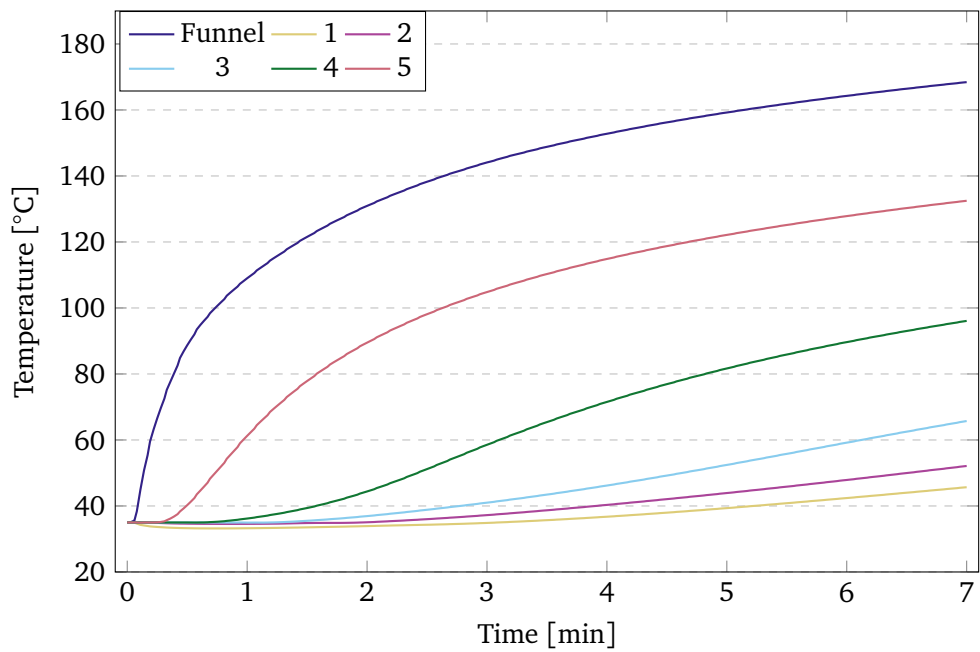
COMSOL simulation with a 20 mm insulation around the funnel tube. Temperature in the top funnel and the storage from bottom (1) to top (5).
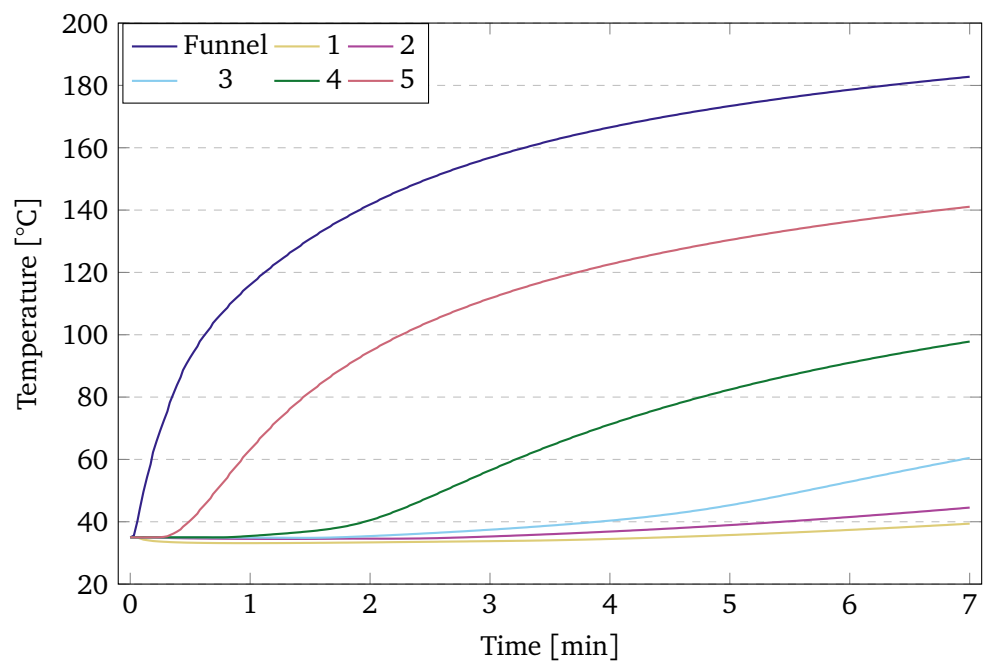
COMSOL simulation with perfect insulation at the funnel tube. Temperature in the top funnel and the storage from bottom (1) to top (5).

Appendix B

Additional Results from Experiments with PV panels
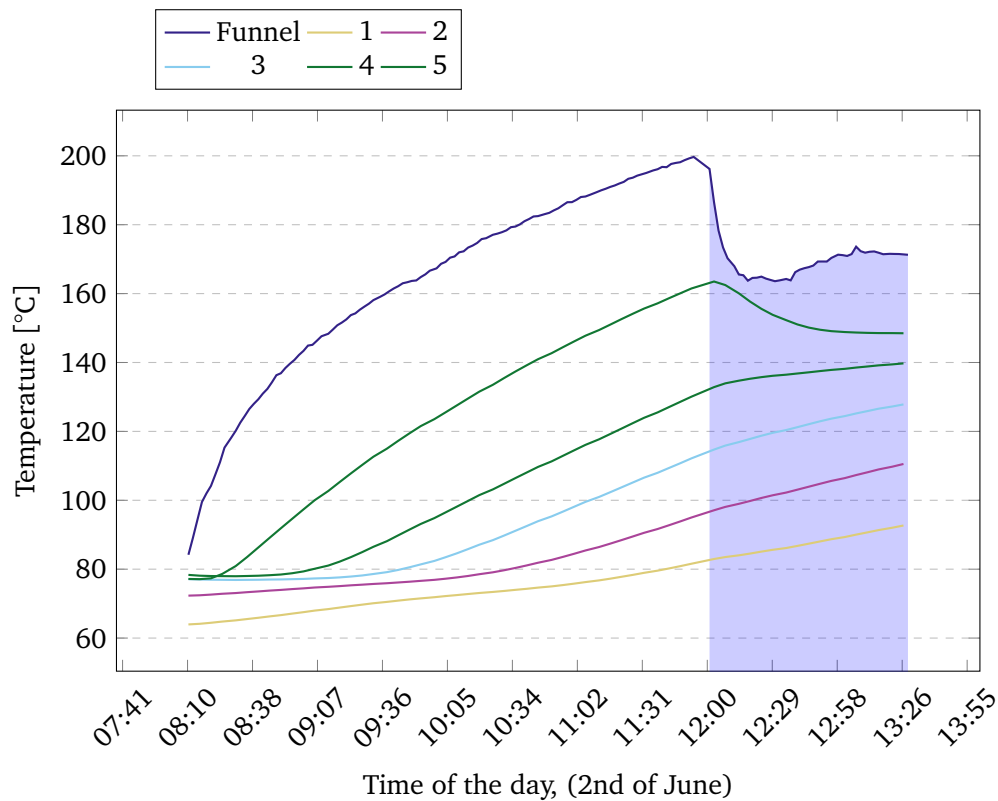
Temperature in the top funnel and the storage from bottom (1) to top (5) during charging with PV panels and cooking beans. The blue shaded area is when beans where cooked.
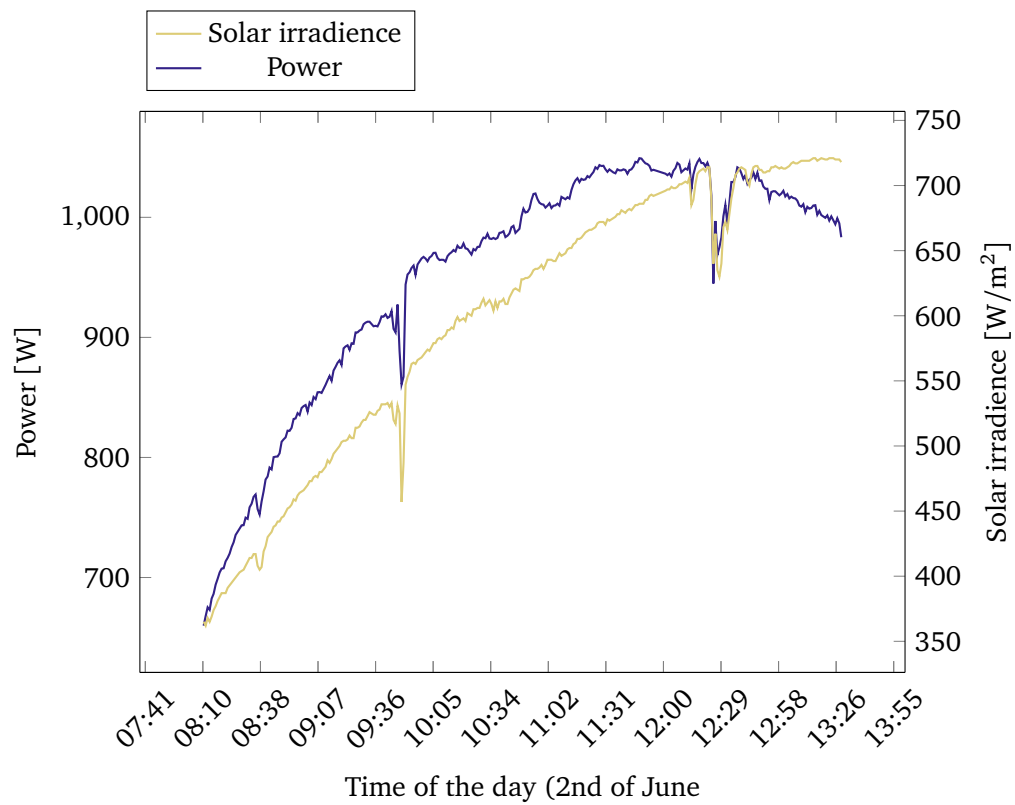
Power from the PV panels and the solar irradience during charging during the bean cooking experiment.

Appendix C

Detailed Drawing of the New System
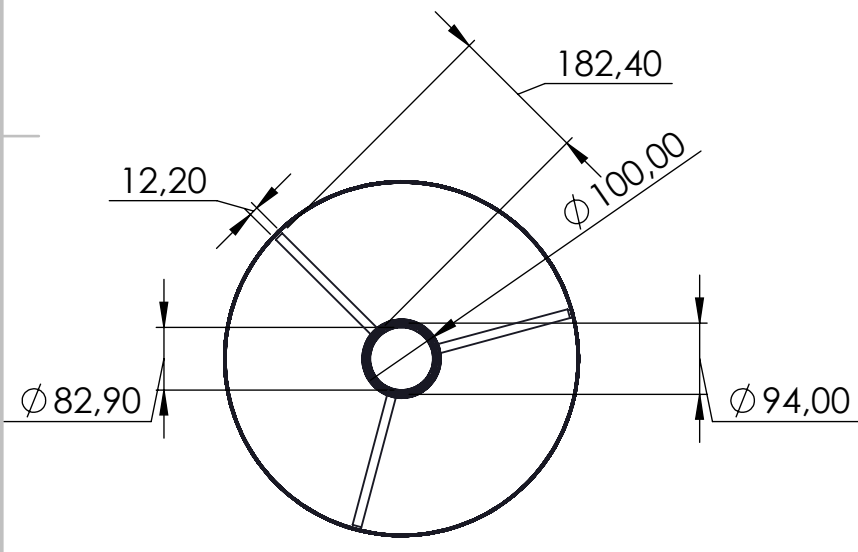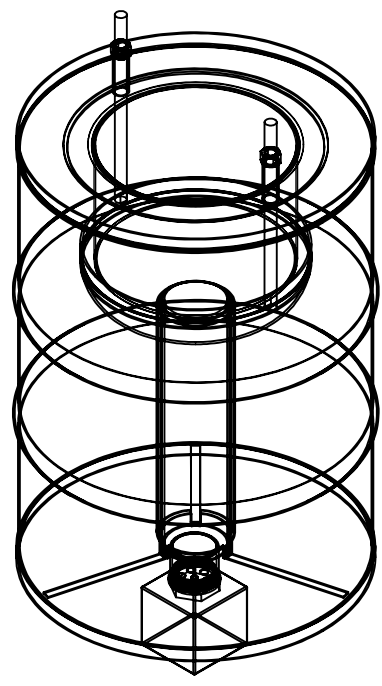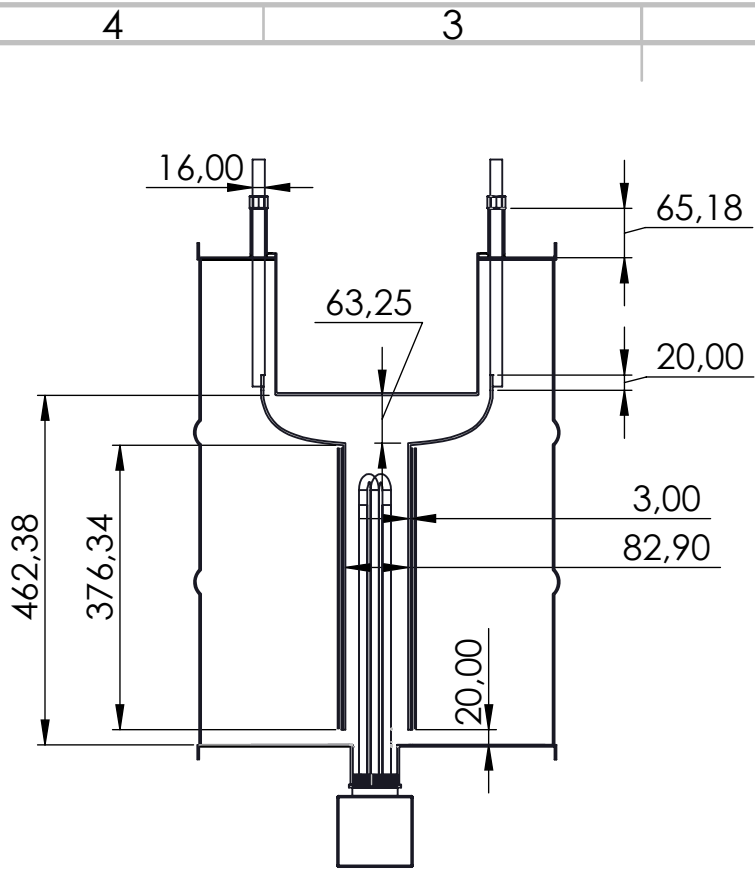
16,00

65,18

63,25

20,00

462,38

376,34

3,00

82,90

20,00

182,40

12,20

⌀100,00

⌀82,90

⌀94,00

	NAME	SIGNATURE	DATE				TITLE:
DRAWN							
CHK'D							
APPV'D							
MFG							
Q.A							

MATERIAL:

DWG NO.

A4

WEIGHT:

SCALE:1:10

SHEET 1 OF 1

Appendix D

PV Power Potential

Norway
(up to parallel 60°N)
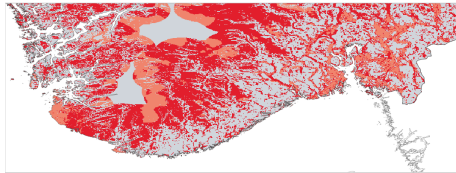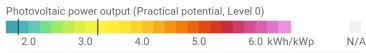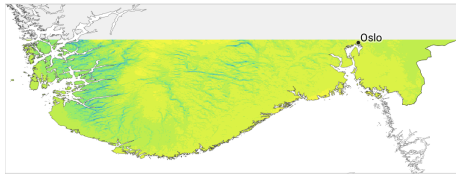
Photovoltaic power output (Practical potential, Level 0)

2.0   3.0   4.0   5.0   6.0 kWh/kWp   N/A

Practical potential zonation: ■ Level 2 ■ Level 1 ■ Level 0

The boundaries, colors, denominations and any other information shown on the maps do not imply, on the part of The World Bank, any judgment on the legal status of any territory, or any endorsement or acceptance of such boundaries.

INDICATORS

Total area / Evaluated area	625,217 / 53,892 km²
Population (2018)	5,314,336
GDP per capita (2018)	81,807 USD
HDI / rank (2017)	0.95 / 1
Electricity consumption per capita (2014)	23,000 kWh/year
PV installed capacity (2018)	68 MWp
Average theoretical potential (GHI) / rank	2.583 kWh/m² / 209
Average practical potential, level 1 / rank	2.761 kWh/kWp / 208
PV equivalent area	4.28%
PVOUT seasonality index (country range)	14.97 (5.79 − 66.81)
LCOE average (country range)	0.13 (0.12 − 0.16)

DISTRIBUTION OF PHOTOVOLTAIC POWER OUTPUT

kWh/kWp	41.3 %	55.0 %	100.0 %	of evaluated area
over 3.0	0.8 %	1.9 %	2.3 %	
3.0 − 2.8	17.0 %	25.4 %	45.8 %	
2.8 − 2.6	15.1 %	18.4 %	32.5 %	
2.6 − 2.4	6.6 %	7.3 %	13.2 %	
2.4 − 2.2	1.5 %	1.7 %	4.2 %	
below 2.2	0.3 %	0.4 %	2.0 %	

Practical potential: ■ Level 2 ■ Level 1 ■ Level 0

SUMMARY STATISTICS

Theoretical potential (kWh/m²) ■ GHI		Practical potential, Level 1 (kWh/kWp) ■ PVOUT	
Maximum	2.80	Maximum	3.06
Percentile 75	2.66	Percentile 75	2.88
Median	2.61	Median	2.80
Average	**2.59**	**Average**	**2.76**
Percentile 25	2.55	Percentile 25	2.67
Minimum	2.23	Minimum	2.17
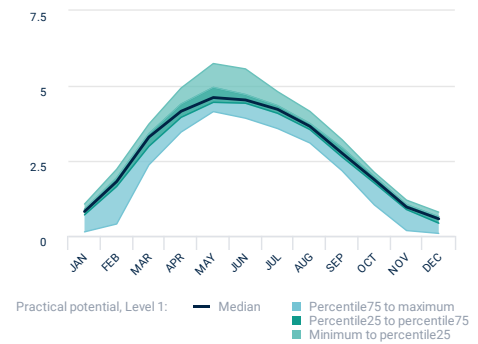
MONTHLY VARIATION OF PHOTOVOLTAIC POWER OUTPUT

Practical potential, Level 1: — Median   ■ Percentile75 to maximum   ■ Percentile25 to percentile75   ■ Minimum to percentile25

globalsolaratlas.info/global-pv-potential-study/

Norway

Average theoretical potential (GHI, kWh/m²) **2.583**

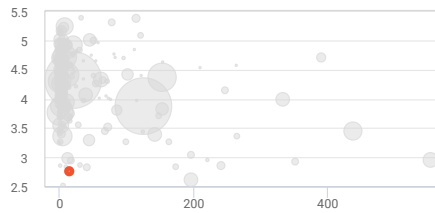
Seasonality index **14.97**

Human development index (2018) **0.95**
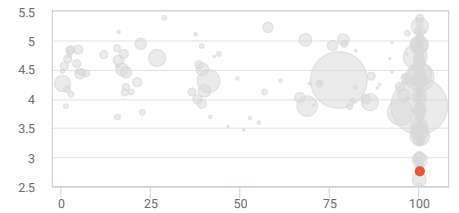

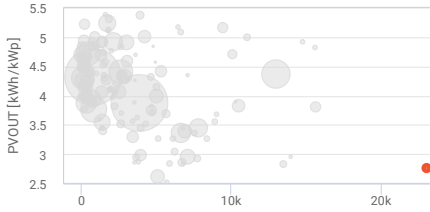**PV installed capacity** (MWp, 2018) **68**

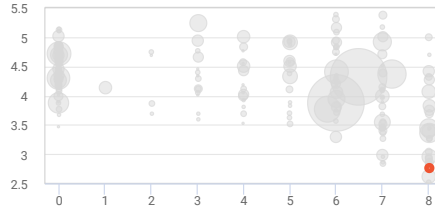**PV installed capacity per capita** (Wp, 2018) **13**

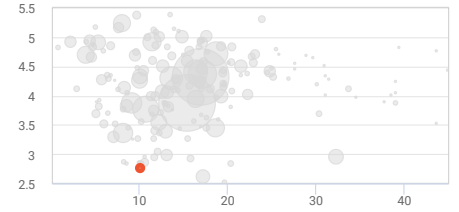**Access to electricity** (% of rural population, 2016) **100.0**

Electricity consumption (kWh/capita/year, 2014) **23,000**

Reliability of supply and transparency of tarrif **8.0**

Approximate electricity tarriffs (USD cents, 2019) **10.0**

© 2021 The World Bank Group

globalsolaratlas.info/global-pv-potential-study/

ABOUT

The World Bank Group publishes this factsheet as a part of the Global Photovoltaic Power Potential study, analyzing data from the Global Solar Atlas, World Bank Open Data, and other public sources. It is a part of the ESMAP initiative on Renewable Energy Resource Mapping, to support the appropriate scale-up of solar power in the worldwide energy mix.

The methodology and details behind the data analytics, explaining the graphics and figures in this factsheet, are discussed in the study.The findings aim to address the needs of policymakers, project developers, financial and academic sectors, as well as professionals and individuals interested in solar energy.

This factsheet involves numerical and graphical components:

- Photovoltaic power potential map of the country with the unified color legend for all countries worldwide (thus maps from various factsheets are comparable). Minima and maxima intervals for the country are marked in the legend.
- Country zonation map, showing how the country area is split into practical potential levels 0, 1 and 2
- Indicators section present basic country facts and statistics relevant to PV status in the country
- Summary statistics provide selected results of country-based evaluation of theoretical (GHI) and practical potential on level 1 (PVOUT)
- Distribution of photovoltaic power output histogram communicates how much land in the country is available in practical potential levels 0, 1 and 2, and various PVOUT ranges. It helps to understand, what might be the approximate area for PV development available in the best or moderate parts of the country.
- Monthly variation of the photovoltaic power potential details the seasonal PV electricity generation throughout a typical year; it is an important supplement to the seasonality index
- The bubble charts portray the position of the country in the global context of socio-economic and energy-related indicators. The bubble size is proportional to the population of the country. Current country is highlighted, other countries are in grey. Axis X represents the given indicator, axis Y represents the average practical PV potential at level 1.

Explore more

For more country fact-sheets, country and regional maps, interactive tools, PV calculator, statistics, reports and raster data in GIS formats visit Global Solar Atlas at https://globalsolaratlas.info.
More detailed data and technical solutions for specialists are provided by Solargis company (https://solargis.com).

© 2021 The World Bank Group

GLOSSARY

Theoretical PV Potential

Global horizontal irradiation (GHI, measured in $kWh/m^2/day$), the long-term amount of solar resource available on a horizontal surface on Earth.

Practical PV Potential

Photovoltaic power output of a PV system (specific yield, measured in kWh/kWp/day); in this case, the long-term power output produced by a utility-scale installation with fixed-mounted, monofacial c-Si modules with optimum tilt

- **Level 0** – Practical potential disregarding any land-use constraints
- **Level 1** – Level 0 practical potential, excluding land with identifiable physical obstacles to utility-scale pv plants
- **Level 2** – Level 1 practical potential, excluding land possibly under land use regulations due to nature and cropland protection

Economic PV Potential

Levelized cost of electricity (USD/kWh) – the lifetime costs associated with construction and operation of the power plant divided by the electricity produced during this lifetime (the lower the cost, the higher is the economic potential)

PV seasonality index

Ratio between the highest and the lowest of monthly long-term PVOUT averages.

PV equivalent area

Presumed country area proportion to be covered by PV plants producing the equivalent of yearly electricity consumption. The estimated area includes both the active area of PV modules and the area between the module rows (assuming the optimum row spacing).

Total / Evaluated area

Total area is a surface area of a country derived from official statistics, including inland water bodies and some coastal waterways. Evaluated area is a true area, from which the statistics were calculated. It includes land areas, without coastal waters, interior parts of the large water bodies, areas with missing input data and minor outliers caused by input data resolution.

Acronyms

DIF – Diffuse horizontal irradiance
DNI – Direct normal irradiance
GDP – Gross domestic product
GHI – Global horizontal irradiance
HDI – Human development index
LCOE – Levellized cost of electricity
PVOUT – Photovoltaic power output
PV – Photovoltaic

DATA SOURCES

Solargis

Average theoretical potential – GHI $(kWh/m^2/day)$
Average practical potential – PVOUT (kWh/kWp/day)
Distribution of photovoltaic power output
Monthly variation of photovoltaic power output
PV equivalent area (% of the total country area)
PV seasonality index

The World Bank

Total area (2018, km^2). Accessed on 2019-11-06.
https://data.worldbank.org/indicator/ag.srf.totl.k2

Population, total (2017). Accessed on 2019-11-06.
https://data.worldbank.org/indicator/sp.pop.totl

GDP per capita (2017, current USD). Accessed on 2019-11-06.
https://data.worldbank.org/indicator/ny.gdp.pcap.cd

Human Development Index (2017). Accessed on 2019-16-10.
https://datacatalog.worldbank.org/human-development-index-hdi

Electric power consumption (2014, kWh per capita). Accessed on 2019-11-06.
https://data.worldbank.org/indicator/eg.use.elec.kh.pc

Access to electricity (2016, % of rural population). Accessed on 2019-11-06.
https://data.worldbank.org/indicator/eg.elc.accs.ru.zs

Reliability of supply and transparency of tariff. Accessed on 2020-01-24.
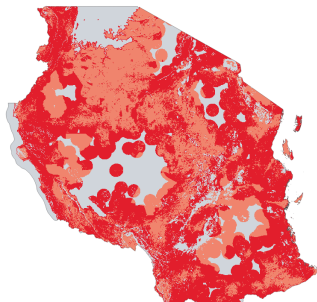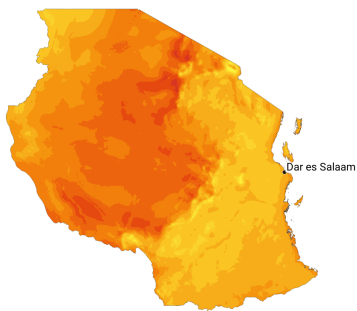World Bank, Doing Business, Measuring Business Regulations, Getting Electricity indicators.
https://www.doingbusiness.org/en/data/exploretopics/getting-electricity

Approximate electricity tariffs. Accessed on 2020-01-24.
World Bank, Doing Business, Measuring Business Regulations, Getting Electricity indicators.
https://databank.worldbank.org/reports.aspx?source=3001&series=IC.ELC.PRI.KH.DB1619

International Renewable Energy Agency (IRENA)

PV installed capacity (2018, MWp)
IRENA, Renewable Capacity Statistics 2019. Accessed on 2019-06-10.
https://www.irena.org/publications/2019/Mar/Renewable-Capacity-Statistics-2019

Levelized cost of electricity (2018, USD/kWh)
IRENA, Renewable power generation cost report 2018. Accessed on 2019-06-10.
https://www.irena.org/publications/2019/May/Renewable-power-generation-costs-in-2018

Tanzania

Photovoltaic power output (Practical potential, Level 0)

| | | | | | |
|2.0|3.0|4.0|5.0|6.0| kWh/kWp|

Practical potential zonation: ■ Level 2 ■ Level 1 ■ Level 0

The boundaries, colors, denominations and any other information shown on the maps do not imply, on the part of The World Bank, any judgment on the legal status of any territory, or any endorsement or acceptance of such boundaries.
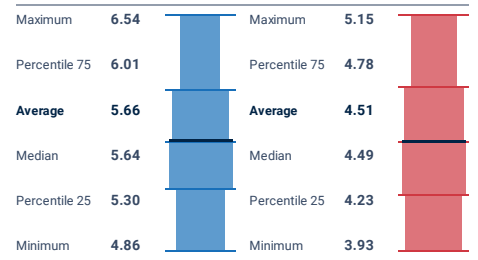
INDICATORS

Total area / Evaluated area	947,300 / 945,306 km²
Population (2018)	56,318,348
GDP per capita (2018)	1,051 USD
HDI / rank (2017)	0.54 / 150
Electricity consumption per capita (2014)	104 kWh/year
PV installed capacity (2018)	25 MWp
Average theoretical potential (GHI) / rank	5.657 kWh/m² / 46
Average practical potential, level 1 / rank	4.507 kWh/kWp / 73
PV equivalent area	0.003%
PVOUT seasonality index (country range)	1.31 (1.09 – 1.67)
LCOE average (country range)	0.09 (0.08 – 0.11)

SUMMARY STATISTICS

Theoretical potential	kWh/m²		Practical potential, Level 1	kWh/kWp
Maximum	6.54		Maximum	5.15
Percentile 75	6.01		Percentile 75	4.78
Average	**5.66**		**Average**	**4.51**
Median	5.64		Median	4.49
Percentile 25	5.30		Percentile 25	4.23
Minimum	4.86		Minimum	3.93

■ GHI   ■ PVOUT

DISTRIBUTION OF PHOTOVOLTAIC POWER OUTPUT

kWh/kWp	48.0 %	80.7 %	100.0 %	of evaluated area
over 5.0	1.9 %	3.1 %	3.7 %	
5.0 — 4.8	7.4 %	15.4 %	20.4 %	
4.8 — 4.6	7.8 %	16.5 %	20.1 %	
4.6 — 4.4	5.7 %	10.2 %	12.7 %	
4.4 — 4.2	13.9 %	18.3 %	21.5 %	
4.2 — 4.0	10.5 %	16.0 %	19.3 %	
below 4.0	0.9 %	1.2 %	2.3 %	

Practical potential: ■ Level 2 ■ Level 1 ■ Level 0

MONTHLY VARIATION OF PHOTOVOLTAIC POWER OUTPUT

Practical potential, Level 1: —— Median   ■ Percentile75 to maximum   ■ Percentile25 to percentile75   ■ Minimum to percentile25
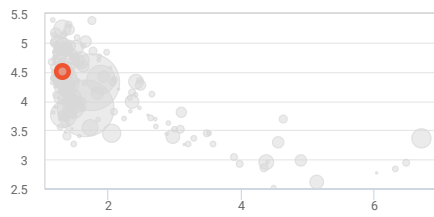
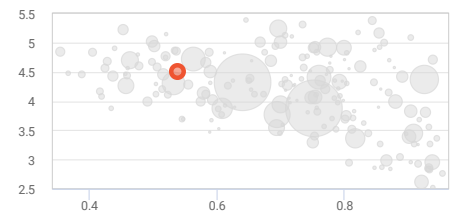globalsolaratlas.info/global-pv-potential-study/
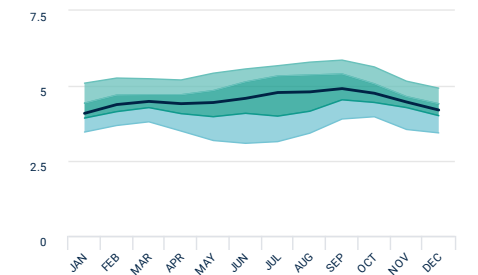
Tanzania

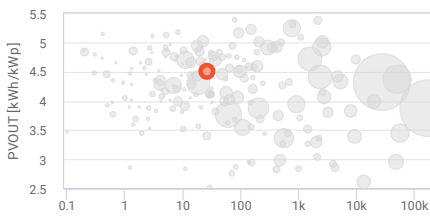**Average theoretical potential** (GHI, kWh/m²)   **5.657**
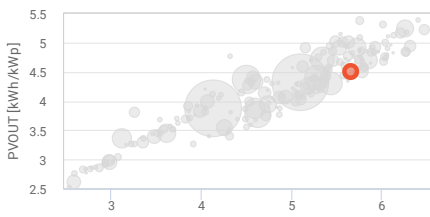
Seasonality index   **1.31**
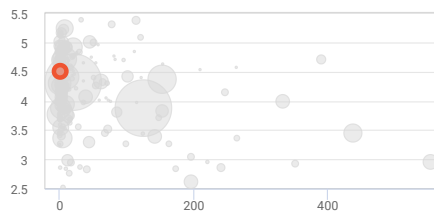

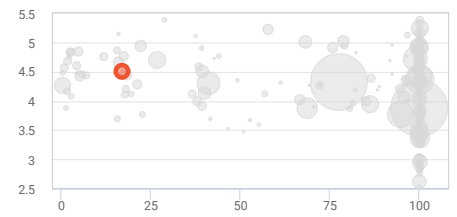**Human development index** (2018)   **0.54**

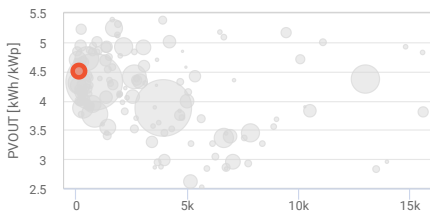**PV installed capacity** (MWp, 2018)   **25**

PV installed capacity per capita (Wp, 2018)   **0**
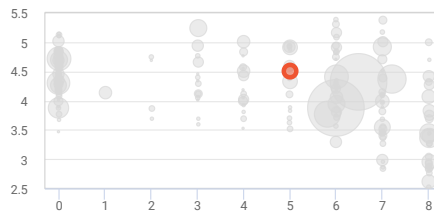

Access to electricity (% of rural population, 2016)   **16.9**
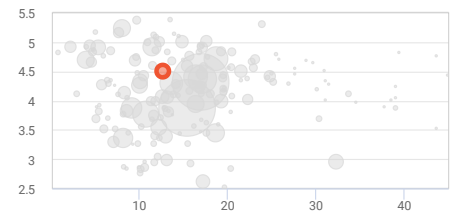

Electricity consumption (kWh/capita/year, 2014)   **104**

Reliability of supply and transparency of tarrif   **5.0**

Approximate electricity tarriffs (USD cents, 2019)   **12.6**

WORLD BANK GROUP   ESMAP   SOLARGIS

© 2021 The World Bank Group

The World Bank Group has published this fact-sheet as a part of the Global Photovoltaic Power Potential study. Disclaimer: Neither Solargis nor the World Bank Group shall be held responsible for the accuracy and/or completeness of the data and liable for any errors or omissions. It is strongly advised that the data be limited to use in informing policy discussions on the subject. As such, neither Solargis nor the World Bank Group will be liable for any damages related to the use of the study for financial commitments or any similar cases.

globalsolaratlas.info/global-pv-potential-study/

ABOUT

The World Bank Group publishes this factsheet as a part of the Global Photovoltaic Power Potential study, analyzing data from the Global Solar Atlas, World Bank Open Data, and other public sources. It is a part of the ESMAP initiative on Renewable Energy Resource Mapping, to support the appropriate scale-up of solar power in the worldwide energy mix.

The methodology and details behind the data analytics, explaining the graphics and figures in this factsheet, are discussed in the study. The findings aim to address the needs of policymakers, project developers, financial and academic sectors, as well as professionals and individuals interested in solar energy.

This factsheet involves numerical and graphical components:

- Photovoltaic power potential map of the country with the unified color legend for all countries worldwide (thus maps from various factsheets are comparable). Minima and maxima intervals for the country are marked in the legend.
- Country zonation map, showing how the country area is split into practical potential levels 0, 1 and 2
- Indicators section present basic country facts and statistics relevant to PV status in the country
- Summary statistics provide selected results of country-based evaluation of theoretical (GHI) and practical potential on level 1 (PVOUT)
- Distribution of photovoltaic power output histogram communicates how much land in the country is available in practical potential levels 0, 1 and 2, and various PVOUT ranges. It helps to understand, what might be the approximate area for PV development available in the best or moderate parts of the country.
- Monthly variation of the photovoltaic power potential details the seasonal PV electricity generation throughout a typical year; it is an important supplement to the seasonality index
- The bubble charts portray the position of the country in the global context of socio-economic and energy-related indicators. The bubble size is proportional to the population of the country. Current country is highlighted, other countries are in grey. Axis X represents the given indicator, axis Y represents the average practical PV potential at level 1.

Explore more

For more country fact-sheets, country and regional maps, interactive tools, PV calculator, statistics, reports and raster data in GIS formats visit Global Solar Atlas at https://globalsolaratlas.info.
More detailed data and technical solutions for specialists are provided by Solargis company (https://solargis.com).

© 2021 The World Bank Group

GLOSSARY

Theoretical PV Potential

Global horizontal irradiation (GHI, measured in kWh/m^2/day), the long-term amount of solar resource available on a horizontal surface on Earth.

Practical PV Potential

Photovoltaic power output of a PV system (specific yield, measured in kWh/kWp/day); in this case, the long-term power output produced by a utility-scale installation with fixed-mounted, monofacial c-Si modules with optimum tilt

- **Level 0** – Practical potential disregarding any land-use constraints
- **Level 1** – Level 0 practical potential, excluding land with identifiable physical obstacles to utility-scale pv plants
- **Level 2** – Level 1 practical potential, excluding land possibly under land use regulations due to nature and cropland protection

Economic PV Potential

Levelized cost of electricity (USD/kWh) – the lifetime costs associated with construction and operation of the power plant divided by the electricity produced during this lifetime (the lower the cost, the higher is the economic potential)

PV seasonality index

Ratio between the highest and the lowest of monthly long-term PVOUT averages.

PV equivalent area

Presumed country area proportion to be covered by PV plants producing the equivalent of yearly electricity consumption. The estimated area includes both the active area of PV modules and the area between the module rows (assuming the optimum row spacing).

Total / Evaluated area

Total area is a surface area of a country derived from official statistics, including inland water bodies and some coastal waterways. Evaluated area is a true area, from which the statistics were calculated. It includes land areas, without coastal waters, interior parts of the large water bodies, areas with missing input data and minor outliers caused by input data resolution.

Acronyms

DIF – Diffuse horizontal irradiance
DNI – Direct normal irradiance
GDP – Gross domestic product
GHI – Global horizontal irradiance
HDI – Human development index
LCOE – Levellized cost of electricity
PVOUT – Photovoltaic power output
PV – Photovoltaic

DATA SOURCES

Solargis

Average theoretical potential – GHI (kWh/m^2/day)
Average practical potential – PVOUT (kWh/kWp/day)
Distribution of photovoltaic power output
Monthly variation of photovoltaic power output
PV equivalent area (% of the total country area)
PV seasonality index

The World Bank

Total area (2018, km^2). Accessed on 2019-11-06.
https://data.worldbank.org/indicator/ag.srf.totl.k2

Population, total (2017). Accessed on 2019-11-06.
https://data.worldbank.org/indicator/sp.pop.totl

GDP per capita (2017, current USD). Accessed on 2019-11-06.
https://data.worldbank.org/indicator/ny.gdp.pcap.cd

Human Development Index (2017). Accessed on 2019-16-10.
https://datacatalog.worldbank.org/human-development-index-hdi

Electric power consumption (2014, kWh per capita). Accessed on 2019-11-06.
https://data.worldbank.org/indicator/eg.use.elec.kh.pc

Access to electricity (2016, % of rural population). Accessed on 2019-11-06.
https://data.worldbank.org/indicator/eg.elc.accs.ru.zs

Reliability of supply and transparency of tariff. Accessed on 2020-01-24.
World Bank, Doing Business, Measuring Business Regulations, Getting Electricity indicators.
https://www.doingbusiness.org/en/data/exploretopics/getting-electricity

Approximate electricity tariffs. Accessed on 2020-01-24.
World Bank, Doing Business, Measuring Business Regulations, Getting Electricity indicators.
https://databank.worldbank.org/reports.aspx?source=3001&series=IC.ELC.PRI.KH.DB1619

International Renewable Energy Agency (IRENA)

PV installed capacity (2018, MWp)
IRENA, Renewable Capacity Statistics 2019. Accessed on 2019-06-10.
https://www.irena.org/publications/2019/Mar/Renewable-Capacity-Statistics-2019

Levelized cost of electricity (2018, USD/kWh)
IRENA, Renewable power generation cost report 2018. Accessed on 2019-06-10.
https://www.irena.org/publications/2019/May/Renewable-power-generation-costs-in-2018

Appendix E

Weather Report

Home ⌄ | World Clock ⌄ | Time Zones ⌄ | Calendar ⌄ | Weather ⌄ | Sun & Moon ⌄ | Timers ⌄ | Calculators ⌄ | Apps & API ⌄ | Free Fun ⌄ | 👤 ⌄ | 🔍

Home / Weather / Norway / Trondheim / Past weeks

🇳🇴 Past Weather in Trondheim, Norway — Yesterday and Last 2 Weeks
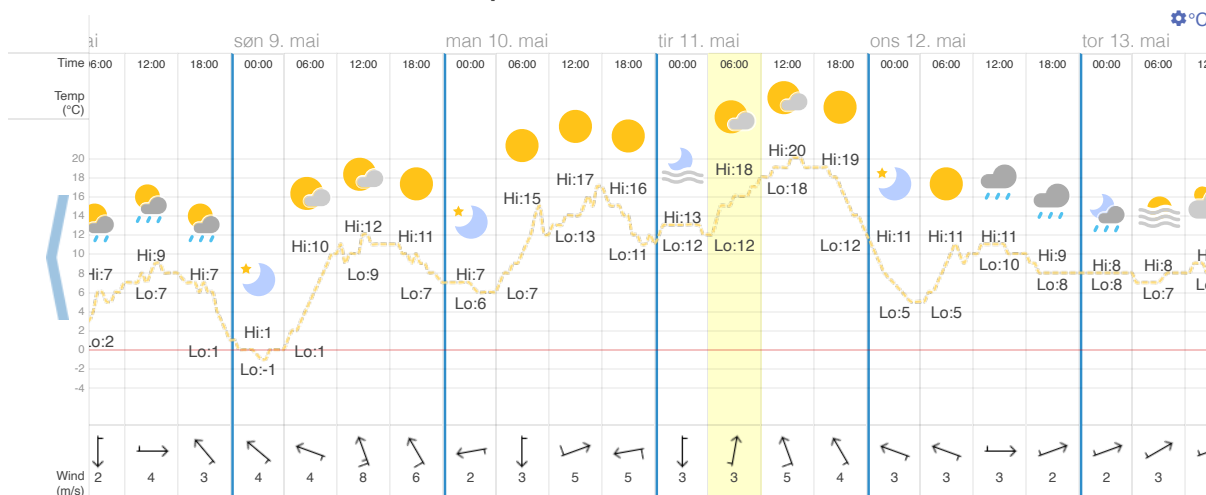
Time/General | Weather ⌄ | Time Zone | DST Changes | Sun & Moon ⌄

Weather Today | Weather Hourly | 14 Day Forecast | **Yesterday/Past Weather** | Climate (Averages)

⛅ **Currently:** 12 °C. Broken clouds. (Weather station: Trondheim / Vaernes, Norway). See more current weather ⌄   ✕

Select month: [Past 2 Weeks ⌄]

Past Weather in Trondheim — Graph

tirsdag 11. mai 2021, 06:00 — 12:00

⛅ **18 / 12 °C** Passing clouds.

Humidity: 46%
Barometer: 1006 mbar

Wind: 2.5 m/s   S

tir 4. mai | ons 5. mai | tor 6. mai | fre 7. mai | lør 8. mai | søn 9. mai | man 10. mai | tir 11. mai | ons 12. mai | tor 13. mai | fre 14. mai | lør 15. mai | søn 16. mai | man 17. mai | tir 18. mai | ons 19. mai

See weather overview ❯

Trondheim Temperature Yesterday

Maximum temperature yesterday: 14 °C (at 13:50)
Minimum temperature yesterday: 8 °C (at 00:50)
Average temperature yesterday: 10 °C

High & Low Weather Summary for the Past Weeks

	Temperature	Humidity	Pressure
High	20 °C (11. mai, 15:20)	100% (12. mai, 20:50)	1015 mbar (12. mai, 20:50)
Low	-3 °C (7. mai, 05:20)	27% (6. mai, 16:50)	998 mbar (11. mai, 01:20)
Average	9 °C	66%	1005 mbar
* Reported 4. mai 14:20 — 19. mai 14:20, Trondheim. Weather by CustomWeather, © 2021			

Note: Actual official high and low records may vary slightly from our data, if they occured in-between our weather recording intervals... More about our weather records

Trondheim Weather History for 11. mai 2021

Time	Conditions		Weather	Comfort			Humidity	Barometer	Visibility
		Temp		Wind					
00:20 Tue, 11 May		12 °C	Passing clouds.	19 km/h	←		77%	999 mbar	N/A
00:50		13 °C	Passing clouds.	6 km/h	↙		72%	999 mbar	N/A
01:20		13 °C	Clear.	6 km/h	↓		72%	998 mbar	16 km
01:50		13 °C	Passing clouds.	9 km/h	↙		72%	999 mbar	N/A
02:20		13 °C	Clear.	19 km/h	↖		67%	999 mbar	16 km
02:50		13 °C	Clear.	6 km/h	↓		67%	999 mbar	16 km
04:50		13 °C	Passing clouds.	7 km/h	↙		55%	1002 mbar	N/A
05:20		12 °C	Sunny.	6 km/h	↓		58%	1003 mbar	16 km
05:50		12 °C	Sunny.	4 km/h	↓		58%	1003 mbar	16 km
06:20		12 °C	Sunny.	No wind	↓		63%	1004 mbar	16 km
07:20		15 °C	Sunny.	4 km/h	↓		48%	1005 mbar	16 km
07:50		15 °C	Passing clouds.	6 km/h	↙		48%	1005 mbar	N/A
08:20		15 °C	Passing clouds.	11 km/h	↑		48%	1006 mbar	N/A
08:50		16 °C	Passing clouds.	7 km/h	↗		45%	1006 mbar	N/A
09:20		16 °C	Sunny.	15 km/h	↑		45%	1006 mbar	16 km
09:50		16 °C	Passing clouds.	15 km/h	↑		45%	1007 mbar	N/A
10:20		16 °C	Passing clouds.	9 km/h	↖		42%	1007 mbar	N/A
10:50		17 °C	Passing clouds.	11 km/h	↖		42%	1007 mbar	N/A
11:20		17 °C	Passing clouds.	9 km/h	↑		42%	1007 mbar	N/A
11:50		18 °C	Passing clouds.	17 km/h	↑		40%	1008 mbar	N/A
12:20		18 °C	Passing clouds.	13 km/h	↑		37%	1008 mbar	N/A
12:50		18 °C	Passing clouds.	17 km/h	↑		37%	1008 mbar	N/A
13:20		19 °C	Sunny.	24 km/h	↑		35%	1008 mbar	16 km
13:50		19 °C	Passing clouds.	19 km/h	↖		32%	1008 mbar	N/A
14:20		19 °C	Passing clouds.	17 km/h	↑		35%	1009 mbar	N/A
14:50		19 °C	Passing clouds.	19 km/h	↖		35%	1009 mbar	N/A
15:20		20 °C	Sunny.	19 km/h	↖		33%	1009 mbar	16 km
15:50		20 °C	Passing clouds.	22 km/h	↖		33%	1009 mbar	N/A
16:20		20 °C	Sunny.	24 km/h	↖		35%	1009 mbar	16 km
16:50		19 °C	Sunny.	20 km/h	↖		35%	1009 mbar	16 km
17:20		19 °C	Sunny.	19 km/h	↑		35%	1010 mbar	16 km
17:50		19 °C	Passing clouds.	15 km/h	↑		32%	1009 mbar	N/A
18:20		19 °C	Passing clouds.	13 km/h	↑		32%	1010 mbar	N/A
18:50		19 °C	Sunny.	13 km/h	↖		32%	1010 mbar	16 km
19:20		19 °C	Passing clouds.	17 km/h	↑		35%	1010 mbar	N/A
19:50		18 °C	Sunny.	15 km/h	↑		37%	1010 mbar	16 km
20:20		18 °C	Sunny.	19 km/h	↖		37%	1010 mbar	16 km
20:50		17 °C	Sunny.	19 km/h	↖		42%	1011 mbar	16 km
21:20		16 °C	Sunny.	20 km/h	↖		42%	1011 mbar	16 km
21:50		15 °C	Sunny.	19 km/h	↖		48%	1011 mbar	16 km
22:20		14 °C	Passing clouds.	13 km/h	←		51%	1011 mbar	N/A
22:50		14 °C	Passing clouds.	9 km/h	←		48%	1011 mbar	N/A
23:20		13 °C	Passing clouds.	9 km/h	↖		51%	1012 mbar	N/A
23:50		12 °C	Passing clouds.	7 km/h	↖		54%	1012 mbar	N/A

Home | World Clock ˅ | Time Zones ˅ | Calendar ˅ | Weather ˅ | Sun & Moon ˅ | Timers ˅ | Calculators ˅ | Apps & API ˅ | Free Fun ˅ | 👤 ˅ | 🔍

Home / Weather / Norway / Trondheim / Past weeks

🇳🇴 **Past Weather in Trondheim, Norway — Yesterday and Last 2 Weeks**

Search for city or place… 🔍

Time/General | Weather ˅ | Time Zone | DST Changes | Sun & Moon ˅

Weather Today | Weather Hourly | 14 Day Forecast | Yesterday/Past Weather | Climate (Averages)

☀️ **Currently:** 16 °C. Passing clouds. (Weather station: Trondheim / Vaernes, Norway). See more current weather ❯ ✕

Select month: Past 2 Weeks ▾

Past Weather in Trondheim — Graph

onsdag 2. juni 2021, 00:00 — 06:00

🌙 **18 / 16 °C**
Clear.

Humidity: 48%
Barometer: 1024 mbar

← E
Wind: 3.333 m/s
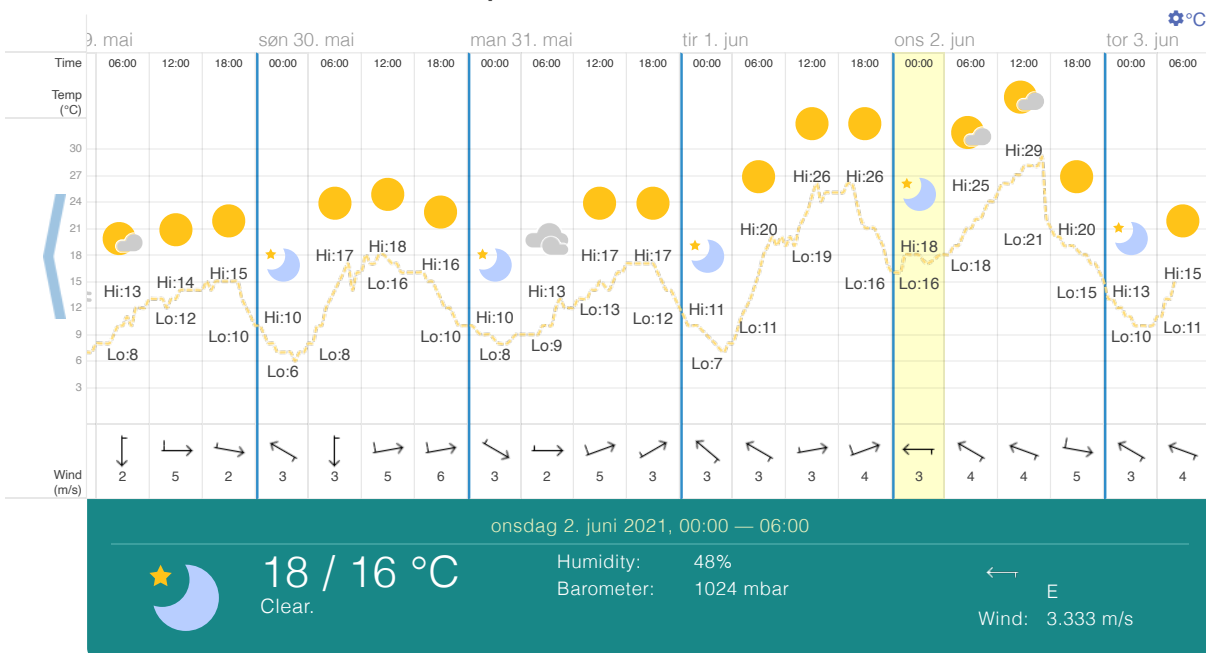
ons 19. mai | tor 20. mai | fre 21. mai | lør 22. mai | søn 23. mai | man 24. mai | tir 25. mai | ons 26. mai | tor 27. mai | fre 28. mai | lør 29. mai | søn 30. mai | man 31. mai | tir 1. jun | ons 2. jun | tor 3. jun

See weather overview ❯

Trondheim Temperature Yesterday

Maximum temperature yesterday: 29 °C (at 16:50)
Minimum temperature yesterday: 15 °C (at 23:50)
Average temperature yesterday: 21 °C

High & Low Weather Summary for the Past Weeks

	Temperature	Humidity	Pressure
High	29 °C (2. jun, 16:50)	93% (19. mai, 07:20)	1029 mbar (19. mai, 07:20)
Low	4 °C (28. mai, 04:50)	23% (2. jun, 14:50)	997 mbar (22. mai, 11:20)
Average	13 °C	62%	1016 mbar
	* Reported 19. mai 07:20 — 3. jun 07:50, Trondheim. Weather by CustomWeather, © 2021		

Trondheim Weather History for 2. juni 2021

Time		Conditions		Comfort				
		Temp	Weather	Wind		Humidity	Barometer	Visibility
00:20 Wed, 2 Jun		16 °C	Clear.	7 km/h	↖	68%	1022 mbar	16 km
00:50		16 °C	Clear.	4 km/h	↓	59%	1023 mbar	16 km
01:20		18 °C	Passing clouds.	11 km/h	←	46%	1023 mbar	N/A
01:50		18 °C	Clear.	19 km/h	←	43%	1023 mbar	16 km
02:20		18 °C	Clear.	17 km/h	←	43%	1023 mbar	16 km
02:50		18 °C	Clear.	13 km/h	←	43%	1024 mbar	16 km
03:50		17 °C	Passing clouds.	11 km/h	←	45%	1024 mbar	N/A
05:20		18 °C	Sunny.	17 km/h	↖	43%	1025 mbar	16 km
05:50		18 °C	Sunny.	11 km/h	←	46%	1025 mbar	16 km
06:20		18 °C	Sunny.	11 km/h	←	46%	1025 mbar	16 km
06:50		19 °C	Passing clouds.	11 km/h	↖	43%	1025 mbar	N/A
07:20		19 °C	Passing clouds.	13 km/h	↖	43%	1025 mbar	N/A
07:50		20 °C	Sunny.	13 km/h	↖	43%	1025 mbar	16 km
08:20		21 °C	Sunny.	13 km/h	↖	38%	1025 mbar	16 km
08:50		21 °C	Passing clouds.	13 km/h	↖	43%	1025 mbar	N/A
09:20		22 °C	Passing clouds.	11 km/h	↖	41%	1025 mbar	N/A
09:50		22 °C	Passing clouds.	13 km/h	↖	38%	1025 mbar	N/A
10:20		23 °C	Sunny.	15 km/h	↖	38%	1025 mbar	16 km
10:50		24 °C	Passing clouds.	15 km/h	↖	36%	1025 mbar	N/A
11:20		24 °C	Sunny.	17 km/h	↖	36%	1025 mbar	16 km
11:50		25 °C	Passing clouds.	13 km/h	↖	32%	1025 mbar	N/A
12:20		26 °C	Passing clouds.	11 km/h	↖	30%	1025 mbar	N/A
12:50		26 °C	Passing clouds.	11 km/h	↖	30%	1025 mbar	N/A
13:20		26 °C	Passing clouds.	13 km/h	↖	30%	1024 mbar	N/A
13:50		27 °C	Passing clouds.	9 km/h	↖	28%	1024 mbar	N/A
14:20		27 °C	Passing clouds.	9 km/h	↖	28%	1024 mbar	N/A
14:50		28 °C	Passing clouds.	9 km/h	↖	23%	1024 mbar	N/A
15:50		28 °C	Sunny.	6 km/h	↓	23%	1024 mbar	16 km
16:20		28 °C	Sunny.	6 km/h	↓	25%	1024 mbar	16 km
16:50		29 °C	Passing clouds.	11 km/h	→	23%	1024 mbar	N/A
17:20		22 °C	Sunny.	33 km/h	↗	53%	1024 mbar	16 km
17:50		21 °C	Sunny.	33 km/h	↗	57%	1024 mbar	16 km
18:20		20 °C	Sunny.	33 km/h	↗	64%	1025 mbar	16 km
18:50		20 °C	Sunny.	30 km/h	→	60%	1025 mbar	16 km
19:20		19 °C	Sunny.	30 km/h	↗	56%	1025 mbar	16 km
19:50		19 °C	Sunny.	26 km/h	→	56%	1026 mbar	16 km
20:20		19 °C	Sunny.	22 km/h	→	56%	1026 mbar	16 km
21:20		18 °C	Sunny.	15 km/h	→	56%	1026 mbar	16 km
21:50		18 °C	Sunny.	11 km/h	→	60%	1027 mbar	16 km
22:20		17 °C	Sunny.	6 km/h	↓	64%	1027 mbar	16 km
22:50		17 °C	Sunny.	4 km/h	↓	59%	1027 mbar	16 km
23:20		16 °C	Passing clouds.	6 km/h	↘	63%	1027 mbar	N/A
23:50		15 °C	Clear.	7 km/h	↘	68%	1028 mbar	16 km

Appendix F

PV system

solartek®

PV high-performance modules

Guaranteed positive output tolerance -0/+5Wp by single measuring

Maximum 8000Pa snow load

Maximum stability through aluminum frame Soft Grip

High-quality junction box and connector systems

Made in Europe

PV modules for extreme areas

12 years manufacturer's warranty

25 years linear performance guarantee to 85% output

Modern and fully automated production

GETEK
ENERGY

www.getek.no
post@getek.no

PVP – Polycrystalline series:

–option: black frame

Type	PVP25030	PVP26030	PVP27030
Nominal output Pmpp	250Wp	260Wp	270Wp
Nominal voltage Umpp	30,70V	30,92V	30,94V
Nominal current Impp	8,18A	8,43A	8,80A
Short circuit current Isc	8,41A	9,01A	9,41A
Open circuit voltage Uoc	37,80V	38,00V	39,26V
Module conversion efficiency	15,37%	15,98%	16,40%

Electrical characteristics (at Standard Test Conditions (STC) of irradiance 1000W / m2 , spectrum AM 25°C)

Design

Frontside	3,2mm anti–reflective glass
Cells	60polycrystalline high efficiency cells 156x156 mm (6")
Backside	Composite film
Frame	40mm silver anodized aluminium frame

Mechanical data

LxWxH	1650x992x40 mm
Weight	19,5kg with frame

Power conection

Socket	Protection classe IP65 (3 bypass diodes
Wire	Approx 110 cm / 4 mm2
Plug–in system	Plug / Socket IP67

Limit values

System voltage	1000VDC
NOCT*	45°C +/- 2K
Max. load-carring capacity	5400 N/m² tested to 8000 Pa
Reverse current feed IR	16.0A

*NOCT, irradiance 800 W/m2 AM 1.5; wind speed 1 m/sec; Temperature 20°C

Temperature coefficient

Voltage Uoc	–0,30%K
Current Isc	+0,04%K
Output Pmpp	–0,42%K
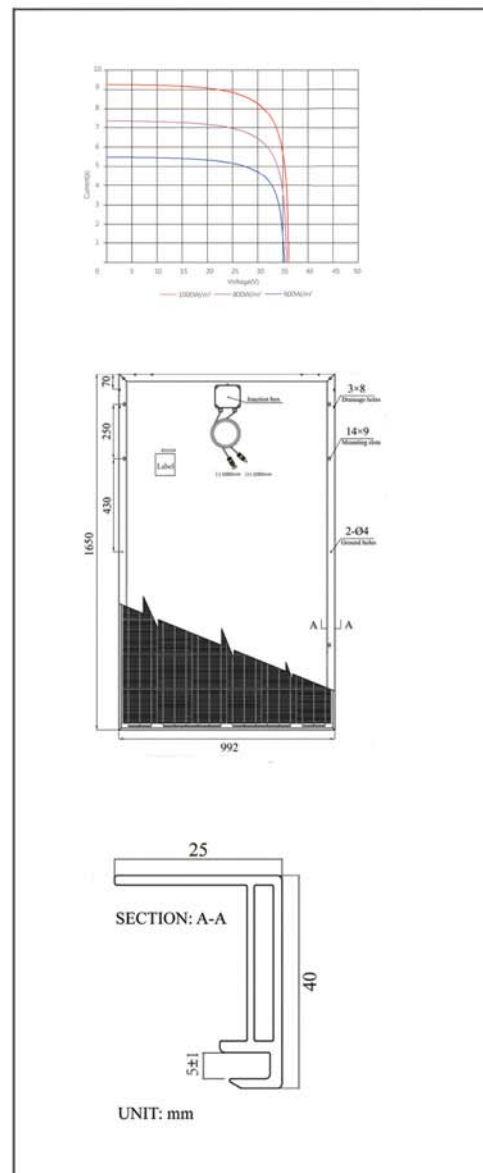
MPPT Load Controller

Features

- 6 thermocouple inputs

- DC/DC buck converter

- P&O MPPT

- Proportional voltage MPPT

- RMS power measurement

- Datalogging to microSD card and real-time clock.

- Manual load adjustment mode

Maximum ratings

Parameter	Min	Nominal	Max	Unit
Voltage (single panel)	16	38	40	V
Voltage (6 panels in series)	96	220	230	V
Load current	0		10	A
Aux. power voltage	16	24	42	V

WARNING: Parts at high voltage potential are exposed inside the enclosure. Connection should only be done by a qualified person.

WARNING: Always make sure polarity and voltages are correct. Reverse polarity and over-voltage can destroy the system.

Quick start guide

Content: PC with remote monitoring software, PC power supply, Load controller, box with accessories: USB cable, microSD card adapter, spare Wago connectors.

How to connect PV panels and load (heater):

Connect PV panels and load using the pre-attached Wago lever-connectors.
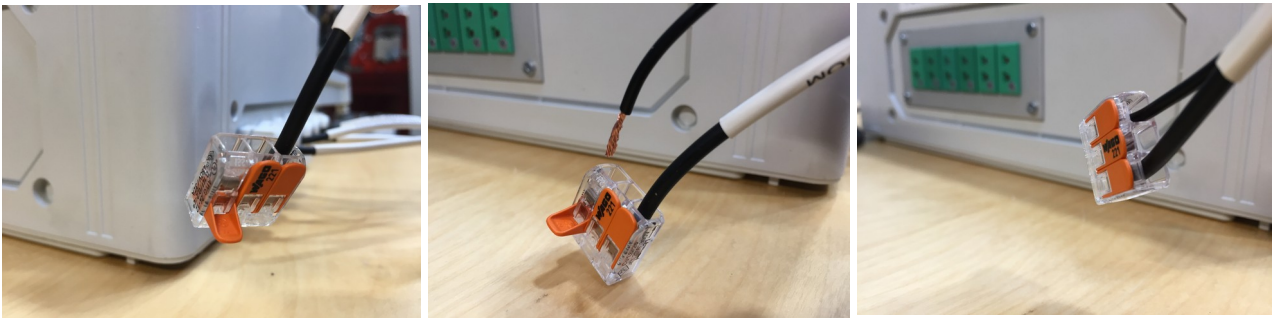
1. Pull lever down.

2. Insert stripped wire (Use maximum 4 mm2 copper wire.)

3. Press lever all the way back to lock the wire in place.

4. Please make sure connection is good both electrically and mechanically by visual inspection and pulling the wire respectively.

2

Connections (Follow the steps in the correct order. See connection diagram below as well.)

1. Turn main switch to OFF position.

2. Connect LOAD (Heater) to the wires marked `LOAD HEATER +` and `LOAD HEATER -` . The polarity of the load does not matter.

3. Connect the 0V (Minus/Negative) of the lowest panel in the PV array to the wire marked `PV ARRAY: 0V/COM` .

4. Connect the plus/positive from the top panel in the PV array to the wire marked `PV ARRAY: +220V DC` . **(WARNING: High voltage)**

5. Connect the plus/positive from the **lowest (!)** panel in the PV array to the wire marked `PV ARRAY: +38V DC` .

6. **Before** turning the main switch to the ON-position, carry out the measurements descibed on the next page. **(Reverse polarity or over-voltage can completely destroy the controller)**

7. If all measurements are good, turn the main switch ON.
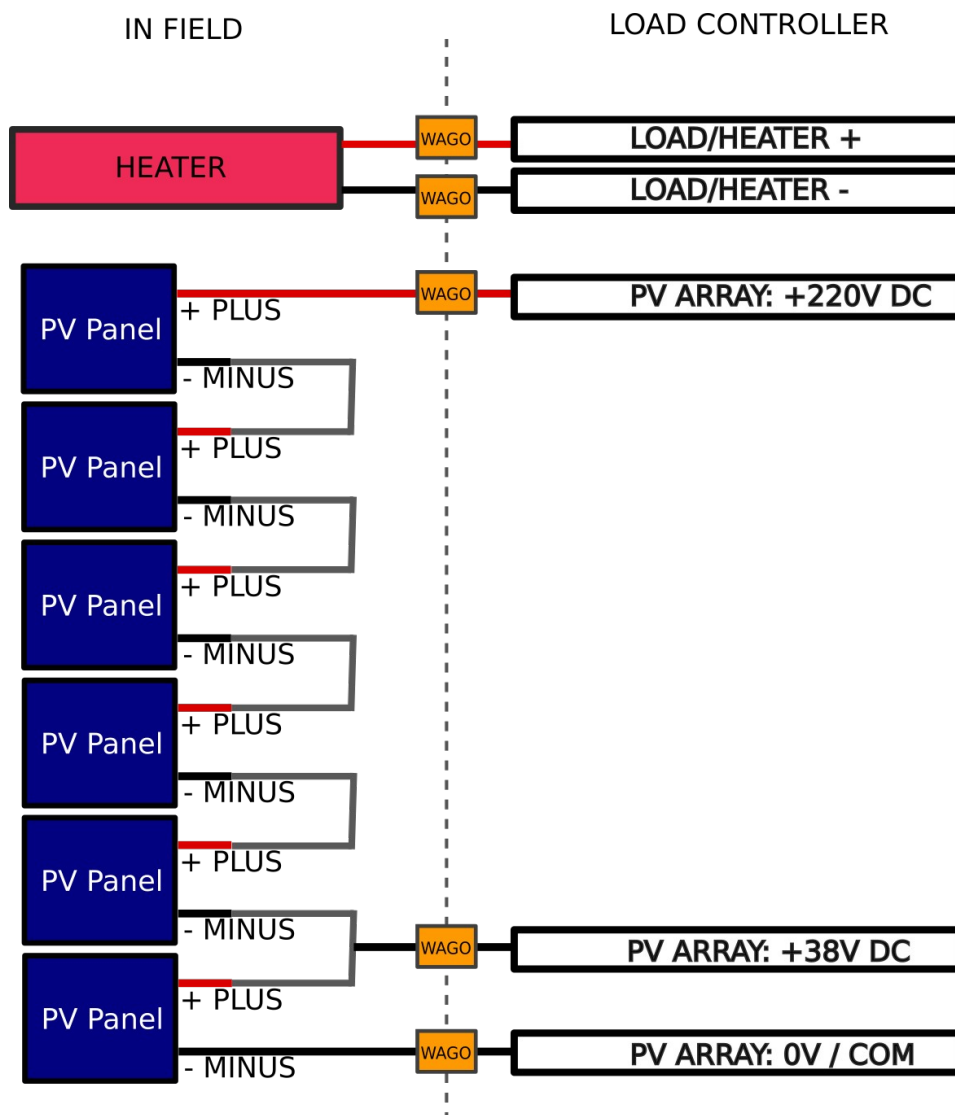
Pre-startup tests (please do not skip these)

Connect the **red** test lead to the **V** input of your multimeter and the **black** test lead to the **COM** input.
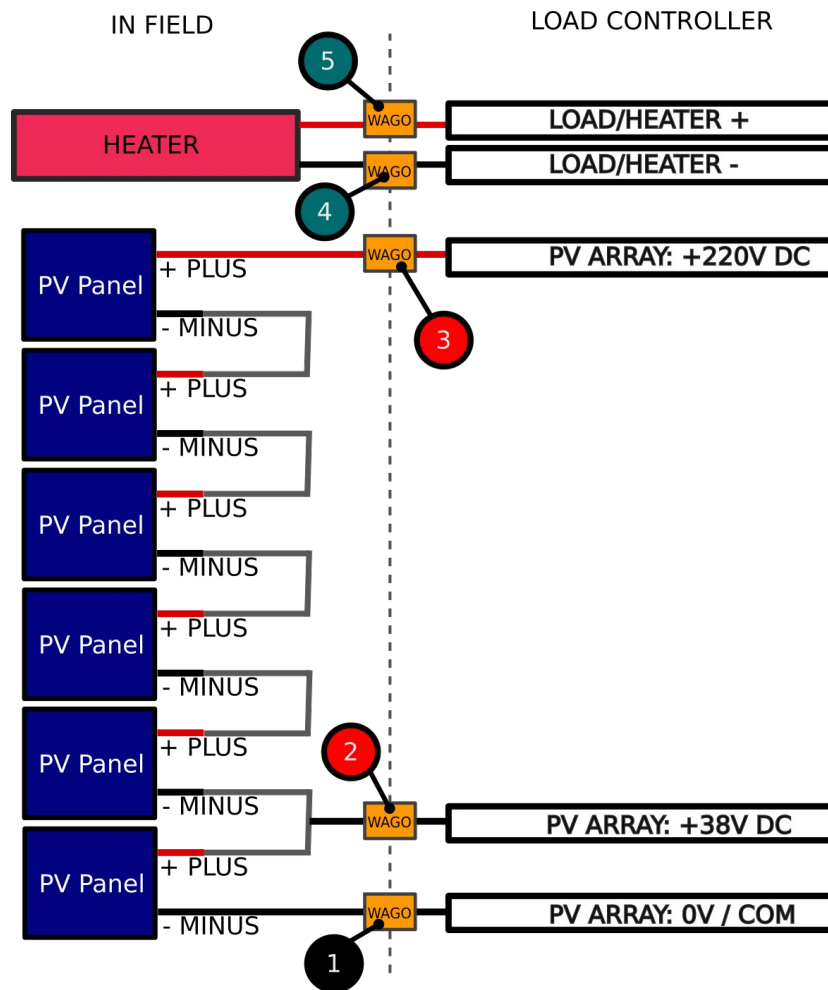
Use a multimeter that can measure DC voltage and resistance. Put the test leads in the Wago connectors.

1. Put the multimeter into resistance mode and measure the resistance between **4** and **5**.
   It should be in the range 10-50Ω (Ohms).

2. Put the multimeter into DC voltage mode and connect the black lead (COM) to **1**.

3. Use the red lead (V) to measure the voltage at **2**.
   *It should be in the range 30-39V DC. The voltage should **not** be negative.*

4. Now take the red lead (V) and measure the voltage at **3**.
   *It should be in the range 180-234V DC. The voltage should **not** be negative.*

If all measurements are within range, the system can be switched ON.

Connect thermocouples with type K miniature plug on the side of the box (The connectors only fit one way around.):
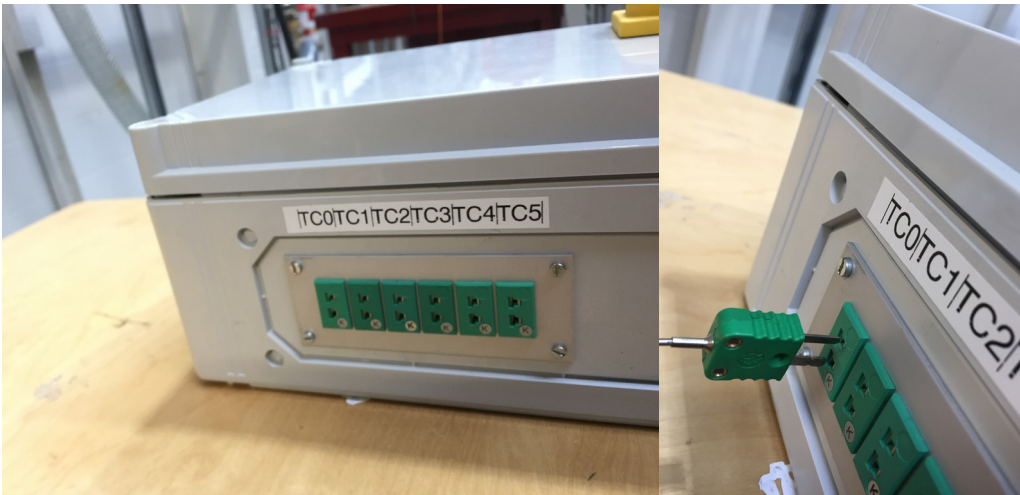
Note: Please place the controller box in a shaded area if possible to keep the temperatures as low as possible.

Overview:
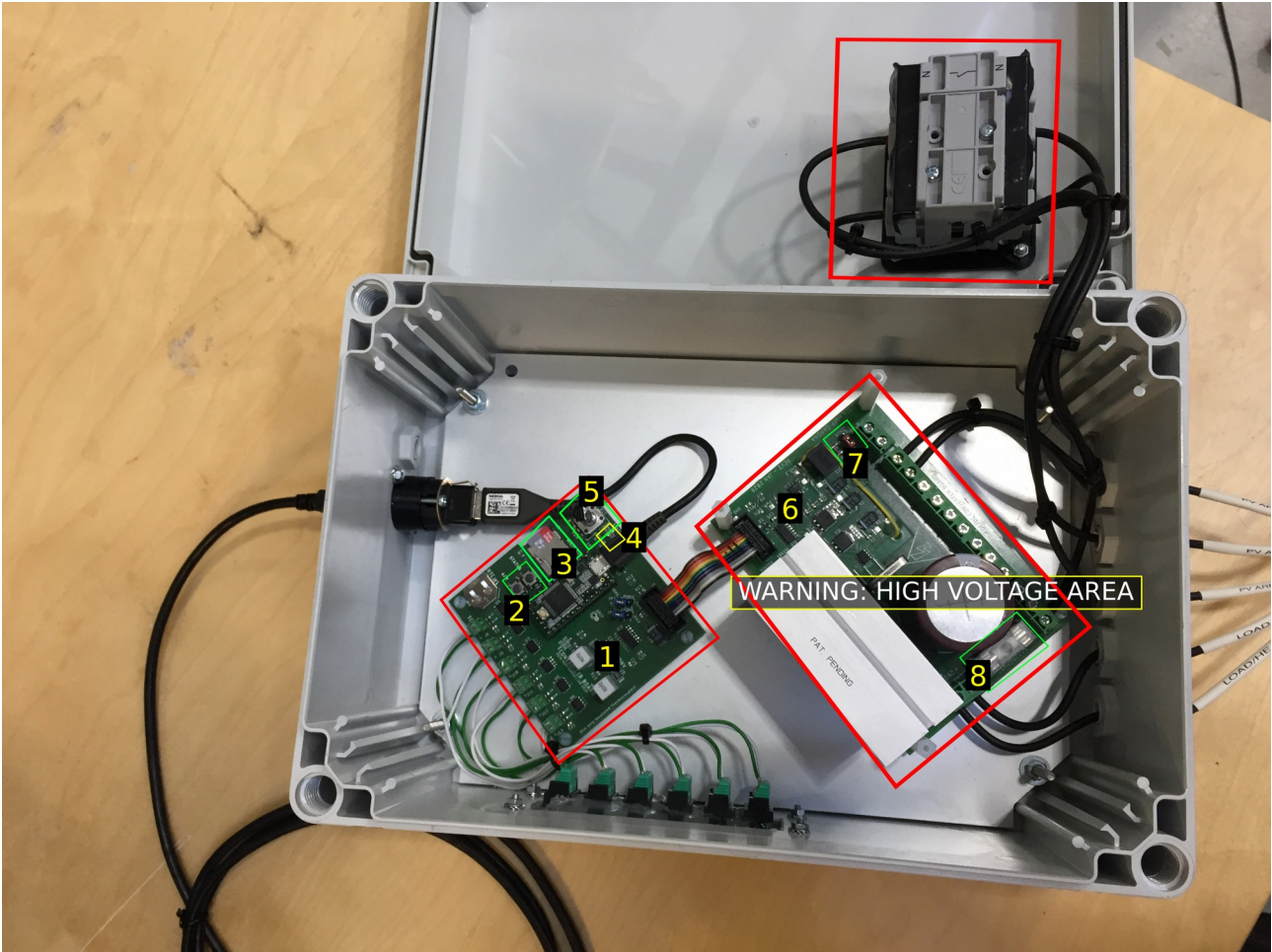
1. Low voltage controller board   2. Push buttons S1 and S2   3. microSD card

4. Status LEDs   5. Potmeter for manual PWM control   6. High voltage power board

7. AUX power jumper   8. Main fuse

How to use the PC monitor software

1. Connect USB cable to the load controller and PC.

2. Make sure the controller is powered on.

3. Double-click the LoadController software shortcut on the desktop.
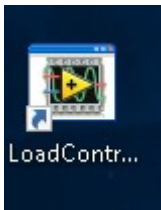
4. Choose COM port (usually COM4) and press «NEXT >>»
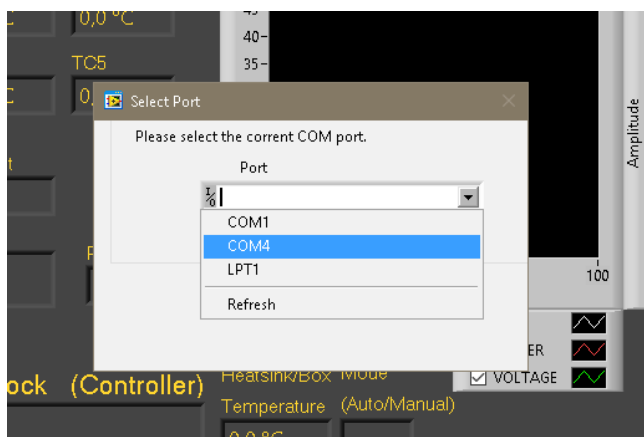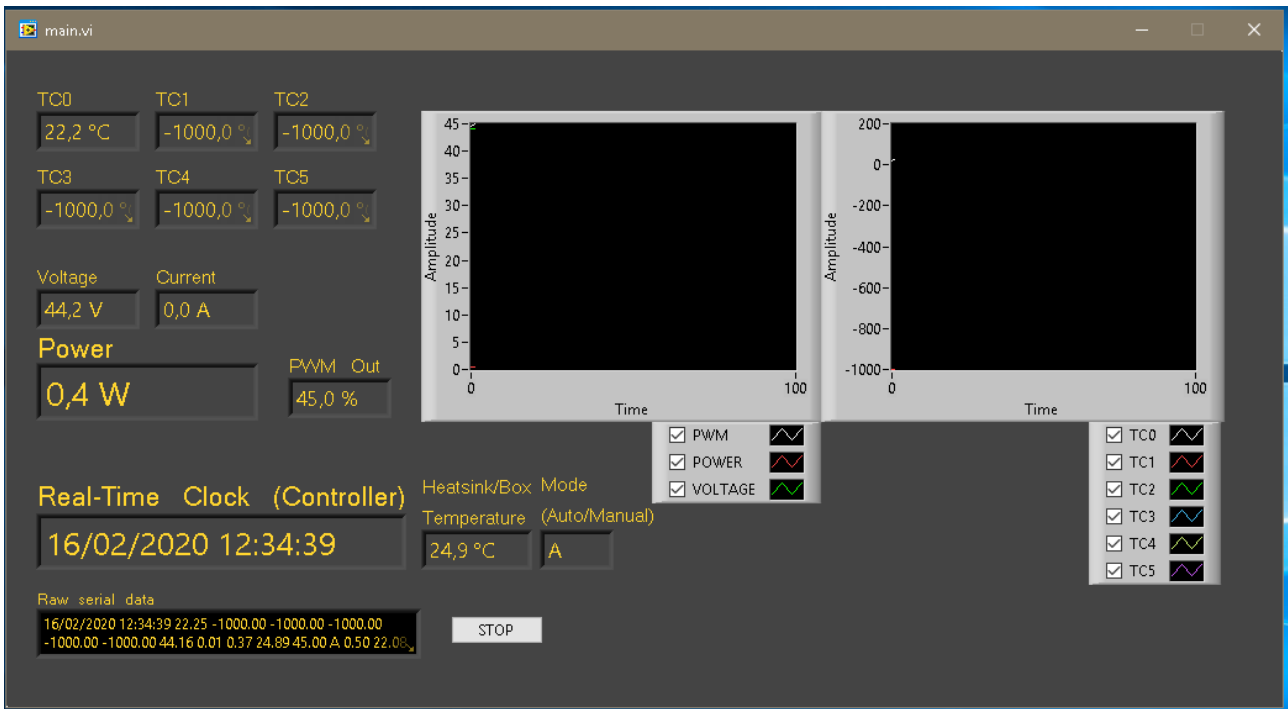
You should now be able to read real-time measurements including: thermocouples, voltage, current, power and PWM output to the DC/DC converter. If nothing happens, try turing the power off and on again on the controller box and restart the software on the PC.

Note: If the Heatsink temperature gets above 40-50 degrees C, consider opening the controller box to reduce the temperature.

Note: Data is logged to files on the computer (in the folder LogFiles on desktop).

8

How to extract logged data from SD card:

1. Turn power off completely.

2. Disconnect the USB cable to access the SD card.

3. Push the SD card into the socket and release.

4. Put the SD card into the microSD-to-SD adapter.

5. Put the SD card into an appropriate card reader and copy the file «log.txt».

6. (Delete the file «log.txt» on the SD card to clear logged data from the controller.)

7. Push the SD card back into the socket on the controller board.

8. Reconnect the USB cable

9. Import as tab-separated CSV into Excel or similar software.

LEDs and push buttons functionality

S1 (A/M): Toggles between auto and manual control. In auto mode, a MPPT algorithm is controlling the load. In manual mode, the PWM duty cycle is controlled using the on-board potentiometer.

Thermocouples

There are six thermocouple inputs. The temperature measurements are logged to SD card. The circuit uses six MAX31855 thermocouple amplifier and communicate with the microcontroller using SPI.

Troubleshooting for thermocouples:

Check the following points:

1. Polarity and connections are correct. (+ and - are marked on the PCB next to screw terminals.)

2. Thermocouple is of type K.

3. Thermocouple is of insulated type (e.g. mineral insulated).

4. Thermocouple and/or wire is not broken.

Certain errors can be detected by the controller board. In that case, the temperature reads as follows:

Temperature reading	Error	Fix
-1000.0	Open circuit	Check thermocouple and connections.
-2000.0	Short to VCC or GND	Check thermocouple. Make sure the thermocouple is insulated. (Electrically disconnected from sleeve)
-3000.0	Other	If the list above does not fix it, something is probably broken.

microSD card

Use only a microSD card formatted to a FAT32 or FAT16 file system. To do this on Windows, use an microSD to SD adapter if needed, right-click the SD card volume in «My Computer» and click format. Choose FAT32 or FAT16 filesystem and perform the formatting.

The log file is named «LOG.TXT».

To clear the logged data, delete the log file. The controller will automatically create a new one.

The data is tab separated and can be imported into your favourite spreadsheet software. The data is always on the following form:

Time	TC0 (°C)	TC1 (°C)	TC2 (°C)	TC3 (°C)	TC4 (°C)	TC5 (°C)	Voltage (V)	Current (A)	Power (W)	Thermistor (°C)	PWM out (%)

Replacing the fuse

WARNING: Always completely disconnect power before replacing the fuse!

Use 8 or 10A, 5x20mm fuse with voltage rating at least 250VDC.

Instructions for replacing fuse:

1. Disconnect power completely! Check using multimeter.

2. Remove fuse cover.

3. Remove old fuse and replace with new suitable fuse.

4. Attach fuse cover.

5. Reconnect power.

If the fuse trips: Check that the load is not shorted by measuring its resistance. Check connections, terminals and wires for damage.

Simplified system diagram

PV6

PLUS +

MINUS -

PV5

PLUS +

MINUS -

PV4

PLUS +

MINUS -

PV3

PLUS +

MINUS -

PV2

PLUS +

MINUS -

PV1

PLUS +

MINUS -

220V

38V

DC/DC BUCK CONVERTER

PWM

µController

RMS to DC Converter LTC1966

RMS to DC Converter LTC1966

Voltage Divider

PSU

AD8210

Shunt amplifier

Heater Load

Shunt Resistor
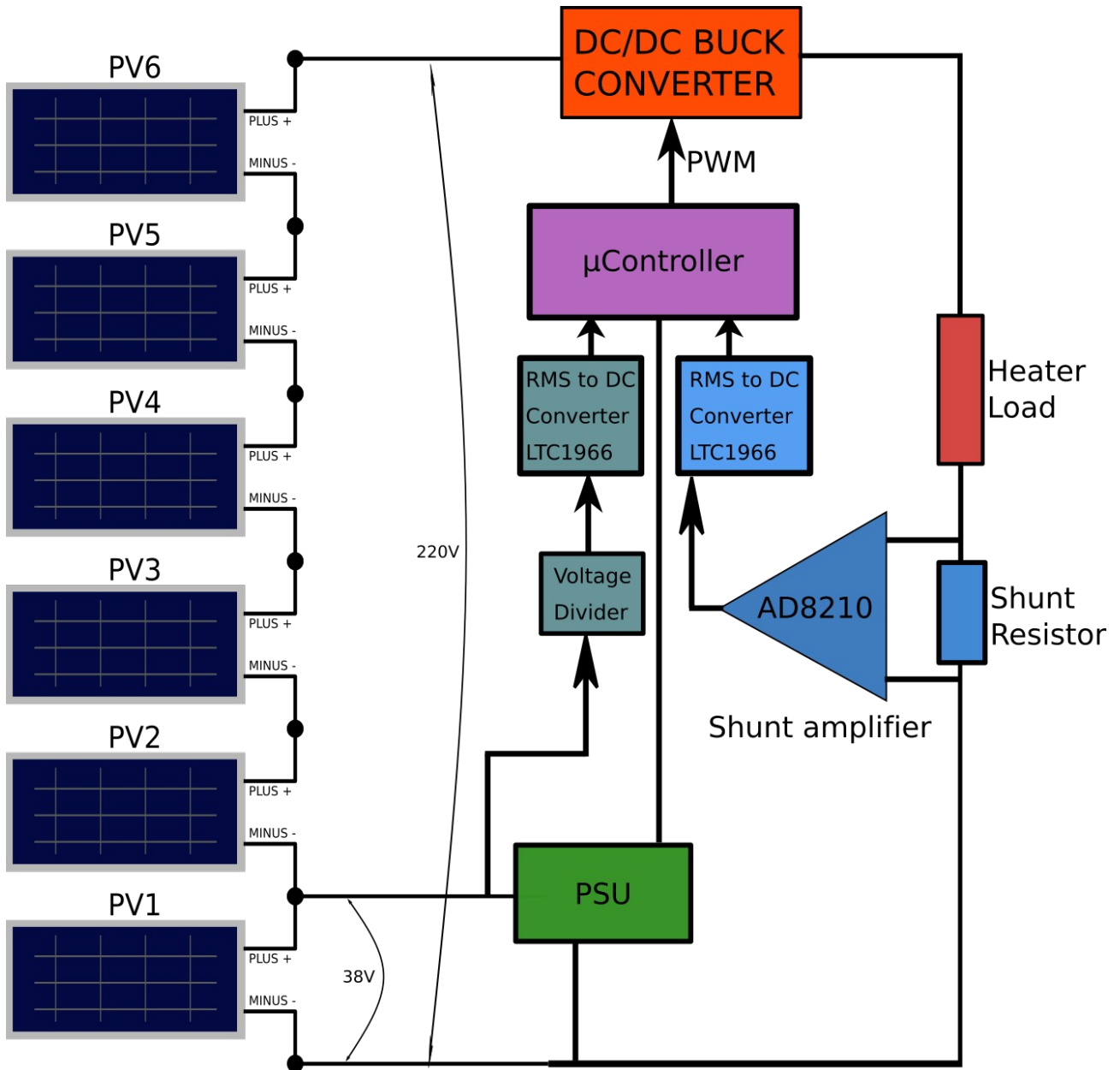
Auxiliary power connection

External power can be connected to drive the controller board so that datalogging and temperatures are logged even when there is no power from the solar PV array present. The voltage must be between 16V and 42V DC. **Do not reverse the polarity.**

AUX power jumper near the connection terminals must be set from **PV** to **AUX**.

RMS voltage and current measurements

The voltage of the lowest panel (PV1) is measured and multiplied by the number of panels to approximate the total voltage of the PV array. RMS calculations are done in hardware using LTC1966 RMS to DC converters.

The current is measured using a 0.025 Ohm shunt resistor together with a current shunt amplifier (AD8210). As with voltage, the RMS is computed using either software or with LTC1966.

Maximum Power Point Tracking (MPPT)

The algorithm begins by the following **pre-tracking routine**:

1. Measure the open circuit voltage.

2. Increase the load until voltage has decreased 10% from the open circuit voltage.

3. Pre-Tracking complete, start MPPT

The MPPT algorithm is of the standard «perturb and observe» type (P&O).

Begin after Pre-tracking complete

↓

Measure V(k) and I(k)

↓

Calculate P(k) = V(k)I(k)

↓

dP = P(k) - P(k-1)
dV = V(k) - V(k-1)

↓

dP > 0

—no→ dV > 0
—yes→ dP > 0

dV > 0: no → $D = D - \Delta D$; yes → $D = D + \Delta D$

dP > 0: no → $D = D + \Delta D$; yes → $D = D - \Delta D$

↓

V(k-1) = V(k)
I(k-1) = I(k)
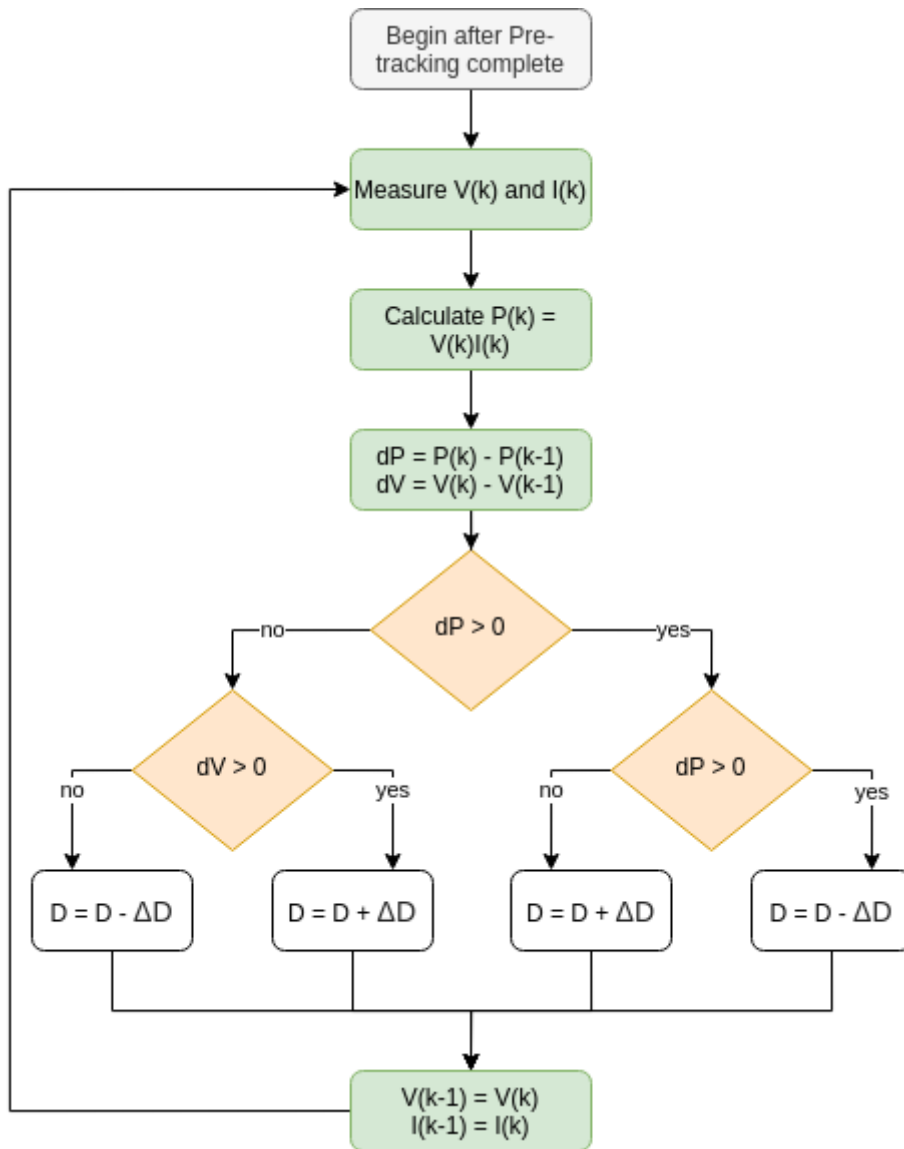
V(k)   Voltage at time k
I(k)   Current at time k
D   PWM Duty cycle
ΔD   Stepsize

Note: In the actual implementation, the stepsize depends on the system voltage.

I/O overview for programming (Teensy 3.2)

MAX31855 SPI

Pin function	Pin	Description/Notes
TC0 CS	14	Chip select (active low w/ external pullup)
TC1 CS	15	Chip select (active low w/ external pullup)
TC2 CS	16	Chip select (active low w/ external pullup)
TC3 CS	17	Chip select (active low w/ external pullup)
TC4 CS	18	Chip select (active low w/ external pullup)
TC5 CS	19	Chip select (active low w/ external pullup)
HW SPI SCK	13	HW SPI clock line
HW SPI DI (MISO)	12	HW SPI Master In Slave Out
SW SPI SCK	20	SW SPI clock line
SW SPI DI (MISO)	10	SW SPI Master In Slave Out

Note: Jumper JP1 and JP4 on controller board PCB must be changed if SW/bit banged SPI is to be used.

microSD SPI

Pin function	Pin	Description/Notes
HW SPI SCK	13	HW SPI clock line
HW SPI DI (MISO)	12	HW SPI Master In Slave Out
microSD CS	2	Chip select (active low w/ external pullup)
HW SPI DO (MOSI)	11	HW SPI Master Out Slave In
microSD CD	3	Card detect switch (low = card inserted)

Analog inputs

Pin function	Pin	Description/Notes
TEMP	A7/21	NTC thermistor for thermal shutdown
VSENSE	A8/22	RAW or RMS voltage
ISENSE	A9/23	RAW or RMS current
POT	A10	Potentiometer for manual PWM control

Note: Jumpers JP2 and JP3 can be used to change between RAW or RMS input. RAW input requires software RMS calculations, RMS input uses the LTC1966 DC to RMS converter.

Digital inputs

Pin function	Pin	Description/Notes
S1	6	Push button S1 Auto/Manual (active high w/ external pulldown)
S2	4	Push button S2 Status (active high w/ external pulldown)

Digital outputs

Pin function	Pin	Description/Notes
PWM	5	PWM output to MOSFET driver chip (external pulldown)
D1	9	Status LED D1
D2	8	Status LED D2
D3	7	Status LED D3

15

Special assembly instructions (rev2)

Assembly notes Teensy 3.2:
- Cut trace to Vin from USB power
- Solder on RTC crystal on Teensy
- Connect reset signal to reset pad

Mount NTC thermistor on heatsink by M3 screw.
Solder thin wire from reset pad on Teensy 3.2 to the reset pad on the controller board.
Hot glue capacitor and heatsink for support.

Appendix G

Risk Analysis

Risk Assessment Report

Sensible heat storage for cooking

Prosjektnavn	Sensible heat storage for cooking
Apparatur	Oil based heat storage rig
Enhet	NTNU
Apparaturansvarlig	Ole Jørgen Nydal
Prosjektleder	Ole Jørgen Nydal
HMS-koordinator	Morten Grønli
HMS-ansvarlig (linjeleder)	Terese Løvås
Plassering	Varmetekniske laboratorier
Romnummer	Multiphase lab
Risikovurdering utført av	Gunn Helen Nylund, Andreas Bjørshol

Approval:

Apparatur kort (UNIT CARD) valid for:	8 months
Forsøk pågår kort (EXPERIMENT IN PROGRESS) valid for:	8 months

Rolle	Navn	Dato	Signatur
Prosjektleder	Ole Jørgen Nydal		
HMS koordinator	Morten Grønli		
HMS ansvarlig (linjeleder)	Terese Løvås		

TABLE OF CONTENTS

1   INTRODUCTION

The experiment setup consists of one tank partly filled with thermal oil (Duratherm 630). A heating element is also placed inside the tank (1800 W), together with a funnel inside and a cooking pot at the top. The oil will be heated up to a decided temperature and then turned off to start a cooking test. The purpose of the cooking test is to see how the temperature profile of the oil will be in the tank, and if the funnel inside the tank works. Therefore, thermocouples are placed in the tank.
The experimental rig is located at room C 162, in Varmeteknisk Lab.

2   DESCRIPTIONS OF EXPERIMENTAL SETUP

The rig consist of the following components (see figure below):
1. Heat storage tank
2. Cooker
3. Heat funnel
4. Heating element
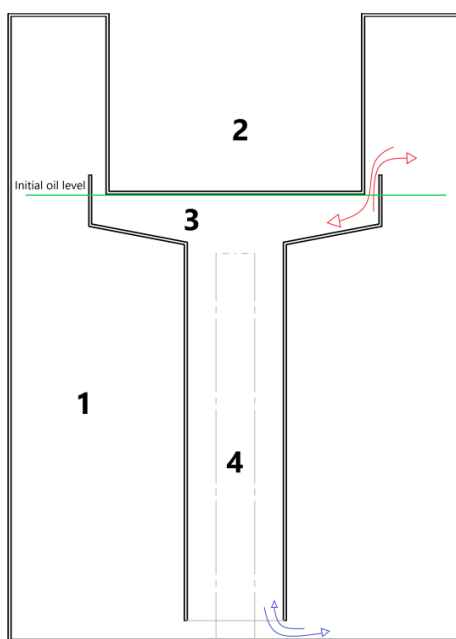
Figure 1: Oil-tank

The oil tank is filled with Duratherm 630 oil. The heating element, a group of thermocouples for monitoring the temperature in the tank, and the heat funnel are placed inside the oil tank. The heating element is a 1800W electric resistance.

The current system will not be closed as shown in the figure, it will have an opening between the cooker and the top of the tank to be able to monitor the level of the oil, but this will be possible to close with a steel ring attached to the pot.

The initial level of the oil (when the oil is cold) will be below the top of the funnel (as indicated in figure 1), the oil will overflow the funnel when it reaches a certain temperature.

3   EVACUATION FROM THE EXPERIMENTAL AREA

Evacuate at signal from the alarm system or local gas alarms with its own local alert with sound and light outside the room in question

Evacuation from the rigging area takes place through the marked emergency exits to the assembly point, (corner of Old Chemistry Kjelhuset or parking 1a-b.)

Action on rig before evacuation:
Turn off the electricity supply

4   WARNING

4.1   Before experiments

Send an e-mail with information about the planned experiment to:
experiments@ept.ntnu.no

The e-mail must include the following information:
- Name of responsible person:
- Experimental setup/rig:
- Start Experiments: (date and time)
- Stop Experiments: (date and time)

You must get the approval back from the laboratory management before start up. All running experiments are notified in the activity calendar for the lab to be sure they are coordinated with other activity.

4.2   Abnormal situation

<u>**FIRE**</u>
If you are NOT able to extinguish the fire, activate the nearest fire alarm and evacuate area.
Be then available for fire brigade and building caretaker to detect fire place.
If possible, notify:

NTNU
Morten Grønli, Mob: 918 97 515
Terese Løvås: Mob: 918 97 007

![NTNU logo]

NTNU – SINTEF Beredskapstelefon

GAS ALARM

If a gas alarm occurs, close gas bottles immediately and ventilate the area. If the level of the gas concentration does not decrease within a reasonable time, activate the fire alarm and evacuate the lab. Designated personnel or fire department checks the leak to determine whether it is possible to seal the leak and ventilate the area in a responsible manner.

PERSONAL INJURY

- First aid kit in the fire / first aid stations
- Shout for help
- Start life-saving first aid
- **CALL 113** if there is any doubt whether there is a serious injury

OTHER ABNORMAL SITUATIONS

NTNU:

You will find the reporting form for non-conformance on:
https://innsida.ntnu.no/wiki/-/wiki/Norsk/Melde+avvik

5   ASSESSMENT OF TECHNICAL SAFETY

5.1   HAZOP

The experiment set up is divided into the following nodes:

Node 1	Complete setup

Attachments, Form: HAZOP

Conclusion: Full safety equipment should be used when experimenting/operating with hot oil, including full coverage clothing, gloves, protective footwear and protective glasses. Also, it is important to always see how the temperature develops inside the tank.

5.2   Flammable, reactive and pressurized substances and gas

Are any flammable, reactive and pressurized substances and gases in use?

NO	

Attachments: EX zones?
Conclusion:

5.3   Pressurized equipment

Is any pressurized equipment in use?

NO	

ATTACHMENTS D:

Conclusion:

5.4 Effects on the environment (emissions, noise, temperature, vibration, smell)

Will the experiments generate emission of smoke, gas, odour or unusual waste?
Is there a need for a discharge permit, extraordinary measures?

NO	

Attachments:

Conclusion: The oil should be stored safe in a designated container and considered as special waste when the experiments are done.

5.5 Radiation

NO	

Attachments:
Conclusion:

5.6 Chemicals

Will any chemicals or other harmful substances be used in the experiments? Describe how the chemicals should be handled (stored, disposed, etc.) Evaluate the risk according to safety datasheets, MSDS. Is there a need for protective actions given in the operational procedure?

YES	Duratherm 630 thermal oil

Attachments: Material Safety Data Sheet

Conclusion: The oil used is a high heat transfer oil but is not dangerous for health. It is declared as to have no known significant effects or critical hazard, so it is safe to smell and touch, like the common oils for use in domestic houses. It is however not applicable for edible use.

5.7 Electricity safety (deviations from the norms/standards)

NO	

Attachments:
Conclusion:

6 ASSESSMENT OF OPERATIONAL SAFETY

Ensure that the procedures cover all identified risk factors that must be taken care of. Ensure that the operators and technical performance have sufficient expertise.

6.1 Procedure HAZOP

The method is a procedure to identify causes and sources of danger to operational problems.
Procedure:
1. Insulate the whole system
2. Minimize the gap between the cooker and the tank
3. Put the rig inside an open box that can contain the whole oil volume.
4. Pretest the system at lower temperatures

Attachments: HAZOP Prosedyre
Conclusion: Use safety equipment at all times and pay attention to the temperature development in the system. Always be able to reach the stop button.

6.2 Operation procedure and emergency shutdown procedure

Attachments: Procedure for running experiments
Emergency shutdown procedure: Pull out the plug connected to the heat element box (no power means no heat).

6.3 Training of operators

A Document showing training plan for operators
- *What are the requirements for the training of operators?*
- *What it takes to be an independent operator*
- *Job Description for operators*

 Attachments*:* Training program for operators

6.4 Technical modifications

- The cooker is not insulated/closed properly, so the hot oil is open to air. Since water is used as the heating medium in the cooker and has a lower boiling point than the oil, it is extremely important to not spill any water into the oil to avoid water expanding in the hot oil.

Conclusion: No water should enter the system, due to the low boiling point of water compared to oil. One must be careful when using water as the heating medium in the cooker.

6.5 Personal protective equipment

- Eye protection should always be used in the rig zone.
- Gloves should be used when handling the tubes, as some of them can be hot.
- Protective clothing should be used when doing experiments with hot oil.
- Protective shoes should be used when setting up the rig/moving heavy objects and when doing experiments with hot oil.

Conclusion: Plastic glasses and loves is always necessary special equipment, while protective clothing and shoes should be using during experiments and testing.

6.6   General Safety

• *Gantry crane and truck driving should not take place close to the experiment.*
• *Warning signs must be close to the hot elements.*
• *An operator must be controlling the rig.*
Conclusion: Signs and monitoring by operator.

6.7   Safety equipment

• *Warning signs, see the Regulations on Safety signs and signalling in the workplace*
• *Fire extinguisher should be available in case of emergencies*
• *Fire blanket should be available for emergencies*
• *The area around the staging attempts shielded.*

6.8   Special predations

There should be a welding screen (not flammable) located around the set up to protect form possible oil spill.

7   QUANTIFYING OF RISK - RISK MATRIX

The risk matrix will provide a visualization and an overview of activity risks so that management and users get the most complete picture of risk factors.

IDnr	Aktivitet-hendelse	Frekv-Sans	Kons	RV
1	Hot oil in contact with skin	1	E	E1
2	Water inside the tank	2	D	D2
3	Temperature above tank limits	3	C	C3
4	Too big expansion of the oil inside the tank	2	C	C2
5	Overheating of oil	2	D	D2

Actions:
- IDnr1 requires adequate safety equipment; fully covering clothing, shoes, protective glasses and gloves during operation and experiments. Also, the tank should be placed inside an open box that has the same volume as the oil inside the tank, so if leakages would happen, it would not be oil all over the floor. Otherwise it would be of a greater probability and characterized as a E3 (unacceptable) risk.
- IDnr2 will be caused by water in the tank, because water have a much lower evaporation point than the thermal oil. It is unlikely that water will enter below the cover ring and into the tank because only half of the cooking pot will be filled with water. However, the consequences are major so safety equipment always need to be worn, and one should be careful when adding water to the pot.
- IDnr3 will be caused if the temperature of the tank gets above what it can handle. This could lead to small or big leakages. To avoid the consequences of this to get too big, the box as mentioned in IDnr 1 must be implemented.
- IDnr4 Will be caused if the expansion of the oil inside the tank is too big, so there is not enough room for the oil to expand inside the tank. To minimize the probability of this one will have to monitor the expansion of the oil very carefully. Calculations are

also done to check that this will not be a problem. The consequences are only moderate because the box that the tank must be placed in.
- IDnr5 is most likely to occur in the extension tube of the heating element at the bottom. It would be a major risk, but it is unlikely due to Duratherm 630 being stable up to temperatures of 332 degrees C.

Conclusion: There are some risk doing this experiment, mostly related to the uncertainty of the expansion of the oil, and how much the tank can handle. Therefore it is concluded that the whole rig should be placed in an open box, so if leakages should occur, it would not be all over the floor.

RISK MATRIX

CONSEQUENSE	(E) Catastrophic	E1	E2	E3	E4	E5
	(D) Extensive	D1	D2	D3	D4	D5
	(C) Moderate	C1	C2	C3	C4	C5
	(B) Negligible	B1	B2	B3	B4	B5
	(A) Insignificant	A1	A2	A3	A4	A5
		(1) Rare	(2) Unlikely	(3) Possible	(4) Likely	(5) Almost certain
		PROBABILITY				

The principle of the acceptance criterion. Explanation of the colors used in the matrix

COLOUR		DESCRIPTION
Red		Unacceptable risk Action has to be taken to reduce risk
Yellow		Assessment area. Actions has to be considered
Green		Acceptable risk. Action can be taken based on other criteria

ATTACHMENT A: PROCESS AND INSTRUMENTATION DIAGRAM (PID)

1. Heat storage tank
2. Cooker
3. Heat funnel
4. Heating element

NTNU
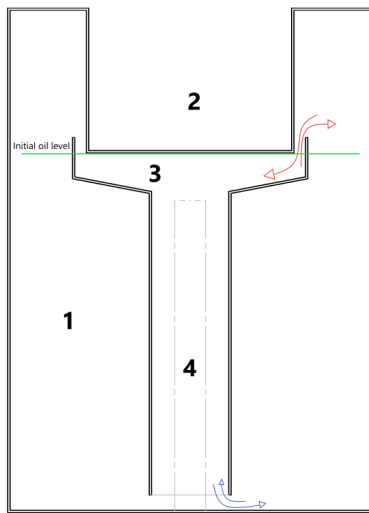
ATTACHMENT B: HAZOP TEMPLATE

Project: Node: 1 Complete setup						Page	
Ref #	Guideword	Causes	Consequences	Safeguards	Recommendations	Action	Date Sign
1	No flow	NA					
2	Reverse flow	NA					
3	More flow	NA					
4	Less flow	NA					
5	Higher level	To high expansion	Overflow of hot oil	Safety equipment	Heat gradually and pay attention to the temperature in the oil	Turn off the power supply	
6	Lower level	Leakages, underfilled	Overheating of the heating element, spill of hot oil	Safety equipment			
7	Higher pressure	NA					
8	Lower pressure	NA					
9	Higher temperature	Increasing the temperature of the oil above autoignition point (367°	Fire	Manual temperature control			
10	Lower temperature	NA					
11	More viscosity	NA					
12	Less viscosity	NA					

NTNU

Project: Node: 1 Complete setup							Page
Ref #	Guideword	Causes	Consequences	Safeguards	Recommendations	Action	Date Sign
13	Composition Change	NA					
14	Contamination	Overcooking the oil that is vented to ambient	Smell in the lab, health issues	Manual temperature control	Use an oil without significant contamination effects	Using Duratherm 630	
15	Relief	Leaks	Spill of oil	Manually check for leaks using water and cold oil			
16	Instrumentation	NA					
17	Sampling	NA					
18	Corrosion/erosion	NA					
19	Service failure	Problems with the heating element	Overheating of the tank, or no heating	Manual temperature control			
20	Abnormal operation	NA					
21	Maintenance	NA					
22	Ignition	Exceed autoignition point (367 °C)	Fire inside the tank	Manual temperature control	Use safety equipment during operation/experiments		
23	Spare equipment	NA					
24	Safety						

x

NTNU

ATTACHMENT C: HAZOP PROCEDURE (TEMPLATE)

Project: Node: 1						Page	
Ref#	Guideword	Causes	Consequences	Safeguards	Recommendations	Action	Date/Sign
	Not clear procedure	Procedure is to ambitious, or confusingly					
	Step in the wrong place	The procedure can lead to actions done in the wrong pattern or sequence					
	Wrong actions	Procedure improperly specified					
	Incorrect information	Information provided in advance of the specified action is wrong					
	Step missing	Missing step, or step requires too much of operator					
	Step unsuccessful	Step has a high probability of failure					
	Influence and effects from other	Procedure's performance can be affected by other sources					

ATTACHMENT E: PROCEDURE FOR RUNNING EXPERIMENTS

Project Sensible heat storage for cooking	Date	Signature
Facility Oil based heat storage tank		
Project leader Ole Jørgen Nydal		

	Conditions for the experiment:	Completed
	Experiments should be run in normal working hours, 08:00-16:00 during winter time and 08.00-15.00 during summer time. Experiments outside normal working hours shall be approved.	
	One person must always be present while running experiments, and should be approved as an experimental leader.	
	An early warning is given according to the lab rules, and accepted by authorized personnel.	
	Be sure that everyone taking part of the experiment is wearing the necessary protecting equipment and is aware of the shut down procedure and escape routes.	
	Preparations	**Carried out**
	Post the "Experiment in progress" sign.	
	Make sure that the ventilation is on and placed over the ventilation hole in the tank	
	Make sure that the safety screen is properly placed between us and the tank	
	During the experiment	
	Always have control on the different temperature measurements	
	Regularly control that there are no oil leakages from the tank	
	Test with colder oil than 150 deg in the first experiments. Start with 110 deg and increase for each experiment	
	Turn off the heating elements before starting cooking test, or if max temperature is reached.	
	Carefully fill half the pot (about 5 l) with water	
	End of experiment	
	Let the system cool down	
	Take the pot with water out to dry it, and place it back	
	Remove all obstructions/barriers/signs around the experiment.	
	Tidy up and return all tools and equipment.	
	Tidy and cleanup work areas.	
	Return equipment and systems back to their normal operation settings (fire alarm)	
	To reflect on before the next experiment and experience useful for others	

	Was the experiment completed as planned and on scheduled in professional terms?	
	Was the competence which was needed for security and completion of the experiment available to you?	
	Do you have any information/ knowledge from the experiment that you should document and share with fellow colleagues?	

Operator(s):

Navn	Dato	Signatur
Gunn Helen Nylund		
Andreas Bjørshol		

ATTACHMENT F: TRAINING OF OPERATORS

Project Sensible heat storage for cooking	Date	Signature
Facility Oil based heat storage tank		
Project leader Ole Jørgen Nydal		

	Knowledge about EPT LAB in general	
	Lab • Access • routines and rules • working hour	
	Knowledge about the evacuation procedures.	
	Activity calendar for the Lab	
	Early warning, experiments@ept.ntnu.no	
	Knowledge about the experiments	
	Procedures for the experiments	
	Emergency shutdown.	
	Nearest fire and first aid station.	

I hereby declare that I have read and understood the regulatory requirements has received appropriate training to run this experiment and are aware of my personal responsibility by working in EPT laboratories.

Operator(s):

Navn	Dato	Signatur
Gunn Helen Nylund		
Andreas Bjørshol		

NTNU

APPARATURKORT / UNITCARD

Dette kortet SKAL henges godt synlig på apparaturen!
This card MUST be posted on a visible place on the unit!

Apparatur (Unit)	
Prosjektleder (Project Leader)	**Telefon mobil/privat** (Phone no. mobile/private)
Apparaturansvarlig (Unit Responsible)	**Telefon mobil/privat** (Phone no. mobile/private)
Sikkerhetsrisikoer (Safety hazards)	
Sikkerhetsregler (Safety rules)	
Nødstopp prosedyre (Emergency shutdown)	

Her finner du (Here you will find):

Prosedyrer (Procedures)	aaa
Bruksanvisning (Users manual)	bbb

Nærmeste (Nearest)

Brannslukningsapparat (fire extinguisher)	aaaa
Førstehjelpsskap (first aid cabinet)	bbbb

NTNU
Institutt for energi og prosessteknikk

Dato

_____

Signert

_____

FORSØK PÅGÅR /EXPERIMENT IN PROGRESS

Dette kortet SKAL henges opp før forsøk kan starte!
This card MUST be posted on the unit before the experiment startup!

Apparatur (Unit)	
Prosjektleder (Project Leader)	**Telefon mobil/privat** (Phone no. mobile/private)
Apparaturansvarlig (Unit Responsible)	**Telefon mobil/privat** (Phone no. mobile/private)
Godkjente operatører (Approved Operators)	**Telefon mobil/privat** (Phone no. mobile/private)
Prosjekt (Project)	
Forsøkstid / Experimental time (start - stop)	
Kort beskrivelse av forsøket og relaterte farer (Short description of the experiment and related hazards**)**	

NTNU
Institutt for energi og prosessteknikk

Dato

_____

Signert

_____

ATTACHMENT H GUIDANCE TO RISK ASSESSMENT

Chapter 5 Assessment of technical safety.

Ensure that the design of the experiment set up is optimized in terms of technical safety.
Identifying risk factors related to the selected design, and possibly to initiate re-design to ensure that risk is eliminated as much as possible through technical security.
This should describe what the experimental setup actually are able to manage and acceptance for emission.

5.1 HAZOP

The experimental set up is divided into nodes (eg motor unit, pump unit, cooling unit.). By using guidewords to identify causes, consequences and safeguards, recommendations and conclusions are made according to if necessary safety is obtained. When actions are performed the HAZOP is completed.
(e.g. "No flow", cause: the pipe is deformed, consequence: pump runs hot, precaution: measurement of flow with a link to the emergency or if the consequence is not critical used manual monitoring and are written into the operational procedure.)

5.2 Flammable, reactive and pressurized substances and gas.

According to the Regulations for handling of flammable, reactive and pressurized substances and equipment and facilities used for this:

Flammable material: Solid, liquid or gaseous substance, preparation, and substance with occurrence or combination of these conditions, by its flash point, contact with other substances, pressure, temperature or other chemical properties represent a danger of fire.
Reactive substances: Solid, liquid, or gaseous substances, preparations and substances that occur in combinations of these conditions, which on contact with water, by its pressure, temperature or chemical conditions, represents a potentially dangerous reaction, explosion or release of hazardous gas, steam, dust or fog.
Pressurized : Other solid, liquid or gaseous substance or mixes having fire or hazardous material response, when under pressure, and thus may represent a risk of uncontrolled emissions

Further criteria for the classification of flammable, reactive and pressurized substances are set out in Annex 1 of the Guide to the Regulations "Flammable, reactive and pressurized substances"
http://www.dsb.no/Global/Publikasjoner/2009/Veiledning/Generell%20veiledning.pdf
http://www.dsb.no/Global/Publikasjoner/2010/Tema/Temaveiledning_bruk_av_farlig_stoff_Del_1.pdf

Experiment setup area should be reviewed with respect to the assessment of Ex zone
• Zone 0: Always explosive atmosphere, such as inside the tank with gas, flammable liquid.
• Zone 1: Primary zone, sometimes explosive atmosphere such as a complete drain point
• Zone 2: secondary discharge could cause an explosive atmosphere by accident, such as flanges, valves and connection points

5.4 Effects on the environment

With pollution means: bringing solids, liquid or gas to air, water or ground, noise and vibrations, influence of temperature that may cause damage or inconvenience effect to the environment.
Regulations: http://www.lovdata.no/all/hl-19810313-006.html#6
NTNU guidance to handling of waste:http://www.ntnu.no/hms/retningslinjer/HMSR18B.pdf

5.5 Radiation

Definition of radiation

Ionizing radiation: Electromagnetic radiation (in radiation issues with wawelength <100 nm) or rapid atomic particles (e.g. alpha and beta particles) with the ability to stream ionized atoms or molecules.
Non ionizing radiation: Electromagnetic radiation (wavelength >100 nm), og ultrasound$_1$ with small or no capability to ionize.
Radiation sources: All ionizing and powerful non-ionizing radiation sources.
Ionizing radiation sources: Sources giving ionizing radiation e.g. all types of radiation sources, x-ray, and electron microscopes.
Powerful non ionizing radiation sources: Sources giving powerful non ionizing radiation which can harm health and/or environment, e.g. class 3B and 4. MR$_2$ systems, UVC$_3$ sources, powerful IR sources$_4$.
$_1$Ultrasound is an acoustic radiation ("sound") over the audible frequency range (> 20 kHz). In radiation protection regulations are referred to ultrasound with electromagnetic non-ionizing radiation. $_2$MR (e.g. NMR) - nuclear magnetic resonance method that is used to "depict" inner structures of different materials. $_3$UVC is electromagnetic radiation in the wavelength range 100-280 nm. $_4$IR is electromagnetic radiation in the wavelength range 700 nm - 1 mm.

For each laser there should be an information binder (HMSRV3404B) which shall include:
- General information
- Name of the instrument manager, deputy, and local radiation protection coordinator
- Key data on the apparatus
- Instrument-specific documentation
- References to (or copies of) data sheets, radiation protection regulations, etc.
- Assessments of risk factors
- Instructions for users
- Instructions for practical use, startup, operation, shutdown, safety precautions, logging, locking, or use of radiation sensor, etc.
- Emergency procedures
- See NTNU for laser: http://www.ntnu.no/hms/retningslinjer/HMSR34B.pdf

5.6 The use and handling of chemicals.

In the meaning chemicals, a element that can pose a danger to employee safety and health
See: http://www.lovdata.no/cgi-wift/ldles?doc=/sf/sf/sf-20010430-0443.html
Safety datasheet is to be kept in the HSE binder for the experiment set up and registered in the database for chemicals.

Chapter 6 Assessment of operational procedures.

Ensures that established procedures meet all identified risk factors that must be taken care of through operational barriers and that the operators and technical performance have sufficient expertise.

6.1 Procedure Hazop
Procedural HAZOP is a systematic review of the current procedure, using the fixed HAZOP methodology and defined guidewords. The procedure is broken into individual operations (nodes) and analyzed using guidewords to identify possible nonconformity, confusion or sources of inadequate performance and failure.

6.2 Procedure for running experiments and emergency shutdown.
Has to be prepared for all experimental setups.
The operating procedure has to describe stepwise preparation, startup, during and ending conditions of an experiment. The procedure should describe the assumptions and conditions for starting, operating parameters with the deviation allowed before aborting the experiment and the condition of the rig to be abandoned.

Emergency procedure describes how an emergency shutdown have to be done,
- *what happens when emergency shutdown, is activated. (electricity / gas supply) and*
- *which events will activate the emergency shutdown (fire, leakage).*

Chapter 7 Quantifying of RISK
Quantifying of the residue hazards, Risk matrix.

To illustrate the overall risk, compared to the risk assessment, each activity is plotted with values for the probability and consequence into the matrix. Use task IDnr.
Example: If activity IDnr. 1 has been given a probability 3 and D for consequence the risk value become D3, red. This is done for all activities giving them risk values.

In the matrix are different degrees of risk highlighted in red, yellow or green. When an activity ends up on a red risk (= unacceptable risk), risk reducing action has to be taken

RISK MATRIX

CONSEQUENSE		(1) Rare	(2) Unlikely	(3) Possible	(4) Likely	(5) Almost certain
	(E) Catastrophic	E1	E2	E3	E4	E5
	(D) Extensive	D1	D2	D3	D4	D5
	(C) Moderate	C1	C2	C3	C4	C5
	(B) Negligible	B1	B2	B3	B4	B5
	(A) Insignificant	A1	A2	A3	A4	A5

		PROBABILITY

The principle of the acceptance criterion. Explanation of the colors used in the matrix

COLOUR		DESCRIPTION
Red		Unacceptable risk Action has to be taken to reduce risk
Yellow		Assessment area. Actions has to be considered
Green		Acceptable risk. Action can be taken based on other criteria

NTNU
Norwegian University of
Science and Technology